MUSCARINIC CHOLINERGIC MODULATION OF LONG-LASTING SYNAPTIC PLASTICITY IN THE RAT DENTATE GYRUS

1990

BURGARD

UNIFORMED SERVICES UNIVERSITY OF THE HEALTH SCIENCES
F. EDWARD HEBERT SCHOOL OF MEDICINE
4301 JONES BRIDGE ROAD
BETHESDA, MARYLAND 20814-4799

GRADUATE AND
CONTINUING EDUCATION

TEACHING HOSPITALS
WALTER REED ARMY MEDICAL CENTER
NAVAL HOSPITAL, BETHESDA
MALCOLM GROW AIR FORCE MEDICAL CENTER
WILFORD HALL AIR FORCE MEDICAL CENTER

APPROVAL SHEET

Title of Dissertation: **"Muscarinic Cholinergic Modulation of Long-Lasting Synaptic Plasticity in the Rat Dentate Gyrus"**

Name of Candidate: Edward C. Burgard
Doctor of Philosophy Degree
December 14, 1990

Dissertation and Abstract Approved:

Committee Chairperson	12/14/90 Date
Committee Member	12/14/90 Date
Committee Member	12/14/90 Date
Committee Member	12-14-90 Date
Committee Member	12/14/90 Date
Committee Member	12/14/90 Date

The author hereby certifies that the use of any copyrighted material in the dissertation manuscript entitled:

"Muscarinic Cholinergic Modulation of Long-lasting Synaptic Plasticity in the Rat Dentate Gyrus"

beyond brief excerpts is with the permission of the copyright owner, and will save and hold harmless the Uniformed Services University of the Health Sciences from any damage which may arise from such copyright violations.

Edward C. Burgard
Department of Pharmacology
Uniformed Services University
of the Health Sciences

ABSTRACT

Title of dissertation: Muscarinic Cholinergic Modulation of Long-Lasting Synaptic Plasticity in the Rat Dentate Gyrus

Edward Charles Burgard III, Doctor of Philosophy, 1990

Dissertation directed by: John M. Sarvey, Ph.D., Associate Professor, Department of Pharmacology

The effects of muscarinic cholinergic receptor activation on the induction of long-lasting synaptic plasticity were investigated in an *in vitro* tissue slice preparation of dentate gyrus from rat hippocampus. Responses evoked by stimulation of medial perforant path axons were measured using extracellular microelectrodes positioned in either or both the granule cell layer and the mid-molecular layer of the dentate gyrus. Two examples of long-lasting synaptic plasticity of medial perforant path/granule cell synapses were studied. The first, long-term potentiation (LTP), was induced by application of a high-frequency stimulus train to the medial perforant path, and was measured as a long-lasting increase in synaptic efficacy at these synapses. The second, ß-adrenergic-induced long-lasting potentiation (LLP), was induced by perfusion of slices with artificial cerebrospinal fluid containing

either norepinephrine or isoproterenol, and was also measured as a long-lasting increase in synaptic function. The induction of both LTP and LLP was found to be dependent on activation of N-methyl-D-aspartate (NMDA) receptors.

The nonselective muscarinic receptor agonist, muscarine, produced a concentration-dependent depression of evoked responses in the dentate gyrus. At a low concentration (1μM) that had no effect on evoked responses, muscarine facilitated induction of LTP, but not LLP. This facilitation was prevented by pirenzepine, an M1 muscarinic receptor antagonist. At a higher concentration of muscarine (10μM) that depressed evoked responses, LTP was not facilitated, and LLP was blocked. The depression of evoked responses produced by 10μM muscarine was not prevented by pretreatment with pertussis toxin, and was blocked by atropine. The muscarinic receptor subtype-selective antagonists pirenzepine (M1), AFDX-116 (M2), and 4-DAMP (M3/M1) all competitively antagonized muscarinic depression of evoked responses, with 4-DAMP exhibiting the greatest potency. In addition, muscarine was unable to modulate either basal or isoproterenol-stimulated accumulation of cyclic 3',5' adenosine monophosphate in slices of dentate gyrus. From these data it was concluded that muscarinic receptor activation differentially modulates two forms of NMDA receptor-dependent synaptic plasticity in the dentate gyrus. Facilitation of LTP and inhibition of LLP by muscarine both appear to be mediated through M1 or M3 receptors.

MUSCARINIC CHOLINERGIC MODULATION OF LONG-LASTING SYNAPTIC PLASTICITY IN THE RAT DENTATE GYRUS

by

Edward C. Burgard III

Dissertation submitted to the Faculty of the Department of Pharmacology
Graduate Program of the Uniformed Services University of the
Health Sciences in partial fulfillment of the
requirements for the degree of
Doctor of Philosophy 1990

This dissertation is dedicated first to my wife, Sheila, and second to my parents, Edward and Barbara, and my sisters, Elise and Anne. Each in his or her own way has made this dissertation possible.

I would like to thank my mentor, John M. Sarvey Ph.D., for his supervision of this dissertation, and for my training as a pharmacologist.

I would like to thank the members of my dissertation committee: Drs. T. Cote, B. Cox, S. Juliano, L. Moore, T. Pellmar and J. Sarvey for their input and their guidance of this dissertation.

A special acknowledgement goes to Gregory Decker, who assisted in much of my training and some of the early experiments.

I would also like to thank Drs. Meta Bonner, Gene Boyer, Dennis Dahl, and all the members of the Friday morning journal club for critical reviews of our manuscripts as well as helpful scientific insight and discussion.

Table of Contents

List of Figures..... x

List of Tables..... xii

Introduction..... 1

Synaptic plasticity in the hippocampus..... 2

NMDA receptors and synaptic plasticity..... 2

ß-Adrenergic involvement in synaptic plasticity..... 6

Muscarinic cholinergic involvement in synaptic plasticity... 9

Cyclic AMP and synaptic plasticity..... 16

Summary and specific aims..... 18

Materials and Methods..... 19

Preparation and maintenance of hippocampal slices..... 19

Pharmacological manipulations..... 21

Electrophysiology..... 22

Cyclic AMP assay..... 28

Pertussis toxin injections..... 30

Materials..... 31

Data analysis..... 31

Results..... 33

I. Evoked responses recorded in the dentate gyrus..... 33

Orthodromic and antidromic responses..... 33

Medial vs lateral perforant path isolation..... 34

II. Characterization of LTP and LLP in the dentate gyrus..... 39
Induction of LTP and LLP..... 39
Thresholds for induction of LTP and LLP..... 43

III. The role of NMDA receptors in synaptic plasticity and evoked synaptic activity in the dentate gyrus..... 44
NMDA receptors in LTP and LLP..... 44
NMDA receptors in evoked synaptic activity..... 54

IV. Muscarinic receptor activation in the dentate gyrus..... 62
Effects of muscarine on evoked responses..... 62
Antagonist sensitivity of muscarinic effects..... 65
Pertussis toxin sensitivity of muscarinic depression..... 70
Muscarinic facilitation of LTP..... 78
Muscarinic inhibition of LLP..... 82

V. Stimulation of [cAMP] in the dentate gyrus..... 86
ß-Adrenergic-induced changes in [cAMP]..... 86
Muscarinic-induced changes in [cAMP]..... 89

Discussion..... 90
NMDA receptors and synaptic plasticity..... 90
Muscarinic receptors and synaptic plasticity..... 95

References..... 107

List of Figures

1. Schematic representation of the hippocampal slice..... 24

2. Orthodromic and antidromic responses recorded in the dentate gyrus..... 36

3. Medial vs lateral perforant path isolation..... 38

4. LTP and β-adrenergic-induced LLP 41

5. NMDA receptor antagonists block both LTP and LLP..... 47

6. APV posttreatment does not block LLP..... 50

7. APV blocks phorbol ester-induced potentiation..... 53

8. NMDA receptor antagonists depress orthodromic transmission..... 56

9. High [Mg^{++}] does not block D(-)APV-induced depression..... 58

10. NMDA receptor antagonists depress medial, but not lateral EPSPs..... 61

11. Concentration-dependent depression of evoked responses by muscarine..... 64

12. Competitive antagonism of muscarinic depression by pirenzepine..... 68

13. Antagonism of muscarinic depression by muscarinic receptor antagonists..... 72

14. Representative traces demonstrating the efficacy of muscarinic receptor antagonists..... 74

15. Pertussis toxin insensitivity of muscarinic depression..... 77

16. Pirenzepine-sensitive facilitation of LTP by a low concentration of muscarine..... 80

17. Blockade of LLP by a high concentration of muscarine..... 84

18. Inability of muscarine to block isoproterenol-stimulated increase in cAMP..... 88

List of Tables

1. Summary of muscarinic receptor pharmacology..... 13

List of Abbreviations

AHP	afterhyperpolarization
APV	2-amino-5-phosphonovaleric acid
cAMP	cyclic 3',5'-adenosine monophosphate
EAA	excitatory amino acid
EPSP	excitatory postsynaptic potential
G protein	GTP-binding protein
HFT	high frequency stimulus train
IBMX	3-isobutyl-1-methylxanthine
ISI	interstimulus interval
ISO	isoproterenol
I/O	input/output
I/V	current/voltage
KRB	Krebs-Ringer buffer
LLP	long-lasting potentiation
LTP	long-term potentiation
NE	norepinephrine
NMDA	N-methyl-D-aspartate
PDA	phorbol 12,13-diacetate
PP	perforant path
PS	population spike
PTx	pertussis toxin
SNK	Student-Newman-Keuls test

Introduction

What are the mechanisms underlying synaptic plasticity in the central nervous system? In 1949, D. O. Hebb proposed his theory of the neurophysiological basis of learning, now known as Hebb's postulate. In this, Hebb proposed that learning is not a result of establishing new connections in the brain, but rather modifying or enhancing existing ones. His postulate can be paraphrased as: if an afferent fiber repeatedly takes part in exciting a postsynaptic cell, then some physiological change will take place to facilitate the firing of that cell by that presynaptic element. If this is true, then synaptic connections within the brain have the innate ability to modify or become modified, to facilitate the flow of impulses from one neuron to the next. One of the first pieces of evidence to support Hebb's postulate came from the work of Bliss and Lømo (1973). In this report the authors described a long-lasting enhancement of the evoked synaptic response in the dentate gyrus/perforant path synapse of the anesthetized rabbit produced by high frequency stimulation of the perforant path. Here was the first demonstration of Hebb's postulate in a mammalian brain structure associated with mnemonic functions. This long-lasting effect was labelled long-term potentiation (LTP), and since that time, LTP has become a widely studied model for synaptic plasticity (Bliss and Gardner-Medwin, 1973; Douglas and Goddard, 1975; Alger and Teyler, 1976) and a candidate for the cellular mechanism underlying learning and memory (Berger, 1984; Matthies et al., 1986; Morris et al., 1986).

Synaptic plasticity in the hippocampus

Since the first demonstration by Bliss and Lømo, the basic properties behind hippocampal LTP have been well studied. LTP is induced by high-frequency stimulation of afferents, and is produced by pairing of presynaptic activity with postsynaptic depolarization (Kelso et al., 1986; Malenka et al., 1989). Neither presynaptic activity (Scharfman and Sarvey, 1985), nor postsynaptic depolarization (Kelso et al., 1986) alone will induce LTP. The initiation of LTP appears to be Ca^{++}-dependent (Lynch et al., 1983), and dependent on the activation of N-methyl-D-aspartate (NMDA) receptors (Collingridge et al., 1983) at most synapses. LTP is measured as a long-lasting increase in synaptic efficacy (Sarvey, 1988), and this long-lasting aspect is referred to as the 'maintenance phase' of LTP. Whereas NMDA receptors are responsible for induction of LTP, maintenance appears to be mediated by changes in non-NMDA receptor function (Davies et al., 1989). The importance of NMDA receptors in the induction of other forms of synaptic plasticity has been investigated by a number of groups (Kleinschmidt et al., 1987; Burgard and Sarvey, 1989; Cline and Constantine-Paton, 1990).

NMDA receptors and synaptic plasticity

The cellular mechanisms responsible for the induction and

maintenance of LTP are now becoming clear. A recent breakthrough was the discovery that antagonists of NMDA receptors could block LTP in field CA1 of the hippocampus (Collingridge et al., 1983; Harris et al., 1984) and the dentate gyrus (Wigstrom et al., 1986; Errington et al., 1987). The NMDA receptor is one of three subclasses of excitatory amino acid (EAA) receptors whose endogenous ligand is either glutamate or aspartate (Olverman et al., 1984; Fagg et al., 1986). The major excitatory neurotransmitter throughout the central nervous appears to be an EAA, and the five subtypes of excitatory amino acid receptors associated with this neurotransmitter are the kainate, AMPA (formerly quisqualate), 4AP, metabotropic quisqualate, and NMDA receptors (Watkins et al., 1990). The kainate, AMPA and NMDA receptors are named after the ligand which binds to its respective high affinity site (Foster and Fagg, 1984; Watkins and Olverman, 1987). The kainate and AMPA receptors can be placed together into one general class of EAA receptor which regulates a fast Na^+/K^+ conductance producing a fast dendritic EPSP. These two act primarily to mediate the fast excitatory effects of glutamate in synaptic transmission. Mayer and Westbrook (1984, 1985, 1987) and Nowak et al. (1984) have described the current/voltage (I/V) relationship produced across the neuronal membrane with activation of the various EAA receptors. Kainate and quisqualate receptors show a linear I/V curve across a range of membrane potentials with a reversal potential of approximately zero mV. This accounts for the mixed Na^+/K^+ conductance. NMDA receptors, on the other hand are an example of a receptor/channel complex that is both ligand-gated and voltage-gated. Activation of NMDA receptors requires a sufficient depolarization of the

plasma membrane to eject a Mg^{++} ion which is normally situated within and blocks the channel (Nowak et al., 1984; Mayer et al., 1984). The I/V curve for NMDA receptor activation is 'J'-shaped with a maximal inward conductance at about -30mV. At membrane potentials more hyperpolarized than this, Mg^{++} is drawn into the channel by electrostatic forces, and at more depolarized potentials the positive charge buildup within the cell repels the Mg^{++} ion to unmask the channel. Again, the NMDA receptor-mediated response displays a reversal potential of approximately zero mV, suggesting a mixed ion conductance. With depolarization, the NMDA receptor channel allows not only Na^{+} and K^{+} fluxes as do the other EAA channels, but also allows Ca^{++} influx (MacDermott et al., 1986). It is this increased Ca^{++} conductance which may play a role in mediating secondary effects within the cell as a consequence of NMDA receptor activation.

NMDA receptors are not thought to be active at the relatively hyperpolarized membrane potential a neuron maintains at rest, but they may play a small role in low-frequency evoked activity. Various groups have demonstrated an NMDA receptor-mediated component of low-frequency synaptic transmission. It is possible to uncover an NMDA receptor-regulated component by omitting Mg^{++} in the extracellular bathing medium, or by depolarization of the neuron (Coan and Collingridge, 1987; Davies et al., 1988). Others have demonstrated a depression of evoked responses under physiological conditions by bath application of various NMDA receptor antagonists in the cortex (Thompson et al., 1985; Artola and Singer, 1987), in field CA1 (Hablitz and Langmoen, 1986; Muller and Lynch, 1988) and in the dentate gyrus

(Abraham and Mason, 1988). Thus, the idea that NMDA receptors do not function in low-frequency synaptic transmission may be incorrect.

The role of NMDA receptors in synaptic plasticity has best been demonstrated by the ability of NMDA receptor antagonists to block LTP. The competitive antagonists D(-)-2-amino-5-phosphonovaleric acid (D(-)APV) and 3-[(±)-2-carboxypiperazin-4-yl]propyl-1-phosphonic acid (CPP) have high selectivity and affinity for NMDA/glutamate binding sites (Davies et al., 1986; Watkins and Olverman, 1987). Collingridge et al., (1983) were the first to demonstrate that APV could block LTP in field CA1 of the hippocampal slice. Others have since demonstrated this effect in both field CA1 (Harris et al., 1984, 1986; Wigstrom et al., 1986) and the dentate gyrus (Errington et al., 1987), but not in the mossy fiber projections to field CA3 (Harris and Cotman, 1986). Interestingly, field CA1, the dentate gyrus and frontal cortex contain the highest concentrations of NMDA receptors in the entire brain (Monaghan and Cotman, 1985), with CA3 containing a correspondingly high concentration of kainate receptors (Cotman and Monaghan, 1987).

The high-frequency synaptic activity necessary for LTP induction appears to produce a sustained depolarization of the postsynaptic membrane that is sufficient to activate NMDA receptors. It is believed that Ca^{++} entry through NMDA channels is responsible for at least a portion of the potentiation, since chelation of Ca^{++} postsynaptically with intracellular EGTA injections alleviates induction of LTP (Lynch et al., 1983) and postsynaptic injections of Ca^{++} potentiate synaptic transmission (Malenka et al., 1988). The question of whether NMDA receptor activation occurs on pre- or postsynaptic membranes has not

been resolved. There is evidence to suggest that NMDA receptor activation also occurs presynaptically to regulate neurotransmitter release (Skrede and Malthe-Sorenssen, 1981; Errington et al., 1987). Recent evidence suggests that induction of LTP is postsynaptic, whereas maintenance may be presynaptic (Bekkers and Stevens, 1990; Malinow and Tsien, 1990). The initiation and maintenance of LTP are probably due to a combination of pre- and postsynaptic activity, as this is indicative of a Hebbian system.

ß-adrenergic involvement in synaptic plasticity

In 1983, Newman and Harley (1983) reported a long-lasting enhancement of the *in vivo* evoked dentate gyrus population spike in response to application of norepinephrine (NE). This long-lasting effect appeared to be very similar to LTP. Subsequent studies (Lacaille and Harley, 1985), most notably by Stanton and Sarvey (1985a, 1985c, 1987), demonstrated that this norepinephrine-induced long-lasting potentiation (NELLP, or LLP) can be produced in the dentate gyrus but not in field CA1 of the hippocampal formation. It is reproducible in the hippocampal slice preparation, involves ß-adrenergic receptor activation, and is associated with a long-lasting rise in tissue levels of cyclic 3',5'-adenosine monophosphate (cAMP) in the dentate gyrus. A similar potentiation of evoked responses can be produced with bath application of the ß-adrenergic agonist isoproterenol, and is called isoproterenol-induced long-lasting potentiation (also called LLP,

Sarvey, 1988). LTP in the dentate gyrus is blocked by pretreatment with ß-adrenergic receptor antagonists or depletion of norepinephrine from the dentate gyrus (Stanton and Sarvey, 1985b), suggesting a role for ß-adrenergic receptor activation in dentate gyrus LTP. Other studies have also demonstrated a facilitatory effect of norepinephrine on LTP induction in the dentate gyrus as well as in field CA3 of the hippocampus (Hopkins and Johnston, 1984, 1988).

A unique property of the dentate gyrus is the presence of two anatomically and functionally discrete subdivisions of the major excitatory input, the perforant path (PP, Hjorth-Simonsen and Jeune, 1972; McNaughton, 1980). The medial and lateral PPs are comprised of axons arising from neurons located in the medial and lateral areas of the entorhinal cortex, respectively. The medial PP projects to the middle, and the lateral PP to the outer molecular layer of the dentate gyrus (Hjorth-Simonsen, 1972; Steward, 1976). These form glutamatergic synapses on granule cell dendrites (White, et al., 1977). Dahl and Sarvey (1989) have reported that the two PPs display different sensitivities to application of β-adrenergic agonists. Within the dentate gyrus, β-adrenergic agonists produce an LLP of medial PP-evoked responses, but a corresponding long-lasting depression of lateral PP-evoked responses. These results emphasize the need for complete isolation of the two pathways, and discrete stimulation of only the medial PP in studies involving LLP in the dentate gyrus.

The physiological relevance of the actions of β-adrenergic agonists becomes clearer with an understanding of the noradrenergic system within the dentate gyrus. ß-Adrenergic receptors are abundant in

the dentate gyrus as well as in field CA1 (Crutcher and Davis, 1980). Noradrenergic innervation from the locus coeruleus via the dorsal noradrenergic bundle enters the dentate gyrus through both the entorhinal cortex and the fimbria. The majority of noradrenergic terminals seems to be situated in the hilar region adjacent to the dentate gyrus granule cell (somatic) layer (Loy et al., 1980; Crutcher and Davis, 1980; Oleskevich and Descarries, 1988), even though ß-adrenergic receptors are located throughout the molecular (dendritic) layer. Because of the presence of noradrenergic receptors, bath application of norepinephrine in the dentate gyrus can produce a long-lasting increase in the initial negative slope of the evoked dendritic EPSP and in the amplitude of the population spike (Stanton and Sarvey, 1987).

The biophysical effects of norepinephrine on individual neurons have been described by a number of investigators, some of which have described a reversible decrease in a Ca^{++}-dependent K^{+} conductance in granule cells (Haas and Rose, 1987; Lacaille and Schwartzkroin, 1988) which is not long-lasting. Gray and Johnston (1987) described an increased activity of voltage dependent Ca^{++} channels in dentate gyrus neurons in response to either isoproterenol or norepinephrine. Interactions between the glutamatergic and noradrenergic systems in slices of the dentate gyrus or hippocampus have shown: 1) an NMDA-stimulated [^{3}H]norepinephrine release which is blocked by NMDA receptor antagonists (Jones et al., 1987), 2) a norepinephrine-mediated increase in [^{14}C]glutamate release (Lynch and Bliss, 1986), and 3) an opioid-sensitive [^{3}H]norepinephrine release stimulated by NMDA (Werling

et al., 1988). Mueller et al. (1981), have discriminated between α- and ß-receptor mediated effects of norepinephrine in field CA1 of the hippocampal slice. They have found a depression caused by α-agonists and a facilitation of evoked responses by ß-agonists. Neither of these appeared to be long-lasting effects.

Muscarinic cholinergic involvement in synaptic plasticity

A large body of evidence has accumulated implicating the cholinergic septo-hippocampal system in mammalian learning and memory. The ability of muscarinic receptor antagonists such as scopolamine to disrupt certain types of learning (Deutsch, 1971; Piercey et al., 1987), along with memory impairments induced by lesions of the septal nuclei provide evidence for a strong cholinergic contribution to learning and memory (see Durkin, 1989).

The septo-hippocampal projections in the rat arise from cholinergic cell bodies located in the basal forebrain, specifically the medial septal nucleus and nucleus of the diagonal band. Axons from these neurons project largely through the fimbria/fornix and supply almost all of the cholinergic input to the hippocampus (Mosko et al., 1973; Chandler and Crutcher, 1983). Cholinergic terminals project to many hippocampal subregions, but in the dentate gyrus, terminals form a fine network around and synapse on granule cell bodies and their proximal dendrites in the molecular layer (Frotscher and Leranth, 1985;

Clark, 1985). Within the dentate gyrus, muscarinic cholinergic receptors are located both in the granule cell layer and in the molecular layer (Mash and Potter, 1986). It appears that the localization of cholinergic terminals roughly coincides with localization of muscarinic receptors in the dentate gyrus.

Muscarinic receptors have been classified into a number of subtypes based historically on their location in certain tissues and their pharmacological responses to muscarinic ligands. Molecular biological techniques have now surpassed traditional pharmacology in the identification of muscarinic receptor subtypes. Five (m1 - m5) muscarinic receptors have been cloned and sequenced (Bonner et al., 1987) and the localization of their mRNAs within the rat brain has been determined (Buckley et al., 1988). A convention has been established whereby cloned muscarinic receptors are designated m1 - m5, and pharmacologically identified endogenous muscarinic receptors are designated M1 - M5. It should be noted that while muscarinic receptor subtypes are referred to as M1 - M5 in this dissertation, some of the data summarized from other laboratories were obtained from analysis of cloned (m1 - m5) muscarinic receptors.

Selective pharmacological probes exist for only three subtypes (M1 - M3) of muscarinic receptors. *In situ* hybridization has revealed that M1 receptor mRNA is very high in the dentate gyrus, with lower levels of M3 and M4 receptor mRNAs. M2 receptor mRNA is virtually absent from the dentate gyrus, which is not surprising since M2 receptors are thought to be located on presynaptic cholinergic nerve terminals (Buckley et al., 1988). Although the M2 receptor is found in

low levels in the dentate gyrus, the mRNA for that receptor may be restricted to the cell soma in the basal forebrain.

Within the central nervous system, the most studied muscarinic receptor is the M1 receptor. It is found in high concentrations in the cortex and the hippocampal formation (Cortes and Palacios, 1986). The high affinity of the M1 receptor for the muscarinic receptor antagonist pirenzepine (see Table 1) makes it the standard receptor by which other receptors have been termed 'non-pirenzepine-sensitive' (Hammer et al., 1980; Doods et al., 1987). Pirenzepine also has a lower affinity binding site which explains its antagonism of other muscarinic receptor subtypes at higher concentrations (Doods et al., 1987; McKinney et al., 1989). M1 receptor activation has been linked to activation of phospholipase C in a pirenzepine sensitive manner which stimulates the formation of inositol trisphosphate and diacylglycerol (Peralta et al., 1988; Audigier et al., 1988). It is generally accepted that formation of these second messengers occurs via coupling of the receptor to a pertussis toxin (PTx)-insensitive GTP-binding (G) protein (Hulme et al., 1990). This second messenger activation eventually leads to a number of intracellular electrophysiological events. M1 receptor activation produces a slow depolarization in granule cells (Muller and Misgeld, 1986), and blocks a K^+-mediated afterhyperpolarization (AHP) in CA1 pyramidal neurons, producing a depolarization (Cole and Nicoll, 1983; Dutar and Nicoll, 1988). These events are blocked by low concentrations of pirenzepine. Electrophysiological effects produced by cloned M1 receptors are mediated by PTx-insensitive G proteins (Jones et al., 1990). These results indicate that M1 receptor activation produces an

Table 1. Summary of muscarinic receptor pharmacology. Table of ranges of pA_2 values for four different muscarinic receptor antagonists. These values were summarized from studies conducted on both cloned (m1 - m3), and pharmacologically identified endogenous muscarinic receptors (M1 - M3). The asterisk denotes the relative selectivity of each antagonist at each receptor subtype. The ability of each receptor subtype to either inhibit cAMP production, or stimulate PI hydrolysis is indicated at the bottom of the table, along with the PTx-sensitivity of this effect.

MUSCARINIC RECEPTOR SUBTYPES

	M1	M2	M3
		(pA_2 values)	
ANTAGONISTS			
atropine	9.4 - 9.7	8.8 - 9.0	8.8 - 9.8
pirenzepine	7.8 - 8.0 *	6.2 - 6.8	6.4 - 6.7
AFDX-116	5.9 - 6.4	6.7 - 7.0 *	5.3 - 6.1
4-DAMP	8.7 - 9.1	7.5 - 7.9	8.5

* denotes relative selectivity

cAMP inhibition	no	yes PTx-sensitive	no
PI hydrolysis	yes PTx-insensitive	no	yes PTx-insensitive

(Adapted from Mei et al., 1989; Hulme et al., 1990)

overall excitatory effect in the central nervous system.

'Non-pirenzepine sensitive' receptors have been less well characterized in the central nervous system. Originally discovered in cardiac tissue, M2 receptors have been predominantly associated with an inhibition of cAMP accumulation (Ashkenazi et al., 1987; Peralta et al., 1988). Selective antagonists for the M2 receptor have only recently become available. While gallamine exerts moderate selectivity as an M2 antagonist, another compound, AFDX-116 is the most selective competitive antagonist for M2 receptors available. It has a high affinity, non-pirenzepine sensitive M2 binding site (see Table 1), but also becomes non-selective at higher concentrations with a low affinity binding site (Micheletti et al., 1987; Giraldo et al., 1987). M2 receptors are present only in low levels in the dentate gyrus (Regenold et al., 1989).

The latest muscarinic receptor subtype able to be studied pharmacologically is the M3 receptor. Cloned m3 receptors also appear to mediate phosphatidylinositol turnover, similar to M1 receptors, and this effect also appears to be PTx-insensitive (Hulme et al., 1990). In addition, electrophysiological effects produced by cloned M3 receptors are mediated by PTx-insensitive G proteins (Jones et al., 1990). The muscarinic receptor antagonist 4-DAMP has only recently been shown to antagonize M3 receptors with high affinity (see Table 1), but also can antagonize M1 receptors with lower affinity (Quirion et al., 1989; Michel et al., 1989). High affinity 4-DAMP binding has been demonstrated in the dentate gyrus (Quirion et al., 1989).

The electrophysiology of 'non-pirenzepine-sensitive' muscarinic

responses has not been well established in terms of M2 vs M3 responses. Egan and North (1986) showed that acetylcholine hyperpolarizes central nervous system neurons via a non-pirenzepine-sensitive mechanism. It has also been suggested that the EPSP in hippocampal pyramidal cells is reduced by M2 receptor activation based on its sensitivity to gallamine (Dutar and Nicoll, 1988). The 4-DAMP-sensitive effects of muscarinic receptor activation in the hippocampus have only begun to be addressed (Pitler and Alger, 1989).

Studies focusing on the role of the cholinergic system in hippocampal synaptic plasticity have met with mixed results. While muscarinic receptor activation has been reported to block the induction of LTP in field CA3 of the hippocampus (Williams and Johnston, 1988), other studies have suggested that muscarinic receptor antagonists will block (Hirotsu et al., 1989), and acetylcholinesterase inhibitors will enhance, LTP induction in field CA1 (Tanaka et al., 1989). What the electrophysiological and biochemical evidence suggests is that M1 receptors may promote facilitation of neuronal responses. This may be accomplished through mechanisms such as blockade of the AHP and stimulation of phosphoinositide breakdown. On the other hand, M2 receptors may inhibit neuronal responses by inhibition of cyclic AMP accumulation. The opposing effects of various muscarinic subtypes may explain why a definitive role for muscarinic receptor modulation of synaptic plasticity has not been determined.

Cyclic AMP in synaptic plasticity

In the time scale of synaptic events, most activity is on the order of milliseconds in duration. A small number of electrophysiological events last a few seconds, but nonetheless these occur often in response to synaptic activity (Scharfman and Sarvey, 1985). However, in a model of synaptic plasticity possibly linked to learning and memory, the time scale must expand to include events lasting minutes or hours. Clearly, this is beyond the capability of classic transmitter/receptor interactions. What is needed is an intracellular mechanism for establishing long-lasting alterations in either the physiology or morphology of the neuron. One mechanism the cell may use to accomplish this is by activating a second messenger system which in turn induces long-lasting changes in cellular activity. One second messenger system of particular interest is the cyclic AMP/cyclic AMP-dependent protein kinase system.

In the cyclic AMP system, activation of, for example, ß-adrenergic receptors stimulates a G_s protein which in turn activates adenylate cyclase (Gilman, 1987). Adenylate cyclase catalyzes the formation of cAMP from intracellular ATP pools. Cyclic AMP then activates cAMP-dependent protein kinase which may in turn phosphorylate a number of substrate proteins. The role of cAMP in modulating neuronal activity has been described most elegantly by Kandel in Aplysia neurons (Kandel and Schwartz, 1982). They have found that either cAMP or the catalytic subunit of cAMP-dependent protein kinase decreases a serotonin-gated hyperpolarizing K^+ conductance, which in turn leads to

depolarization of the cell. Other studies (Madison and Nicoll, 1986) have demonstrated that norepinephrine, by activating cAMP, reduces a Ca^{++} dependent K^+ channel in hippocampal field CA1 pyramidal cells. Since ß-adrenergic receptors are not receptor/ion channel complexes (as are most EAA receptors, for example) this biochemical cascade beginning with adenylate cyclase and ending with the phosphorylation of a K^+ channel could provide a mechanism for the initiation of long-lasting ß-receptor-mediated actions on neurons. In defense of this hypothesis, the action of cAMP on K^+ channels in Aplysia can last up to 24hr (Schacher et al., 1988; Scholz and Byrne, 1988). Autoradiographic analysis has shown adenylate cyclase to be associated with granule cell dendrites (molecular layer) of the dentate gyrus (Worley et al., 1986). In the dentate gyrus, a long-lasting increased cAMP concentration has been correlated with LLP as opposed to the cAMP profile seen during LTP (an initial increase followed by a rapid return to baseline, Stanton and Sarvey, 1985c). Cyclic AMP presumably functions in this system to stimulate the activity of cAMP-dependent protein kinase, which then phosphorylates various cellular substrates. This could be a direct phosphorylation of postsynaptic proteins leading to long-lasting changes. However, this effect could also occur presynaptically to regulate neurotransmitter release. An increased glutamate release could lead to activation of NMDA receptors postsynaptically. Facilitatory ß-adrenergic effects of norepinephrine on glutamate release have been reported by Lynch and Bliss (1986) in the dentate gyrus. Analysis of dentate gyrus cAMP levels in response to ß-adrenergic and muscarinic receptor activation may indicate the intracellular events underlying the

modulation of synaptic plasticity by these systems.

Summary and specific aims

The background information presented here should indicate possible interactions between the glutamatergic, noradrenergic and muscarinic cholinergic systems resulting in long-lasting changes in synaptic activity. The specific aims of this dissertation were threefold:

1. To characterize the NMDA receptor-mediated activity underlying evoked responses, LTP, and LLP in the dentate gyrus,
2. To characterize the effects of muscarinic receptor activation on evoked responses recorded in the dentate gyrus, and
3. To determine the effects of muscarinic receptor activation on both LTP and LLP in the dentate gyrus.

While all three aims were designed to provide answers to specific questions concerning synaptic activity in the dentate gyrus, it was hoped that general principles concerning the similarities and differences between LTP and LLP would be defined in the process.

Materials and Methods

Preparation and maintenance of hippocampal slices

Male Sprague Dawley rats (100-400 grams, Taconic Farms) were sacrificed by decapitation either with or without ketamine anesthesia (50mg/kg i.p.). The rationale behind using ketamine as an anesthetic is detailed below. Following decapitation, the forebrain was separated from the brainstem, removed from the skull, and immediately immersed in a petri dish filled with cold (20°C) buffer. The brain was then bilaterally dissected along the longitudinal fissure and one hippocampus was dissected free of its surrounding tissue. The left hippocampus was routinely selected for use, although no differences in responses between right and left hippocampi have been noted. The hippocampus was then transferred to the stage of a McIlwain tissue chopper and oriented with its longitudinal axis approximately perpendicular to the chopper blade, but positioned so as to visibly orient the alvear fibers parallel to the blade. Slices (375-400μm thick) were prepared usually from the ventral pole of the hippocampus. This pole was selected because here the molecular layer of the dentate gyrus is more amenable to separation of the medial and lateral perforant paths.

From the tissue chopper, the slices were placed on a nylon screen in a modified Andersen type (Schwartzkroin and Wester, 1975) interface recording chamber. The chamber itself consisted of an outer jacket filled with warm (35°C) water through which a gas mixture of 95% O_2, 5%

CO_2 was bubbled. This produced a fine mist which surrounded and moistened the upper surface of the slices. The slices were bathed in a modified Krebs-Ringer buffer (KRB) which percolated under and around the sides of the slices. The perfusion buffer consisted of (in mM): NaCl:125, KCl:3, $NaHCO_3$:26, NaH_2PO_4:1.25, $CaCl_2$:2.4, $MgSO_4$:1.3, glucose:10, and was constantly oxygenated with a gas mixture of 95% O_2, 5% CO_2 which maintained a pH of 7.4. Warm buffer was fed into the chamber through a peristaltic pump and drugs were introduced into the buffer. Viable slices were maintained in this manner for periods of up to ten hours.

The rationale behind using ketamine as an anesthetic is based on reports (Rothman et al., 1987; Rothman and Olney, 1987) that ketamine is a cytoprotective agent that functions as a non-competitive antagonist at NMDA receptors. Although dissection of the hippocampus from the brain was achieved within 3-4 minutes, the hippocampus inevitably was subjected to a certain amount of hypoxia. A detailed examination of the cytoprotective effects of ketamine on hippocampal slice preparation has not been done. However, our slices appeared qualitatively more healthy than those prepared without ketamine. This improvement was measured by three observations: 1) the evoked population spike routinely was superimposed on a large positive wave that is at least in part a granule cell layer representation of the EPSP. This response appeared similar to that recorded *in vivo* and was not always seen in slices from unanesthetized animals, 2) epileptiform activity which is indicative of unhealthy slices was rarely seen in ketamine-anesthetized animals, but was sometimes seen in slices from unanesthetized animals, and 3) the

ability of the slice to support recurrent and feed-forward inhibitory circuits as measured by paired-pulse inhibition was greatly increased in slices from ketamine treated rats. This is especially important, since inhibitory interneurons are very susceptible to glutamate-induced neurotoxicity (Scharfman and Schwartzkroin, 1989). In ketamine-anesthetized rats, paired pulse inhibition was routinely present up to an interpulse interval of 30 msec whereas in untreated slices inhibition was often undetectable. Slices were routinely incubated for 2-3 hours before obtaining responses, which should have allowed for washout of the drug. As a test for this, ketamine has been shown to be effective in blocking LTP (Stringer and Guyenet, 1983), but LTP could be elicited in slices from anesthetized animals as early as 2 hours after decapitation.

Pharmacological manipulations

Bath application of drugs was achieved directly through the perfusion buffer. Although each experiment may have varied, agonists were often bath applied for a period of 10 to 30 minutes. Administration of antagonists often occurred for 10-15 minutes prior to, during, and for 10-15 minutes following application of the agonist. If two agonists were being studied together, they may have been applied simultaneously. Wash-out of drugs usually occurred for 30 minutes, but may have been continued longer if needed. The wash period chosen to meet the criterion of a 'long-lasting' effect was thirty minutes

LIBRARY USE

following either discontinuation of the drug or delivery of a high frequency stimulus train.

All drug applications for electrophysiology were made through the buffer, and all drugs were water soluble. Stock solutions of drugs were often made at high concentrations in distilled water and frozen at 0°C until use. Solutions of norepinephrine and isoproterenol were always prepared immediately before perfusion in order to minimize oxidation of these compounds. In some experiments, the Mg^{++} concentration in the perfusion buffer was increased from 1.3mM to 2.4mM. In these experiments, $[PO_4]$ was omitted from the buffer to prevent precipitation of phosphate salts. A zero $[PO_4]$ buffer had no measurable effect on viability of slices, and LTP could be induced in slices bathed in zero $[PO_4]$ buffer.

Electrophysiology

Stimulation and recording paradigms in the hippocampal slice were as diagrammed in Fig 1. Stimulating electrodes were either bipolar or unipolar, and were made from 100 micrometer diameter Teflon-insulated stainless steel wire. Unipolar electrodes were used for almost all experiments, with the return path provided by a Ag/AgCl wire in the bath. Stimulation consisted of depolarizing rectangular pulses of constant current and variable duration. Low frequency stimulation was elicited at a frequency of 0.2Hz, whereas high frequency stimulation consisted of stimulus trains given at 100Hz for 2sec. Stimulating

Fig 1. Schematic representation of the hippocampal slice. Stimulating electrodes were placed either in the medial perforant path (Perf), or in the hilar region of the dentate gyrus for stimulation of the mossy fibers (mf). Recording electrodes were placed either in the granule cell layer for recording the population spike (PS), or in the mid-molecular layer of the dentate gyrus for recording the EPSP.

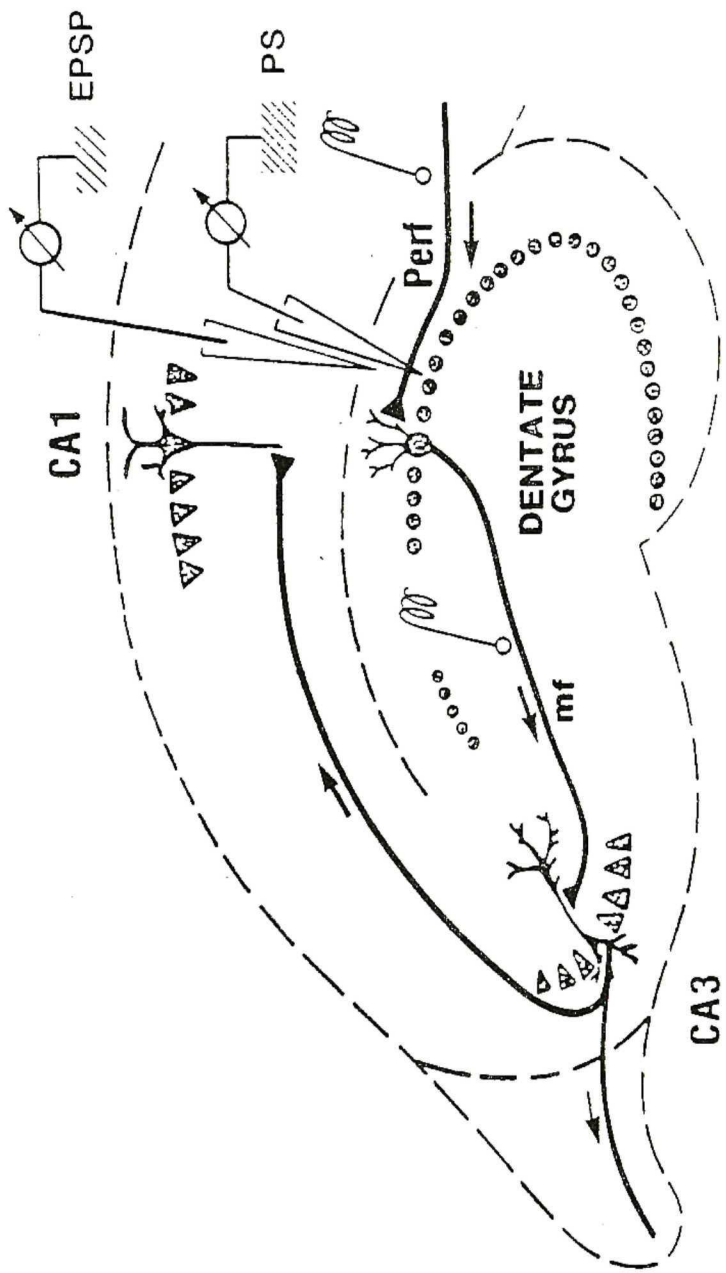
EPSP
PS
Perf
CA1
DENTATE
GYRUS
mf
CA3

electrodes were placed under visual guidance from a dissecting microscope in the middle third of the molecular layer of the dentate gyrus (approximately 150μm from the granule cell layer) for orthodromic stimulation of the medial perforant path. The fine diameter of the stimulating electrode allowed for precise placement in a specific region of the slice. This also allowed stimulus isolation of the medial from the lateral perforant path in the dentate gyrus. Evidence from this laboratory indicates that there are differences in ß-adrenergic sensitivity between the two pathways (Dahl and Sarvey, 1989). For antidromic stimulation, the stimulating electrode was placed in the hilar region, and the axons arising from the dentate granule cells (mossy fibers) were stimulated. The distance between stimulating and recording electrodes was approximately 500μm. Maintaining this distance was important so as not to directly activate inhibitory circuits. Extracellular recording electrodes were made from 1.2mm diameter glass capillary tubes which were drawn out to a fine tip using a Narishige electrode puller. These extracellular electrodes were filled with a 2mM NaCl solution. A Ag/AgCl wire conducted the recorded signal from this electrolyte solution into a preamplifier which amplified the signal and filtered high frequency noise. The signal was simultaneously recorded by the computer and an oscilloscope and the recorded trace was displayed on the screen. Recording electrode tips were manually broken to give a tip resistance of 3-10 MΩ. They were placed in one of two different areas of the slice: 1) the dentate gyrus granule cell layer (to record the population spike, PS), and 2) the dentate medial perforant path (to record the medial dendritic excitatory postsynaptic potential, EPSP).

The recording electrodes were routinely 'stepped' through the molecular layer in 50 micrometer increments starting at the hippocampal fissure, and progressing inward toward the granule cell layer. This allowed a depth profile to be recorded corresponding to current sources and sinks within the dendritic region of the cells. This procedure allowed for electrophysiological separation of the medial from the lateral perforant path (Dahl et al. 1990, see Fig 3).

Slices were preincubated for at least two hours prior to introduction of electrodes. Once a response was obtained, a complete input/output (I/O, i.e. stimulus duration/response) curve was constructed for that response. In other words, a constant current stimulus (0.1 - 0.5mA) delivered at a low frequency (0.2Hz) and of variable durations (10 - 400μsec) was delivered through the stimulating electrode and the response was recorded at 3 - 5 selected durations. I/O curves were usually recorded at intervals of 10 - 15 min, but for some time course experiments, data were sampled every 2 min throughout the experiment. Before beginning the experiment, and once responses had stabilized, a series of at least three baseline responses were recorded over a thirty minute period. A mean and standard deviation of the baseline responses was computed and used in subsequent analyses. Analysis of either the slope or amplitude of traces was restricted to responses that were 20 - 70% of the maximum for that particular response. This region falls on the linear portion of the I/O curve, the region of greatest flexibility of responses. When EPSPs were analyzed, the stimulus strength chosen was always subthreshold for evoking a population spike.

Before recording any responses, the intrinsic inhibition of the slice was measured to ensure that the slice was healthy (as inhibition was lost, the slices exhibited epileptiform activity). Paired-pulse stimulation was delivered to the slice at interstimulus intervals (ISIs) from 20 - 30 msec as a measure of intrinsic inhibition. A response was used only if it exhibited paired-pulse inhibition in this ISI range. A more detailed explanation of paired-pulse inhibition can be found in Burgard and Sarvey (in press).

For LTP experiments, a high frequency stimulus train (HFT) was delivered to the perforant path at 100Hz for 2 seconds. A stimulus intensity which would normally evoke a population spike (at 0.2 Hz) that was 30 - 50% of maximum amplitude and an EPSP of approximately 75% of maximum initial negative slope was chosen for the HFT to induce LTP. This stimulus intensity was termed 'suprathreshold' and the intensity was selected in order to keep the stimulus train from evoking epileptiform afterdischarges and to minimize current spread, yet still reliably induce LTP. An HFT delivered at a stimulus intensity which was just subthreshold for evoking a population spike, but still evoked an EPSP of approximately 50% of maximum slope, rarely induced LTP; this low intensity HFT was termed 'subthreshold.' This stimulus intensity allowed us to examine the facilitatory effects of compounds on the induction of LTP.

Cyclic AMP assay

For studies involving biochemical analysis of cAMP concentrations, hippocampal slices were transferred from the tissue chopper directly into a petri dish filled with ice-cold oxygenated buffer. Any pieces of entorhinal cortex that may have been attached to the slice were removed. The dentate gyrus from each slice was then microdissected from the hippocampus proper. One razor cut was made along the hippocampal fissure, and the other made perpendicular to the mossy fiber projections between fields CA3 and CA4. Only the dentate gyrus slice was used for the cAMP assay. Only one dentate slice was assayed per tube.

The dentate gyrus was then transferred to a 6x50mm borosilicate glass test tube containing ice-cold buffer on ice. This was accomplished by drawing the slice plus 200μl of buffer into a pipettor tip that was cut large enough for the slice to enter. Once all the assay tubes contained a slice (approximately 10 min), all but approximately 20μl of the supernatant was aspirated from around each slice. The original buffer was aspirated in an attempt to minimize background cAMP accumulation. A 150μl aliqout of fresh ice-cold buffer was then added to the tubes. This buffer also contained the final concentrations of any drugs that were used for treatment. For most cAMP experiments, the fresh buffer contained 1mM 3-isobutyl-1-methylxanthine (IBMX) to minimize phosphodiesterase activity. At this time, 100μl of buffer was added to separate tubes to be used for construction of a [cAMP] standard curve. The tubes were individually oxygenated for

approximately 2 seconds with a gas mixture of 95% O_2, 5% CO_2. The tubes were then removed from ice, and the reaction started by incubation at 35°C for 10 min. Standard curve tubes were handled in the same manner as treatment tubes. While incubating, the tubes were oxygenated once with 95% O_2, 5% CO_2. The reaction was terminated by boiling all tubes for 2 min, and placing the tubes back on ice. All standard curves and treatments were performed in triplicate.

For determination of cAMP levels, a modification of the protein binding assay of Brown et al. (1971) was used (Frey and Gosse, 1989). 110μl of the supernatant from the sample tubes was removed from each tube and placed in separate tubes. 2.5 pmol [^{3}H]cAMP, diluted in 100μl of 0.02M citrate-phosphate buffer, was added to all tubes. The pH of the citrate-phosphate buffer was 5.0, and this neutralized the modified KRB (which becomes alkaline as CO_2 is lost) to a pH of approximately 6.0. The standard curve was then constructed by adding increasing concentrations (0,1,2,5,10,20 pmol) of unlabelled cAMP to these tubes (at least three tubes per concentration). 20μl of cAMP binding protein (cAMP-dependent protein kinase, concentrated from bovine adrenal glands) was added to all tubes, the tubes were vortexed and left on ice for at least 1.5 hrs. This allowed the competitive binding of labelled and unlabelled cAMP to reach an equilibrium. The reaction was terminated by addition of an activated charcoal solution (Norit SG Extra, BSA, antifoam A), the tubes were vortexed, and centrifuged at 1500 x g for 10 min, at 0°C. Following centrifugation, 200μl of the supernatant was removed and placed in scintillation counting vials. The remaining pellet was discarded. 3ml of scintillation cocktail was added to the

vials, and they were subjected to liquid scintillation spectroscopy. The more cAMP produced by the tissue, the less bound counts should have accumulated in the supernatant due to competition of cAMP with [^{3}H]cAMP for binding sites on the cAMP-dependent protein kinase.

Pertussis toxin injections

Male Sprague-Dawley rats (120-160 grams) were anesthetized with halothane and placed in a stereotaxic apparatus (David Kopf). Bilateral intrahippocampal injections of pertussis toxin (PTx, 1μg in 2μl sterile saline) were made over a 5 min period using a 10μl Hamilton syringe at the following coordinates (from Bregma): caudal, 0.5 cm; lateral, $\pm$ 0.3 cm; ventral, 0.35 cm; incisor bar, -2.5 mm. These coordinates placed the tip of the needle at the level of the hippocampal fissure just above the dentate gyrus, as confirmed by injections of fast green. The animals were allowed to recover for 3-4 days, then were sacrificed. The injection site was visible on all animals, and slices were prepared from within 1.6 mm dorsal or ventral to the injection site. The slices used for experiments were usually within 800μm of the injection site, and had no visible damage from the injection. A slice was used only if it exhibited healthy responses (a single population spike with paired-pulse inhibition at a minimum ISI of 20 msec).

Materials

The following drugs or compounds of interest were used in these experiments: (-)norepinephrine HCl, (-)norepinephrine bitartrate, (-) isoproterenol HCl, D,L muscarine Cl, atropine sulfate, phorbol 12,13 diacetate, 3-isobutyl-1-methylxanthine (IBMX) (Sigma); D(-) and L(+) 2-amino-5-phosphonovaleric acid (APV), (Cambridge Research Biochemicals); 3-[(±)-2-carboxypiperazin-4-yl]propyl-1-phosphonic acid (CPP), (Tocris Neuramin); pertussis toxin (List); pirenzepine dihydrochloride, 11-2[[2-[(diethylamino)methyl]-1-piperidinyl]acetyl]-5,11-dihydro-6H-pyrido[2, 3-b][1,4]benzodiazepin-6-one (AFDX-116), (Boehringer Ingelheim); 4-diphenylacetoxy-N-methyl-piperidine methiodide (4-DAMP), (Research Biochemicals Inc); [^{3}H]cAMP (32.3 Ci/mmol), (New England Nuclear).

Data Analysis

Responses (voltage traces) were acquired directly from the recording oscilloscope, digitized, and stored on disk in a PDP 11/73 (Andromeda; DEC) computer. Data analysis was performed on a MINC-11 computer (Digital Equipment Corp.). The analysis program was constructed to measure: 1) The amplitude of the population spike, measured as the mean amplitude between the initial positive peak and the second positive peak, both measured in reference to the maximal

negativity of the population spike, 2) The latency of the population spike, measured as the time difference between the stimulus artifact and the negative peak of the population spike, 3) The maximal initial negative slope of the EPSP, measured as the maximal voltage deflection per unit time (dV/dt) of the initial negative wave of the EPSP, 4) the EPSP latency, measured as the time difference between the stimulus artifact and the region of maximal initial EPSP slope, 5) the peak amplitude of the EPSP, measured as the point of maximal EPSP negativity, and 6) the total area under the EPSP, measured as the area under the curve between the points of initial excursion from, and return to, baseline. If traces were required for figures, the digitized trace was reconstructed on a plotter (Hewlett Packard) for a hard copy of the trace. To meet the criterion of 'potentiation' of evoked responses, the magnitude of the response measured at thirty minutes of wash must have exceeded the mean baseline response by more than two standard deviations of the mean baseline response.

Data from the cAMP experiments was analyzed as follows: raw counts of ^{3}H were converted to pmol cAMP from the standard curve for each experiment using a programmable Hewlett-Packard calculator. The program automatically subtracted mean background counts from each concentration. The mean pmol cAMP for each treatment group was calculated from the triplicate samples.

Statistical analysis consisted of Student's t-test, paired t-test, and ANOVA plus either Student-Newman-Keuls (SNK) or Duncan's test for multiple comparisons. Data are expressed as mean $\pm$ SEM.

Results

I. Evoked responses recorded in the dentate gyrus

Orthodromic and antidromic responses

Low frequency orthodromic stimulation (0.2Hz) of the medial perforant path produced evoked responses measured extracellularly in the dentate gyrus. A recording electrode situated in the mid-molecular layer of the granule cell dendrites corresponding to the terminal synapses of the medial perforant path recorded the medial dendritic EPSP. As depicted in Fig 2A, the EPSP was recorded as a graded negative voltage deflection. Analysis of the initial negative slope of the EPSP gave an indication of the synaptic efficacy of perforant path stimulation. The peak amplitude of the EPSP represented the maximal activation of dendritic synapses, and its analysis gave an indication of the possible contribution of voltage-dependent processes involved in synaptic transmission here.

A recording electrode placed in the granule cell layer recorded a graded positive voltage deflection that was mainly the somatic representation of the synaptic EPSP. When the stimulus intensity was sufficient to evoke action potentials in the granule cells, a negative voltage deflection was superimposed on this positive wave. This was the extracellular representation of summed action potential firing and was

termed the population spike (Fig 2A). The latency to peak of the population spike varied according to the distance between stimulating and recording electrodes, but was usually between 3 and 5 msec after the stimulus. The latency to peak was due to synaptic transmission.

Stimulation of the mossy fibers from a stimulating electrode placed in the hilus produced an antidromic spike recorded in the granule cell layer (Fig 2B). Because of its nonsynaptic nature, the latency to peak of the antidromic spike was usually less than 2 msec. Analysis of changes in the amplitude of the antidromic spike gave an indication of nonspecific (nonsynaptic) changes in the excitability of granule cells.

Medial vs lateral perforant path isolation

Stimulus isolation of the medial from the lateral perforant path was achieved before any data were recorded. A stimulating electrode was placed in the mid-molecular layer, and the dendritic recording electrode was placed in the outer molecular layer, approximately 250μm from the granule cell layer (see Fig 3). At low stimulus intensities (to eliminate stimulus current spread), this electrode recorded a positive voltage deflection corresponding to a current source in the outer molecular layer. The electrode was then stepped into the mid-molecular layer (approximately 150μm from the granule cell layer), where the current sink is greatest corresponding to activation of the medial perforant path. A maximum voltage negativity was then obtained in this region. This was recorded as the medial perforant path-evoked EPSP.

Fig 2. Orthodromic and antidromic responses recorded in the dentate gyrus. A. Orthodromic stimulation of the medial perforant path (Perf) produced a population spike (PS) recorded in the granule cell layer, and an EPSP recorded in the mid-molecular layer. The PS is represented as the negative deflection superimposed on top of the large positive voltage deflection (arrow). The EPSP is recorded as a negative voltage deflection. These responses were elicited by a stimulus intensity that was suprathreshold for evoking a population spike. B. Antidromic stimulation of the mossy fibers elicited an antidromic spike recorded in the granule cell layer. Because it is a nonsynaptic response, it exhibits a characteristic short latency-to-peak. In both A and B, the asterisk denotes the stimulus artifact, and the calibration bar is 5mV, 2msec.

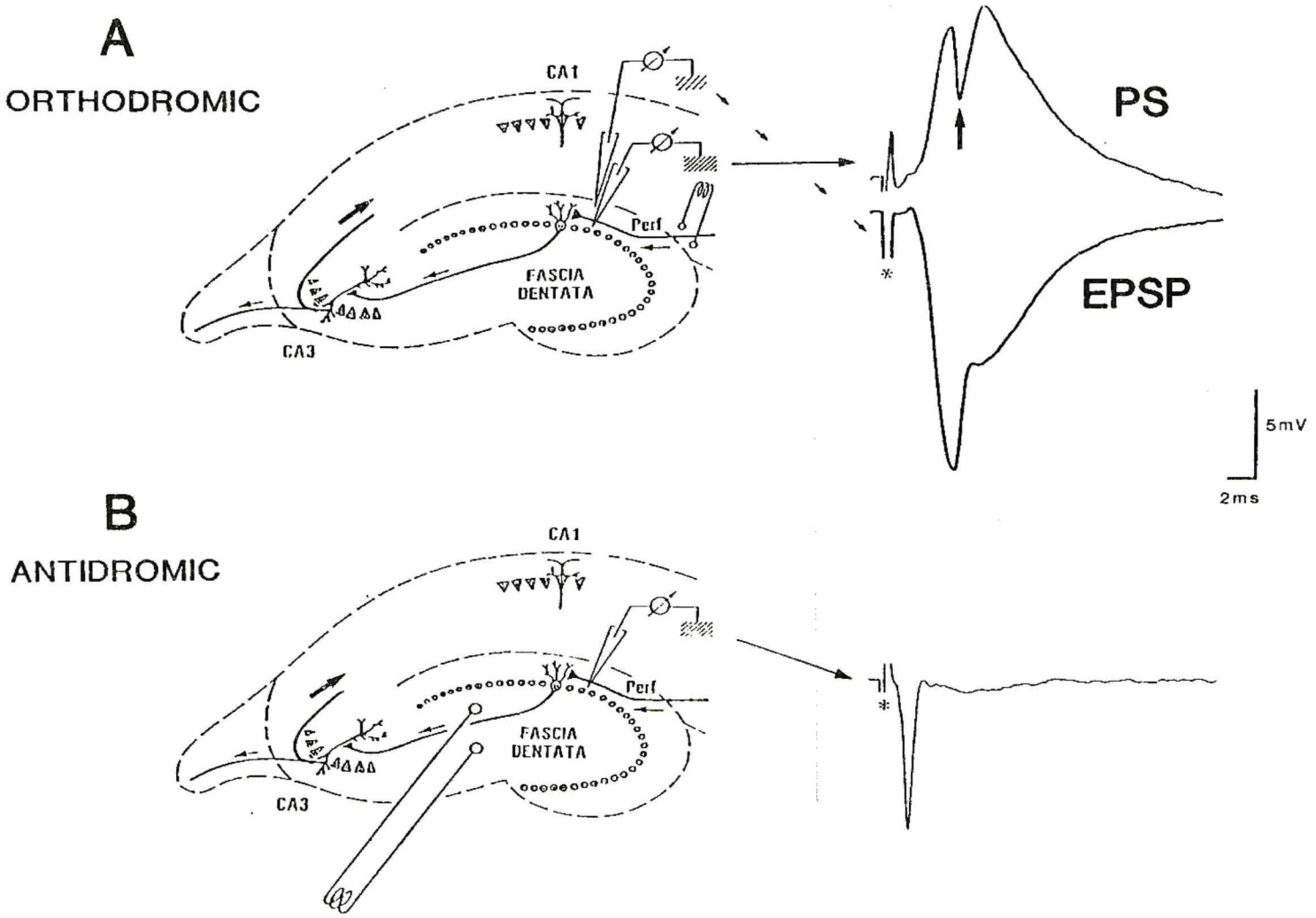
A
ORTHODROMIC
CA1
Perf
FASCIA DENTATA
CA3
PS
EPSP
5mV
2ms
B
ANTIDROMIC
CA1
Perf
FASCIA DENTATA
CA3

Fig 3. Medial vs lateral perforant path isolation. A. Scheme of a hippocampal slice. B. Detail of the dentate gyrus, showing a granule cell and medial and lateral perforant paths (PP) in the molecular layer. The distance between the hippocampal fissure and granule cell layer is approximately 300μm. A stimulating electrode was positioned in the mid-molecular layer to activate the medial PP. Recording electrodes were stepped through the outer- (R1), mid-molecular (R2), and the granule cell layers (R3) to record EPSPs (R1 and R2) or the population spike (R3) in response to medial PP stimulation. C. Responses recorded in three locations in the dentate gyrus. Discrete stimulation (subthreshold for evoking a population spike) of the medial PP evokes a typical negative EPSP in the mid-molecular layer (R2), with a positive deflection recorded in the outer-molecular layer (R1). A higher stimulus intensity evokes a population spike recorded in the granule cell layer (R3). Asterisk denotes stimulus artifact. (Adapted from Dahl et al., 1990)

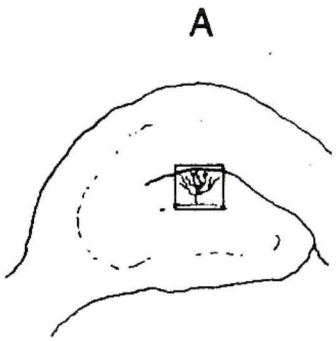
A

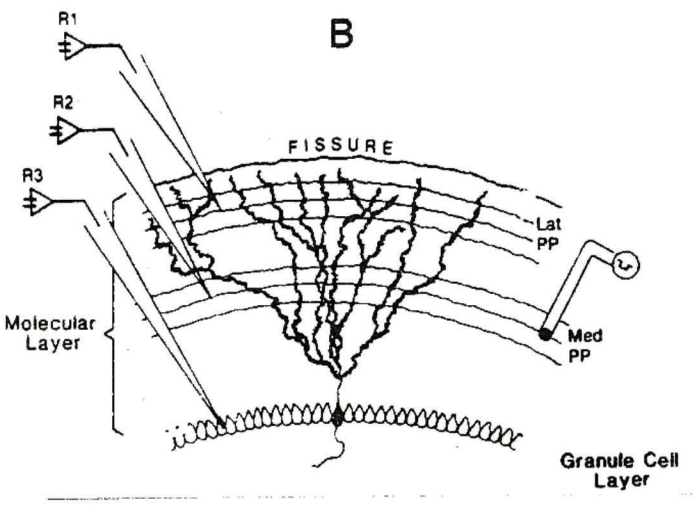
B
R1
R2
R3
FISSURE
Lat
PP
Med
PP
Molecular
Layer
Granule Cell
Layer

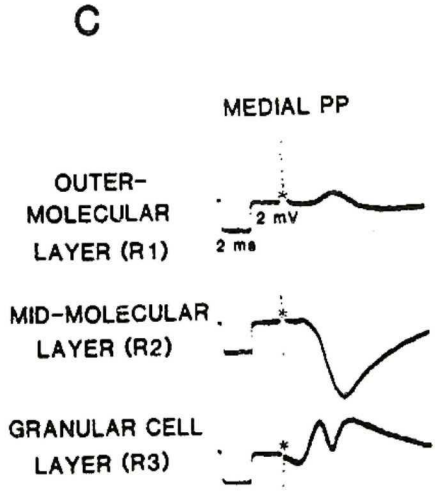
C
MEDIAL PP
OUTER-
MOLECULAR
LAYER (R1)
2 mV
2 ms
MID-MOLECULAR
LAYER (R2)
GRANULAR CELL
LAYER (R3)

Stimulus intensities used for analysis of EPSPs were always subthreshold for evoking a population spike.

II. Characterization of LTP and LLP in the dentate gyrus

Induction of LTP and LLP

A high frequency stimulus train (100Hz for 2 sec) was delivered to the axons of the medial perforant path in the hippocampal slice to induce LTP of the evoked orthodromic population spike (PS) or the dendritic excitatory postsynaptic potential (EPSP). In these experiments examining the similarities between LTP and LLP, LTP was produced in responses in 18 of 20 slices (see Fig 4B for example). The stimulus intensity used for induction of LTP was sufficient to evoke a population spike of approximately 30 - 50% maximum amplitude. This stimulus intensity produced reliable and reproducible LTP which was maintained for at least 30 min. A time course of the population spike amplitude is shown in Fig 4A (responses in 5 of 5 slices potentiated to 253 $\pm$ 27% of baseline, measured at the end of a 30 min wash). As demonstrated in this figure, LTP induction was rapid in onset and was maintained without decrement for at least 30 min. The initial negative slope of the EPSP paralled the time course of the population spike, although to a lesser extent (not shown). The potentiated slope of the EPSP was 149 $\pm$ 6.4% of baseline measured at 30 min following application

Fig 4. LTP and ß-adrenergic-induced LLP. A. Time course of LTP of the population spike. Each data point represents the mean % ± SEM of 5 responses recorded in 5 slices. LTP was induced by the application of a high frequency stimulus train (HFT) delivered at the arrow. Asterisks denote significant difference vs mean baseline values ($P<0.05$, ANOVA plus SNK). B. Representative population spikes and EPSPs recorded before (baseline) and 30 min after the application of an HFT. The stimulus intensity used to evoke the population spike was greater than that used for the EPSP, and asterisk denotes stimulus artifact. C. Time course of LLP of the population spike. Each data point represents the mean % ± SEM of 5 responses. LLP was induced by a 20 min bath application of 1μM isoproterenol (ISO). Asterisks denote significant difference vs mean baseline values ($P<0.05$, ANOVA plus SNK). D. Representative population spikes and EPSPs recorded before (baseline) and after 30 min of wash-out of isoproterenol. The stimulus intensity used to evoke the population spike was greater than that used for the EPSP, and asterisk denotes stimulus artifact. Calibration bar for both B and D is 5mV, 5msec.

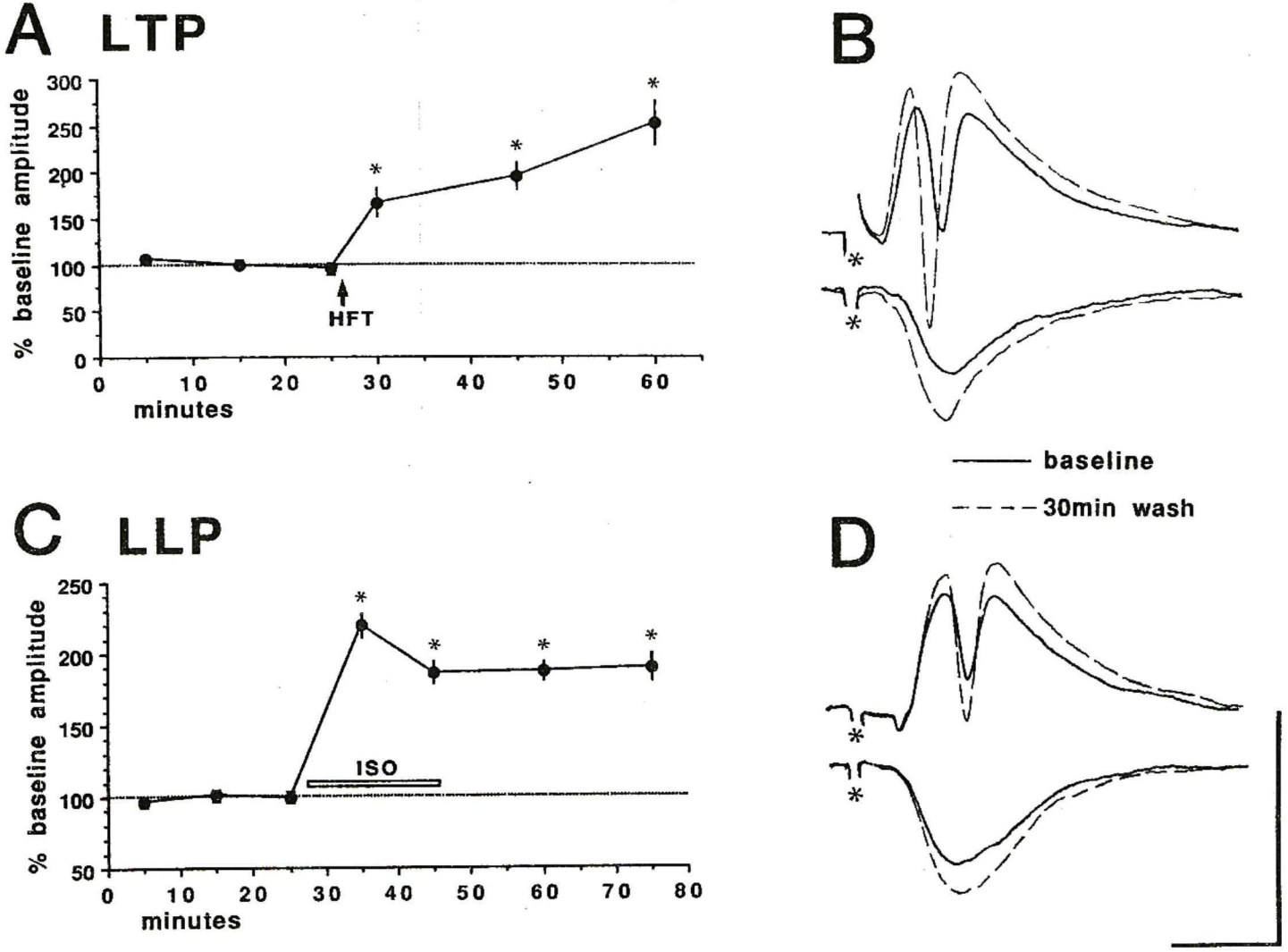
A LTP
% baseline amplitude
300
250
200
150
100
50
0
HFT
0
10
20
30
40
50
60
minutes
B
baseline
30min wash
C LLP
% baseline amplitude
250
200
150
100
50
ISO
0
10
20
30
40
50
60
70
80
minutes
D

of an HFT (responses in 5 of 5 slices potentiated).

For induction of LLP, the adrenergic receptor agonists isoproterenol (ISO) or norepinephrine (NE) were bath applied to hippocampal slices. In most studies, the non-specific ß-adrenergic receptor agonist isoproterenol was used to induce LLP, as LLP is a ß-receptor-mediated phenomenon (Stanton and Sarvey, 1985a). Norepinephrine was not as reliable in inducing LLP, probably because it is a mixed α/ß receptor agonist. It has been demonstrated that norepinephrine has mixed α-inhibitory and ß-excitatory activity in LLP induction (Dahl and Sarvey, 1989). 1μM isoproterenol, bath applied for 20 min produced an LLP of both the population spike and the EPSP (see Fig 4D, for example). A time course of the population spike amplitude is shown in Fig 4C (responses in 5 of 5 slices potentiated to 199 $\pm$ 15% of baseline measured at the end of a 30 min wash). As demonstrated in this figure, the induction of LLP, similar to LTP, was rapid in onset and was maintained without decrement for at least 30 min. Isoproterenol also produced an LLP of the EPSP that followed a time course similar to the population spike (not shown). The potentiated slope of the EPSP was 143 $\pm$ 19% of baseline measured at the end of a 30 min wash period (responses in 4 of 5 slices potentiated). In other studies, a concentration of 50μM norepinephrine applied for 30 minutes reliably induced LLP of the population spike amplitude (151 $\pm$ 7.9%, Fig 5). Norepinephrine-induced LLP was produced in 19 of 27 recorded population spikes. This LLP lasted without decrement throughout a 30 minute wash following norepinephrine application. In separate experiments, bath application of norepinephrine also produced an LLP of the medial

perforant path evoked EPSP (124 ± 5.0% of baseline, responses in 7 of 14 slices potentiated).

Thresholds for induction of LTP and LLP

The stimulus intensity used for reliable induction of LTP is outlined above. The threshold intensity for induction of LTP was defined as the minimum stimulus intensity required for LTP induction, as a function of population spike amplitude. High frequency stimulation at an intensity insufficient to produce a population spike would not induce LTP. This stimulus intensity was then 'subthreshold' for both evoking a population spike and inducing LTP. However, this intensity was still sufficient to produce an EPSP of approximately 50% maximum slope. The high frequency stimulus criteria of 1) approximately 50% maximum EPSP slope and 2) subthreshold for evoking a population spike gave a measure of subthreshold stimulation for LTP induction. By using the concept of a threshold for LTP induction, the facilitation of LTP induction was studied.

In experiments designed to study differences between supra- and subthreshold stimulation, a set of ten slices was used. A suprathreshold HFT reliably induced LTP of both the population spike (responses in 5 of 5 slices potentiated, 253 ± 27% of baseline amplitude) and the EPSP (responses in 5 of 5 slices potentiated, 149 ± 6.4% of baseline slope) as detailed above. The potentiation of both population spike and EPSP was measured 30 minutes after the HFT. In

contrast, a subthreshold HFT seldom induced LTP of either the population spike (responses in 1 of 5 slices potentiated, 99 ± 14% of baseline) or the EPSP (responses in 1 of 5 slices potentiated, 98 ± 4.4%).

Isoproterenol was bath applied at various concentrations for 20 minutes to determine its ability to induce LLP. 1μM isoproterenol produced a reliable potentiation of evoked responses, recorded after 30 minutes of drug-free wash (responses in 5 of 5 slices potentiated to 199 ± 15% of baseline, Fig 4C). However, a concentration of 0.1μM isoproterenol did not produce an LLP of the population spike (99 ± 6.3% of baseline measured at the end of a 30 min wash, see Fig 4 of Burgard and Sarvey, in press), indicating a steep concentration-response curve with an EC50 between 0.1 and 1μM isoproterenol. Determination of a concentration of isoproterenol which was subthreshold for LLP induction provided a basis for studies investigating the facilitation of LLP induction by other neurotransmitter systems (i.e. muscarinic cholinergic).

III. The role of NMDA receptors in synaptic plasticity and evoked synaptic activity in the dentate gyrus

NMDA receptors in LTP and LLP

As outlined in the Introduction, it has been well established

that LTP of perforant path/granule cell synapses is dependent on activation of NMDA receptors. The following experiments were designed to determine if NMDA receptor antagonists would 1) block the induction of LTP of the medial perforant path synapses, and 2) block the induction of LLP in these synapses. Two competitive NMDA receptor antagonists were used in this study: D(-)APV and CPP. To minimize nonspecific effects, concentrations of NMDA receptor antagonists used in these studies were relatively close to the K_i for inhibition of [^{3}H]D(-)APV binding in rat brain membranes (0.48μM for CPP and 0.62μM for D(-)APV) (Davies et al., 1986) but high enough to assure sufficient receptor blockade.

For LTP experiments, D(-)APV was bath applied 10 - 15 min prior to delivery of a high frequency stimulus train to the medial perforant path. This exposure period allowed the antagonist to sufficiently diffuse into the tissue. As can be seen in Fig 5, 10μM D(-)APV blocked LTP of the population spike ($P<0.05$, ANOVA plus Duncan's test, responses in 1 of 8 slices potentiated). 1μM D(-)APV did not block LTP ($P>0.05$, ANOVA, responses in 7 of 10 slices potentiated). Blockade of LTP by these compounds confirms other reports that LTP in perforant path synapses is an NMDA receptor-dependent phenomenon, and extends those findings specifically to the medial perforant path.

For LLP experiments, D(-)APV and CPP were bath applied for 15 min prior to, during and after application of 50μM norepinephrine. The effective concentrations of antagonists used were chosen according to their efficacy in blocking LTP. Only one antagonist was applied per slice. As can be seen in Fig 5, 10μM D(-)APV blocked the induction of LLP ($P<0.05$, ANOVA plus Duncan's test, responses in 4 of 14 slices

Fig 5. NMDA receptor antagonists block both LTP and LLP. Open bars show potentiation of population spike amplitude produced by a high frequency stimulus train (HFT) or 50μM norepinephrine (NE). Black bars show the effects of a 1μM concentration of either D(-)APV or CPP on the potentiation produced by HFT or NE. Hatched bars show the effects of 10μM D(-)APV or CPP on potentiation. Each bar is the mean % baseline amplitude $\pm$ SEM of the population spike taken at the end of the final wash period. The number of experiments in each group appears within the bar. Asterisk denotes a significant difference ($P<0.05$, ANOVA plus Duncan's test) in the mean compared to control potentiation. (From Burgard et al., 1989)

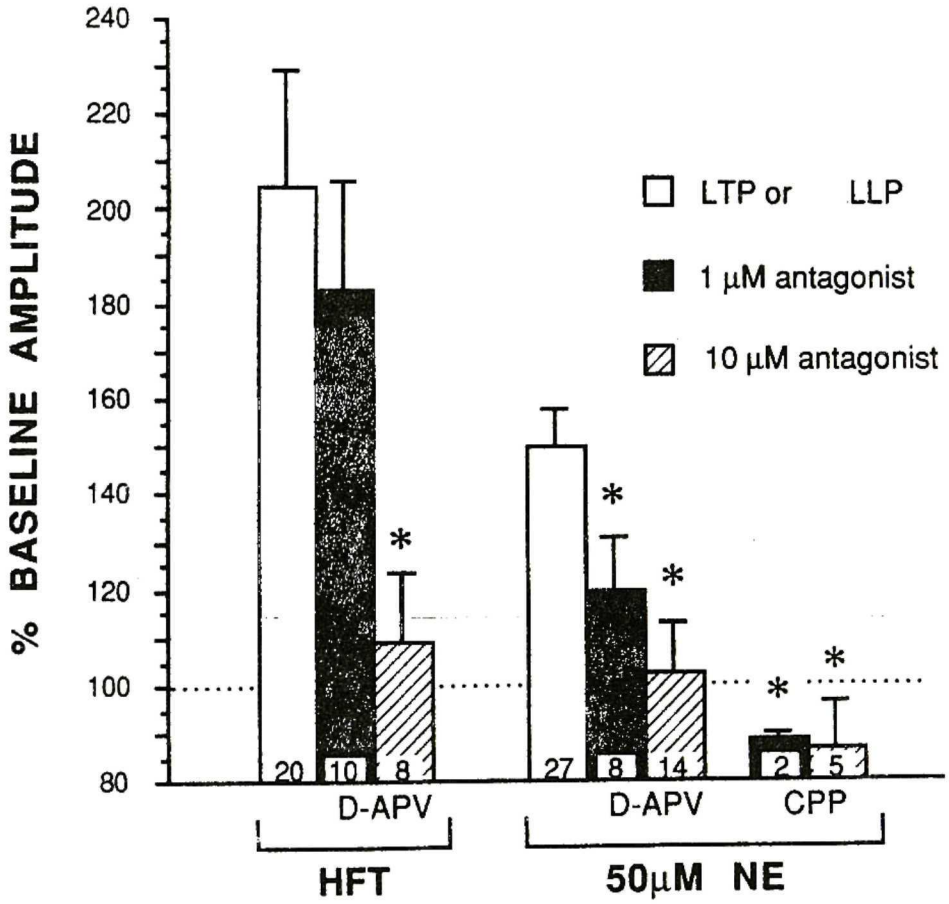
% BASELINE AMPLITUDE
240
220
200
180
160
140
120
100
80
LTP or LLP
1 μM antagonist
10 μM antagonist
20
10
8
27
8
14
2
5
*
D-APV
D-APV
CPP
HFT
50μM NE

potentiated), and 1μM D(-)APV significantly decreased LLP ($P<0.05$, ANOVA, responses in 3 of 8 slices potentiated) of the population spike. In separate experiments (data not shown), 10μM D(-)APV blocked LLP of the EPSP (96 $\pm$ 6%, n=6, responses in 0 of 6 slices potentiated) compared to LLP in the absence of D(-)APV (124 $\pm$ 5% of baseline, $P<0.05$, Student's t-test, responses in 7 of 14 slices potentiated). Fig 5 also shows that CPP, at concentrations of both 1 and 10μM, blocked LLP of the population spike (no responses potentiated in either group). CPP was washed out with drug-free solution for 60 min because CPP produced a reversible depression of the population spike that required a sixty minute wash period to return to baseline.

These results suggest that activation of NMDA receptors is required for induction of both LTP and LLP in medial perforant path synapses. However, is NMDA receptor activation required for maintenance of LLP? To address this question, D(-)APV (10μM) was bath applied after induction of LLP (Fig 6). LLP was induced by a 20 min application of 1μM isoproterenol. Following a 20 min wash period, D(-)APV (10μM for 10 min) depressed the population spike to approximately 65% of baseline amplitude, but this depression was reversed with a subsequent 10 min wash. As demonstrated in this figure, LLP of the population spike in this experiment was not reversed by posttreatment with D(-)APV. In addition, the % depression of the population spike produced by D(-)APV was not changed after LLP induction (see below for depression of evoked responses produced by NMDA receptor antagonists). Similar results were obtained in another experiment. The results from these experiment indicate that 1) LLP, once established, cannot be reversed by blockade

Fig. 6 APV posttreatment does not block LLP. A time course of the amplitude of the population spike, plus representative responses, taken from one experiment. Below, the amplitude of the population spike was plotted against time in minutes. 'Base' represents the mean ± SEM of three consecutive baseline time points, recorded 10 min apart. A 20 min bath application of 1 μM isoproterenol (ISO) produced an acute potentiation and LLP of the population spike that lasted without decrement throughout a 20 min wash. After 20 min of wash, 10μM D(-)APV was bath applied for 10 min, and this was followed by a 10 min wash period. Population spikes are shown above, and were recorded at the time points indicated. APV depressed the population spike, but did not reverse LLP. Asterisks on the traces represent stimulus artifacts, and the calibration bar is 5mV, 2msec.

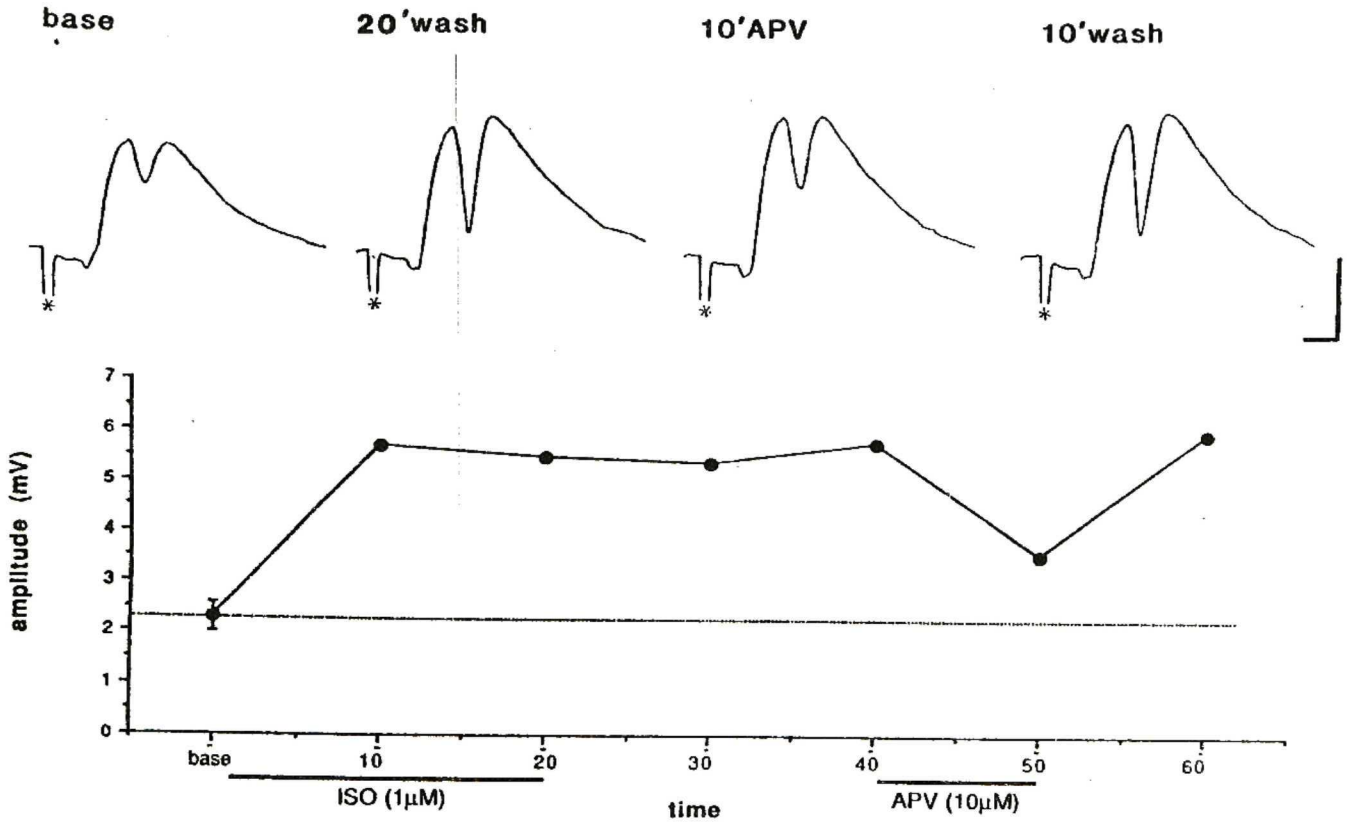
base
20'wash
10'APV
10'wash
amplitude (mV)
0
1
2
3
4
5
6
7
base
10
20
30
40
50
60
ISO (1μM)
time
APV (10μM)

of NMDA receptors, and 2) the contribution of NMDA receptors to low frequency evoked synaptic activity is not changed following LLP.

Another type of long-lasting potentiation of evoked responses can be induced in the dentate gyrus by the bath application of phorbol esters. These relatively lipophilic compounds activate intracellular protein kinase C, a Ca^{++}-dependent enzyme which is thought to play a role in the initiation and/or maintenance of LTP (Linden and Routtenberg, 1989). As a test for the selectivity of D(-)APV in blocking various forms of long-lasting synaptic plasticity, its ability to also block phorbol ester-induced long-lasting potentiation was studied. The relatively water soluble phorbol ester, phorbol 12,13-diacetate (PDA) was dissolved in either distilled water or DMSO (DMSO to a final concentration no greater than 7mM). As shown in Fig 7, a 15 min application of PDA dissolved in distilled water produced a potentiation of the population spike which declined over time, yet was still technically 'potentiated' following a 30 min wash (189 $\pm$ 29% of baseline, n=6). When 10μM D(-)APV was added 15 min prior to and during PDA exposure, the long-lasting potentiation was reduced (121 $\pm$ 8.0% of baseline, n=2), but a transient increase in the population spike was still seen in the presence of PDA (174 $\pm$ 36%, n=4). Similar results were obtained if the PDA was dissolved in DMSO. D(-)APV blocked the potentiation produced by PDA in DMSO measured at the end of a 30 min wash (93 $\pm$ 7.6%, n=6, compared to 237 $\pm$ 72%, n=4 in the absence of D(-)APV). In DMSO, PDA also produced an acute potentiation in the presence of D(-)APV (234 $\pm$ 58% of baseline, n=6). These results suggest that phorbol ester-induced potentiation is another form of NMDA receptor-

Fig 7. APV blocks phorbol ester-induced potentiation. A. Time course of the effects of phorbol 12,13 diacetate (PDA) on the amplitude of the population spike. PDA was dissolved in either distilled water (solid line) or DMSO (broken line), and was bath applied for 15 min shown by the bar. PDA produced an immediate potentiation which declined during the wash period. Each data point is the mean % baseline amplitude ± SEM of either 6 (H_2O) or 4 (DMSO) responses. 'Base' represents the mean ± SEM of three consecutive baseline time points, recorded 10 min apart. B. A time course similar to that displayed in 7A, except that D(-)APV was applied for 15 min prior to, during, and for 5 min after a 15 min application of PDA. Each data point is the mean % baseline amplitude ± SEM of either 2-4 (H_2O) or 6 (DMSO) responses.

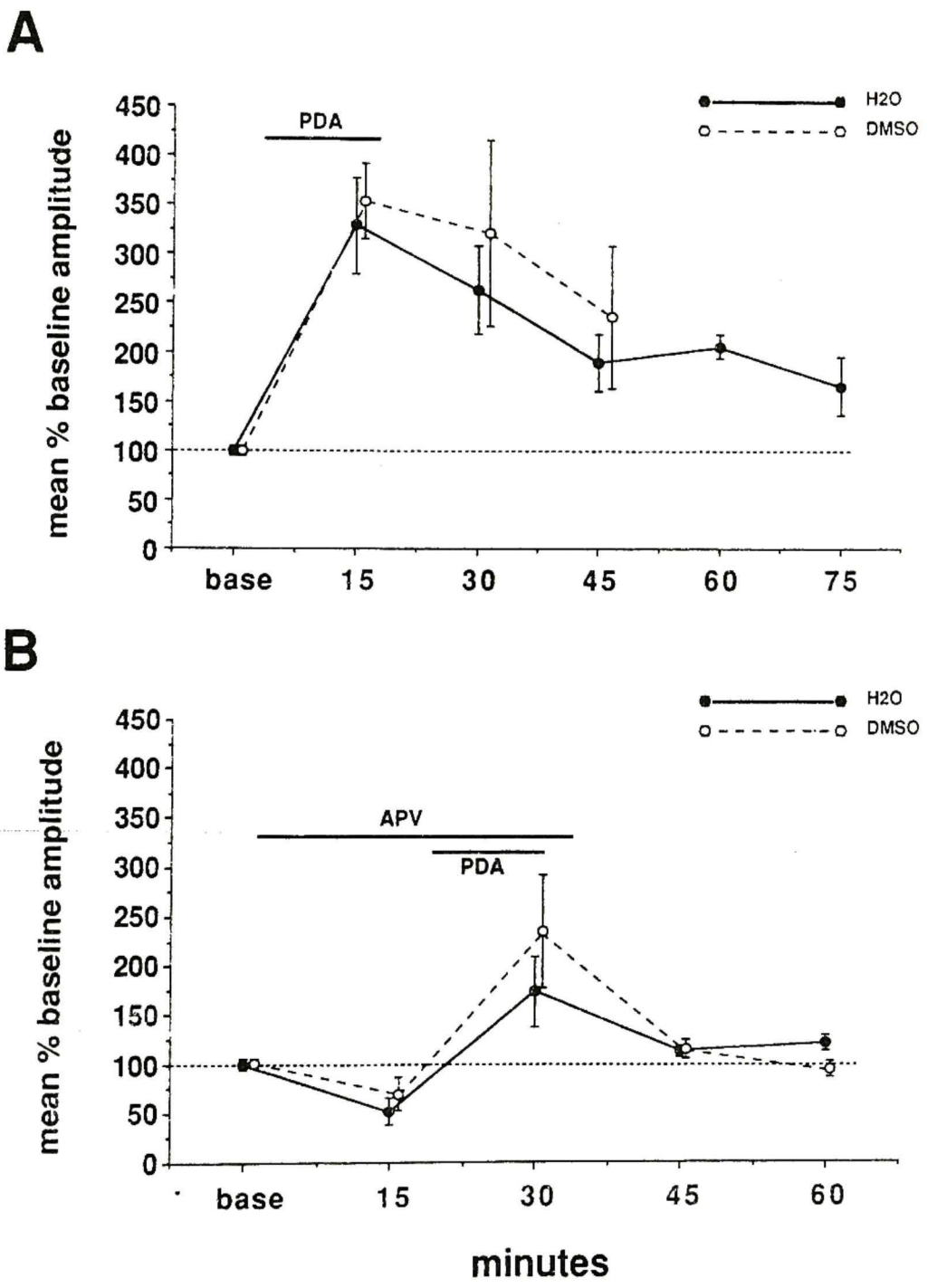
A
mean % baseline amplitude
450
400
350
300
250
200
150
100
50
0
PDA
H2O
DMSO
base
15
30
45
60
75
B
mean % baseline amplitude
450
400
350
300
250
200
150
100
50
0
APV
PDA
H2O
DMSO
base
15
30
45
60
minutes

dependent plasticity.

NMDA receptors in evoked synaptic activity

When measuring evoked responses in the granule cell layer, we consistently observed an initial depression of the population spike produced by both D(-)APV and CPP, so we performed a series of experiments designed to elucidate the nature of this depression. Fig 8 shows the effects of NMDA receptor antagonists on both orthodromic and antidromic evoked responses measured after a 15 min bath application. 1μM D(-)APV depressed the orthodromic population spike amplitude only slightly, but 10μM D(-)APV significantly depressed the response to 71 $\pm$ 3% of baseline. The effects of D(-)APV were reversible and returned to baseline levels following a 30 min wash. This depressant effect was not seen with the inactive isomer L(+)APV (10μM), as can be seen in Fig 8. Thus, it is unlikely that D(-)APV depressed the population spike in a nonspecific manner. CPP produced a significant depression of the orthodromic population spike at concentrations of both 1μM (73 $\pm$ 6% of baseline) and 10μM (57 $\pm$ 6% of baseline). The responses at both concentrations of CPP were completely reversible but required a 60 min wash to return to baseline. Neither 10μM D(-)APV nor 10μM CPP had any effect on the antidromic spike recorded in the granule cell layer of the dentate gyrus (Fig 8).

Because of the nature of the voltage-dependent Mg^{++} block of the NMDA receptor at resting membrane potential, the question arose as to

Fig 8. NMDA receptor antagonists depress orthodromic transmission. This bar graph shows the effects of NMDA receptor antagonists on the amplitude of either the evoked population or antidromic spike. All NMDA receptor antagonists were bath applied for 15 min. Each bar represents the mean % baseline amplitude ± SEM of responses in one treatment group measured at 15 min application. The number of experiments in each group appears within the bar. Numbers below the bar designate the concentration (μM) of antagonist. Asterisk denotes a significant difference ($P<0.05$, paired t-test) in the mean compared to baseline responses. Anti = antidromic spike; ortho = orthodromic spike; D- = D(-)APV; L+ = L(+)APV. (From Burgard et al., 1989)

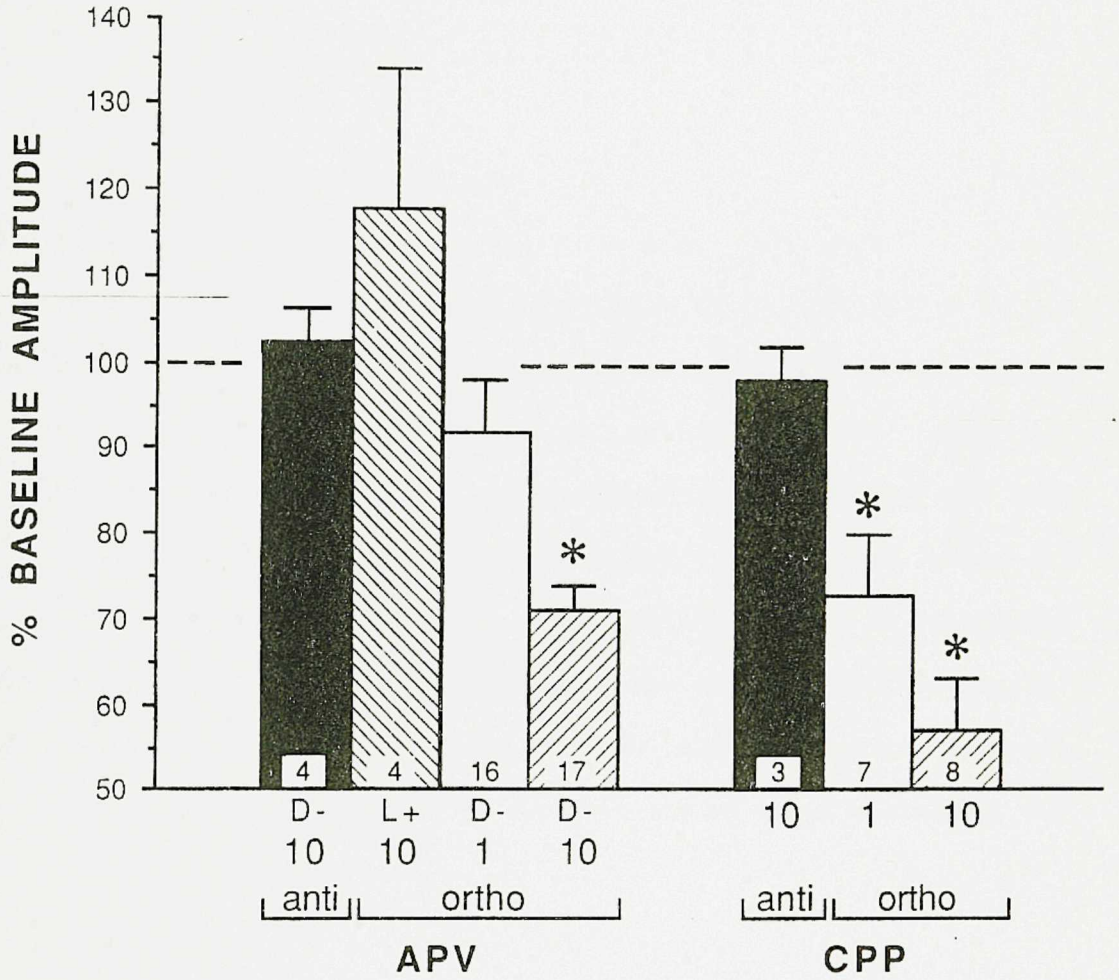
% BASELINE AMPLITUDE
140
130
120
110
100
90
80
70
60
50
4
4
16
17
3
7
8
*
*
*
D-
10
L+
10
D-
1
D-
10
10
1
10
anti
ortho
anti
ortho
APV
CPP

Fig 9. High [Mg^{++}] does not block D(-)APV-induced depression. Time course of the effects of high [Mg^{++}] and D(-)APV on the amplitude of the population spike. Each data point is the mean amplitude $\pm$ SEM of 2-4 responses. Data are expressed as % 'high Mg^{++} baseline' amplitude. This was done because application of a buffer containing 2.4mM Mg^{++} produced a depression of the population spike which eventually stabilized to a new baseline value. This new baseline value was designated 100%. 15 min after the arrival of 2.4mM Mg^{++}, 10μM D(-)APV was co-applied for 15 min. D(-)APV produced a reversible depression of the population spike in the presence of 2.4mM Mg^{++}.

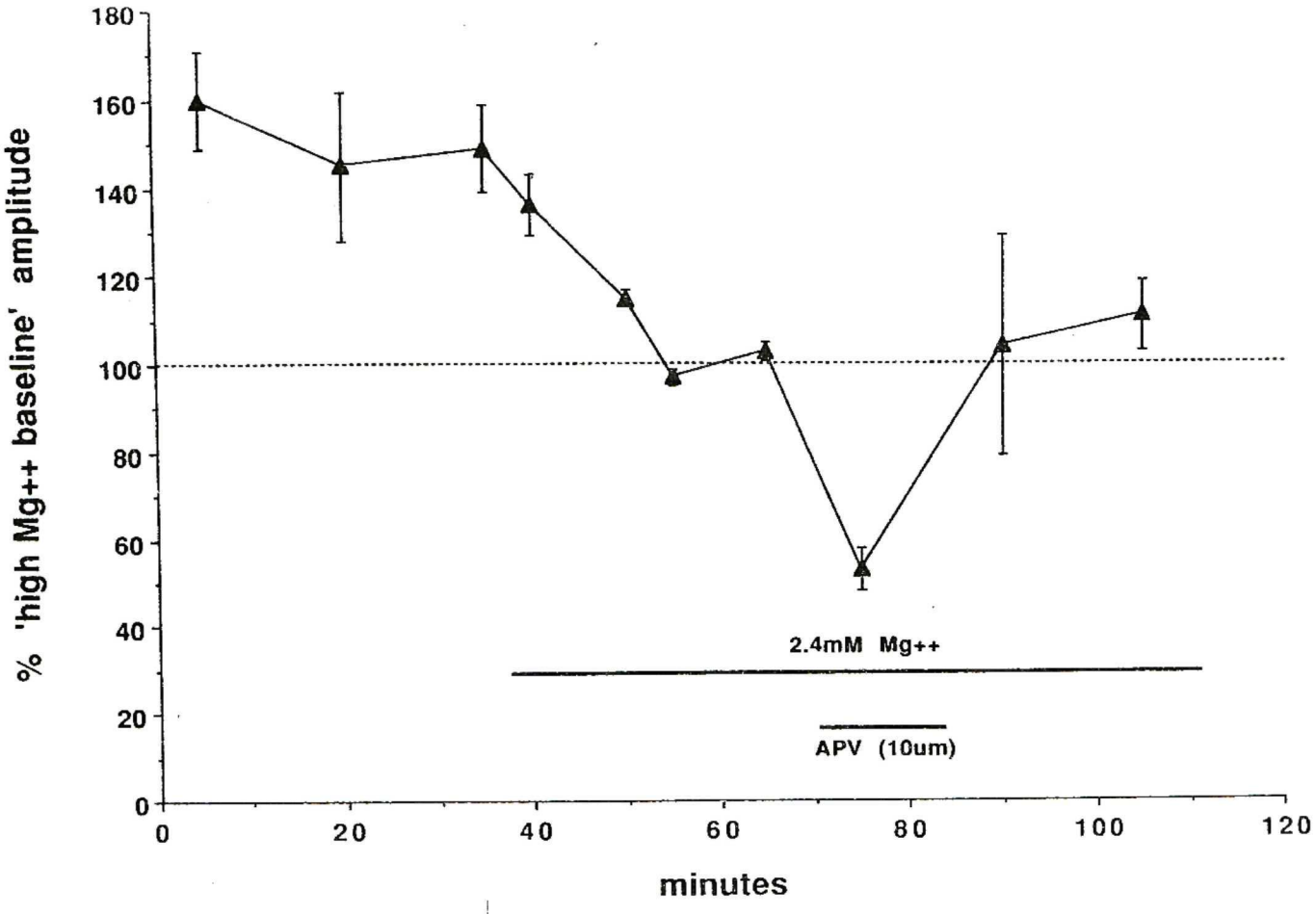
% 'high Mg++ baseline' amplitude
180
160
140
120
100
80
60
40
20
0
0
20
40
60
80
100
120
minutes
2.4mM Mg++
APV (10um)

whether or not the slices were exposed to an adequate [Mg^{++}] to prevent NMDA receptor activity during low frequency evoked activity. Fig 9 is a summary of a number of experiments in which baseline population spike amplitudes were obtained, and then the [Mg^{++}] in the buffer was increased to 2.4mM (from 1.3mM). Increasing the [Mg^{++}] caused a depression of the population spike. Once a new baseline was established, 10μM D(-)APV was applied for 15 min. The reversible depression of the population spike produced by D(-)APV in 2.4mM Mg^{++} (53 $\pm$ 4.9% of baseline) was comparable to that seen in 1.3mM Mg^{++} buffer (51 $\pm$ 6.3%, see Fig 10). These results suggest that D(-)APV-induced depression of the population spike is not due to an inadequate Mg^{++} block of the NMDA receptor.

In separate experiments, neither D(-)APV nor CPP depressed the initial negative slope of the medial perforant path-evoked EPSP. However, as demonstrated in Fig 10, a 30 min bath application of 10μM D(-)APV significantly depressed the peak amplitude and total area of the EPSP (n=6). This depression was reversed to pretreatment values following a 30 min wash (amplitude 103 $\pm$ 0.1% of baseline, area 102 $\pm$ 0.1%). 1μM CPP produced a reversible depression of the amplitude and area of the EPSP similar to D(-)APV (Fig 10). This depression also reversed to baseline values following a 30 min wash (amplitude 98 $\pm$ 0.1% of baseline, area 102 $\pm$ 0.1%). The depressant effects of NMDA receptor antagonists on both the population spike and the EPSP indicates that there is a significant NMDA receptor-mediated component to evoked synaptic activity in the medial perforant path.

Fig 10. NMDA receptor antagonists depress medial, but not lateral EPSPs. A. Effects of D(-)APV on medial perforant path (PP)-evoked responses. The EPSPs (upper row) were recorded in the mid-molecular layer; population spikes (lower row) were recorded in the granule cell layer and were evoked at higher stimulus intensities than the EPSPs. The open arrow indicates pretreatment responses. The solid arrow indicates the peak of the population spike. B and C. Histograms showing means and SEMs of response parameters before and during a 30 min exposure to 10μM D(-)APV or 1μM CPP on medial PP-evoked (B) EPSPs (D(-)APV n=6; CPP n=4) and (C) population spikes (D(-)APV n=6; CPP n=3). Measurements during exposure to compounds are expressed as percent of pretreatment values. The asterisk indicates a significant difference as compared to pretreatment values ($P<0.05$). (Adapted from Dahl et al., 1990)

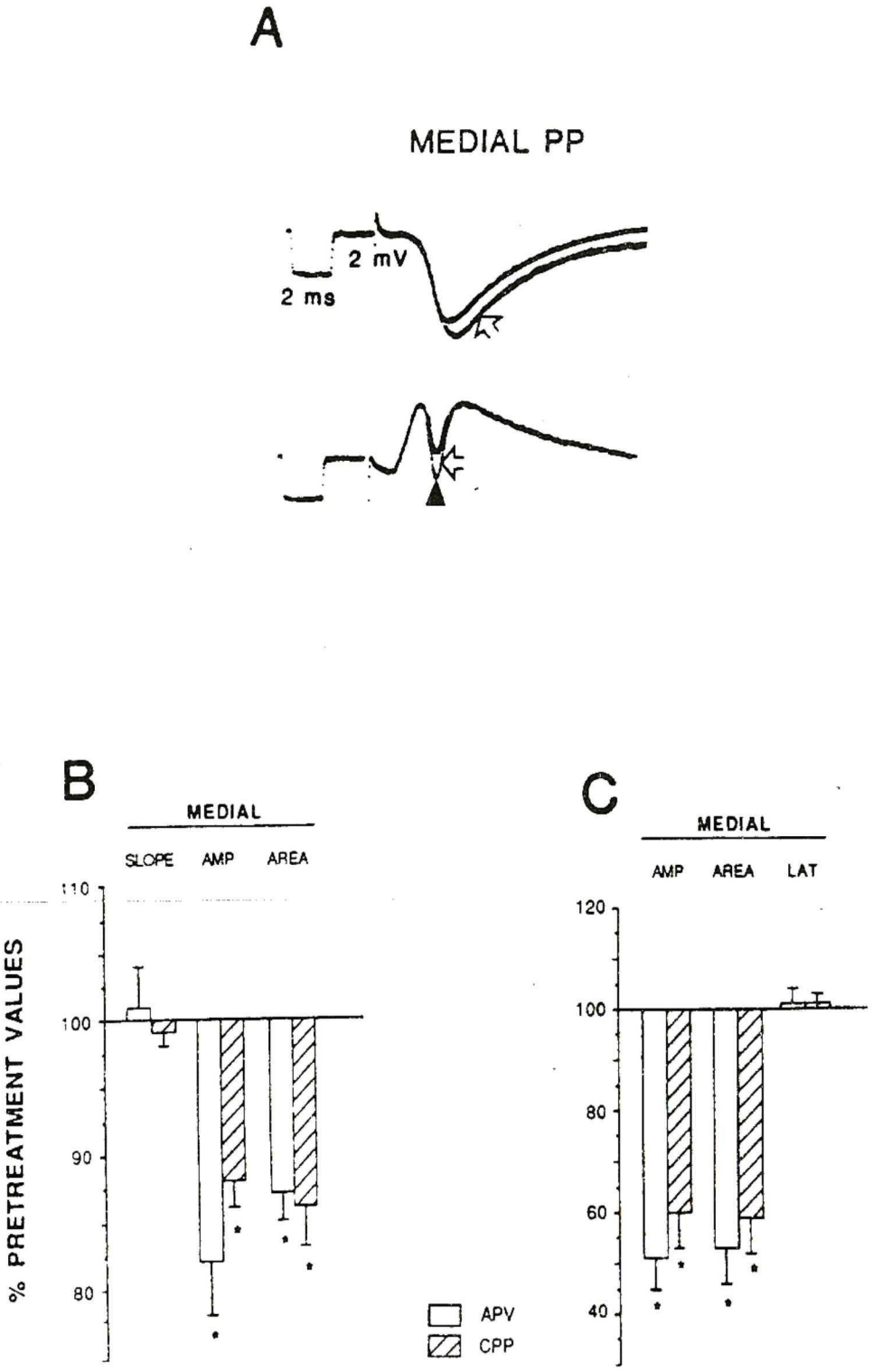
A
MEDIAL PP
2 mV
2 ms
B
MEDIAL
SLOPE
AMP
AREA
% PRETREATMENT VALUES
110
100
90
80
APV
CPP
C
MEDIAL
AMP
AREA
LAT
120
100
80
60
40

IV. Muscarinic receptor activation in the dentate gyrus

Effects of muscarine on evoked responses

The non-selective muscarinic receptor agonist muscarine was bath applied to hippocampal slices at various concentrations. Effects of muscarine on normal synaptic transmission were assessed by monitoring both the population spike and EPSP. Muscarine produced a depression of evoked responses as shown in Fig 11C. This log concentration/response curve demonstrates the concentration-dependent depression of the population spike produced by muscarine. This muscarine-induced depression was also seen in the initial negative slope of the EPSP, however to a lesser extent. Because of the relatively small effects of muscarine on the EPSP as compared to the population spike, and the variability measured within the small range of the EPSP, most of the analysis of the effects of muscarine were confined to those effects produced on the population spike. In general, any effects of muscarinic ligands, alone or in combination, on the population spike were parallelled by lesser muscarinic effects on the EPSP. An effort has been made to include pertinent data on the EPSP where possible.

A concentration of 1μM muscarine had no significant effect on either the population spike (90 $\pm$ 16% of baseline, n=6, Fig 11C) or the EPSP (106 $\pm$ 4.1%, n=6) measured after 10 minutes of muscarine

Fig 11. Concentration-dependent depression of evoked responses by muscarine. A. Time course of the effects of 10μM muscarine (musc) on evoked responses. A 10 min bath application of 10μM muscarine transiently depressed both the mean amplitude of the population spike (left ordinate), and the mean slope of the EPSP (right ordinate). Each data point represents the mean % baseline $\pm$ SEM of 5 responses. Asterisk denotes significant difference as compared to mean baseline values ($P<0.05$, ANOVA plus SNK). B. Representative population spikes (PS) and EPSPs recorded before (baseline) and at the end of a 10 min bath application of 10μM muscarine. The stimulus intensity used to evoke the PS was greater than that used for the EPSP. Asterisk denotes stimulus artifact, and calibration bar is 5mV, 5msec. C. Log concentration-response curve demonstrating the depression of the population spike amplitude produced by muscarine. Each data point represents the mean % depression $\pm$ SEM of at least 2-5 responses, recorded at the end of a 10 min muscarine application.

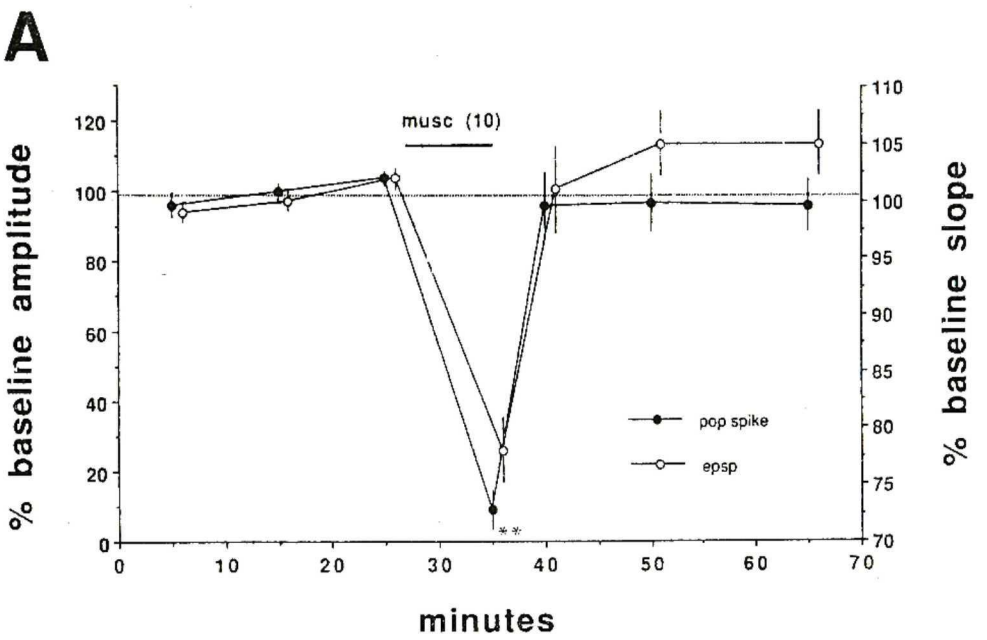
A
musc (10)
% baseline amplitude
% baseline slope
pop spike
epsp
minutes
0
10
20
30
40
50
60
70
120
100
80
60
40
20
110
105
95
90
85
80
75

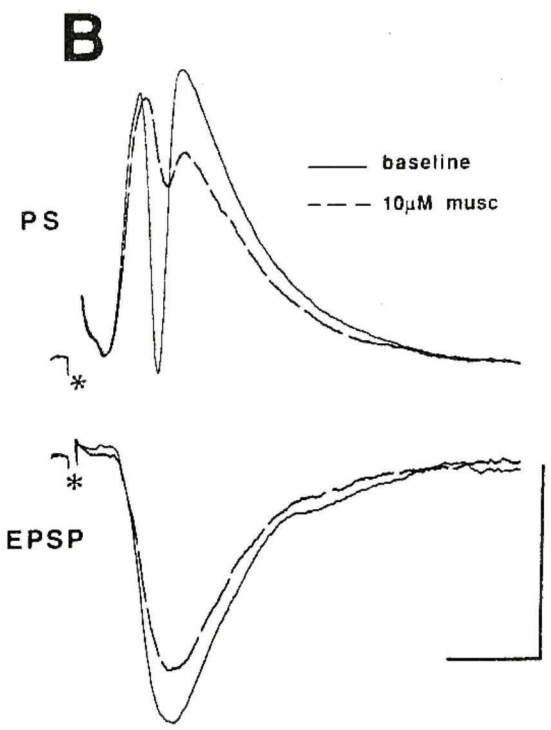
B
baseline
10μM musc
PS
EPSP

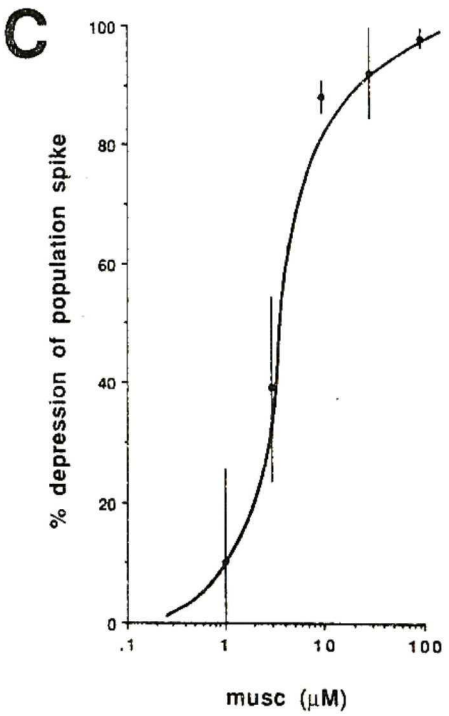
C
% depression of population spike
musc (μM)
.1
1
10
100
0
20
40
60
80
100

application. The estimated EC50 for muscarinic depression of the population spike was 3.3μM. A concentration of 10μM muscarine significantly ($P<0.05$, Student's t-test) depressed both the population spike (9.1 $\pm$ 6.0% of baseline, n=5) and the EPSP (78 $\pm$ 3.0%, n=5). As demonstrated in the time course of Fig 11A, the depression produced by 10μM muscarine was fully reversed following a 5 min wash. Because 10μM muscarine produced almost complete depression of the population spike, and a modest depression of the EPSP (see Fig 11B, for example), this concentration was used in many subsequent experiments. Increasing the concentration of muscarine to 30μM produced a larger depression of the EPSP (69 $\pm$ 7.1% of baseline, n=3) but did not produce a significantly larger depression of the population spike (Fig 11C). Neither the EPSP nor the population spike were analyzed at these higher muscarine concentrations, in an effort to minimize possible nonspecific effects produced at high agonist concentrations.

Antagonist sensitivity of muscarinic responses

In order to determine the subtype(s) of muscarinic receptor responsible for the concentration-dependent depression of evoked responses produced by muscarine, a number of relatively selective muscarinic receptor antagonists were used to block this effect. In addition to the nonselective antagonist atropine, three relatively potent and selective subtype antagonists were used; pirenzepine (M1 receptor antagonist), AFDX-116 (M2), and 4-DAMP (M3/M1). Each displays

selectivity at low concentrations, but all are nonselective muscarinic receptor antagonists at high concentrations. The nonselective muscarinic receptor antagonist atropine (1μM) blocked the depression of both the population spike (97 $\pm$ 3% of baseline, n=2) and the EPSP (104 $\pm$ 5%, n=2) produced by 10μM muscarine.

Because of the abundance of M1 receptors, and the quantity of pharmacological data available on the competitive M1 receptor antagonist pirenzepine, most of this analysis concentrated on the ability of pirenzepine to antagonize muscarinic depression. Pirenzepine was applied 10 min prior to, and during a 10 min application of muscarine. Pirenzepine produced a concentration-dependent blockade of muscarinic depression. As can be seen in Fig 12A, increasing concentrations of pirenzepine in the presence of muscarine produced a series of parallel, rightward shifts of the muscarine concentration-response curve. The shift in the curve followed that for a competitive antagonist, as the EC50 for muscarinic depression of the population spike was increased, and the maximal % depression produced by muscarine remained unchanged. Estimated EC50s for muscarine in the presence of various concentrations of pirenzepine were as follows; pirenzepine (0μM) = 3.3μM, pirenzepine (1μM) = 10μM, pirenzepine (3μM) = 25μM, and pirenzepine (10μM) = 100μM. Higher concentrations of pirenzepine were not used, since this would have required the use of concentrations of muscarine 100μM or higher to overcome the pirenzepine blockade.

The ability of pirenzepine to block muscarinic depression of the EPSP was similar to its ability to affect the population spike. At a concentration of 10μM, muscarine depressed the EPSP to 78 $\pm$ 3.0 %, of

Fig 12. Competitive antagonism of muscarinic depression by pirenzepine. A. Log concentration-response curves of muscarine in the presence of various concentrations of the M1 receptor antagonist pirenzepine. Pirenzepine was bath applied for 10 min prior to and during a 10 min application of muscarine. Each point represents the mean % depression ± SEM of at least 2-5 responses, recorded at the end of the muscarine application. Curves were fit by hand. B. Schild plot of the data displayed in Fig 12A. EC_{50}s for muscarine in the presence of 0, 1, 3 and 10μM pirenzepine were estimated from the concetration-response curves in 12A. The log concentration ratio was plotted against log pirenzepine concentration, and the pA2 estimated from the x-intercept of a line fit by hand through the three points.

A

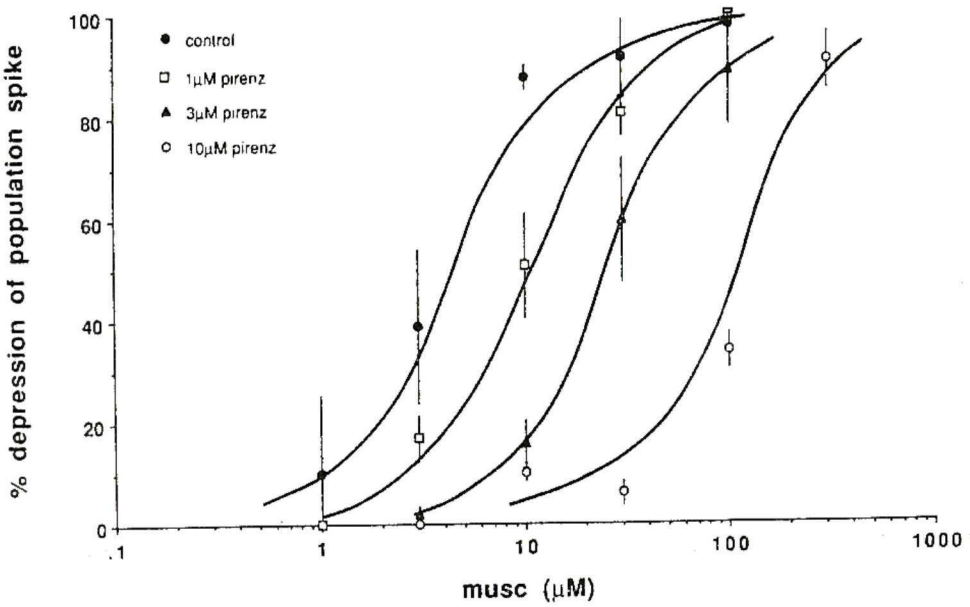
% depression of population spike
100
80
60
40
20
0
control
1μM pirenz
3μM pirenz
10μM pirenz
.1
1
10
100
1000
musc (μM)

B

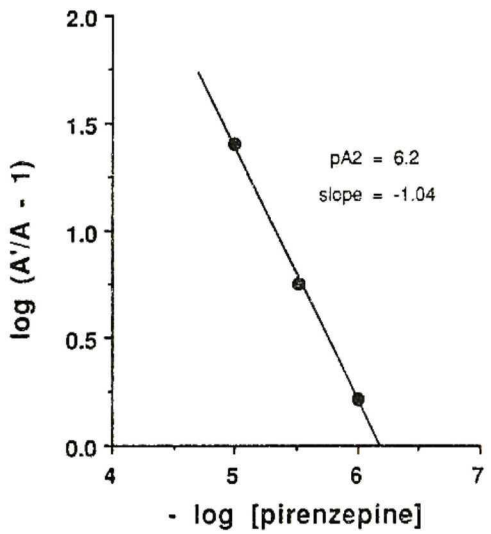
log (A'/A - 1)
2.0
1.5
1.0
0.5
0.0
pA2 = 6.2
slope = -1.04
4
5
6
7
- log [pirenzepine]

baseline (n=5). A 1μM concentration of pirenzepine reduced this depression to 96 $\pm$ 4.1% of baseline (n=7).

An estimate of the affinity of pirenzepine as an antagonist of muscarinic depression of the population spike was determined on the basis of the EC50s for muscarine in the presence of increasing concentrations of pirenzepine. This analysis followed that of Arunlakshana and Schild (1959) and Tallarida et al. (1979). The concentration ratio of the EC50 of muscarine alone (A) and in combination with pirenzepine (A') was determined for each concentration of pirenzepine used. This ratio depends upon the concentration of pirenzepine (B) in the form of the equation:

$$(1)\quad A'/A = 1 + B/K_B$$

where K_B is the antagonist dissociation constant. When the concentration ratio equals 2, then $B/K_B = 1$, or taking the log of both sides:

$$(2)\quad \log B - \log K_B = 0.$$

As defined by Schild, the pA_2 is the negative log of B which produces a concentration ratio of 2. From this is obtained:

$$(3)\quad pA2 = -\log B = -\log K_B = \log 1/K_B,$$

and since $1/K_B = K_A$, the affinity constant, pA_2 is a measure of affinity of the antagonist. Rearranging equation 1, and taking the log of both sides, we obtain:

$$\log (A'/A - 1) = \log B - \log K_B$$

or,

$$(y = m(x) + b),$$

the equation for a straight line with a slope = 1.

Plotted as a straight line, as in Fig 12B, the Schild plot revealed two

important points: 1) the pA_2 value for pirenzepine, measured as the x-intercept, was 6.2, and 2) the slope of the line connecting these points was equal to -1.04. These data suggest that pirenzepine is acting as a selective competitive antagonist in this system.

The fact that pirenzepine was a competitive antagonist of the depression produced by muscarine was an indication that activation of M1 receptors was responsible for this effect. To strengthen this hypothesis, the muscarinic receptor antagonists AFDX-116 and 4-DAMP were examined for their ability to block muscarinic depression induced by 10μM muscarine. A summary of the effects of these compounds is shown in Fig 13. In these experiments, the antagonist was applied for 10 min prior to and during a 10 min application of 10μM muscarine. AFDX-116 produced a concentration-dependent antagonism of muscarinic depression of the population spike with an estimated EC50 of 3.3μM. 4-DAMP produced a similar antagonism, but was much more potent (estimated EC50 = 0.12μM). Pirenzepine displayed an estimated EC50 of 1μM. Representative population spikes recorded in the presence of various concentrations of antagonists plus 10μM muscarine are shown in Fig 14. These traces all show the effect of a 1μM concentration of antagonist, along with a concentration that would completely prevent 10μM muscarine-induced depression. Only atropine and 4-DAMP could completly antagonize the effects of 10μM muscarine at very low concentrations ($\leq$1μM).

Pertussis toxin sensitivity of muscarinic depression

Fig 13. Antagonism of muscarinic depression by muscarinic receptor antagonists. Log concentration-response relationships demonstrating the abilities of three different muscarinic receptor antagonists to block 10μM muscarine-induced depression of the population spike. Three concentrations of each antagonist were used, and applied for 10 min prior to and during a 10 min exposure to muscarine. Each data point represents the mean % depression $\pm$ SEM of 2-5 responses, recorded at the end of the muscarine application. The dotted line indicates the point at which the population spike was depressed by 50%. The curve for each antagonist was drawn by hand, and its intercept with the dotted line gave a measure of the EC_{50} for the antagonist.

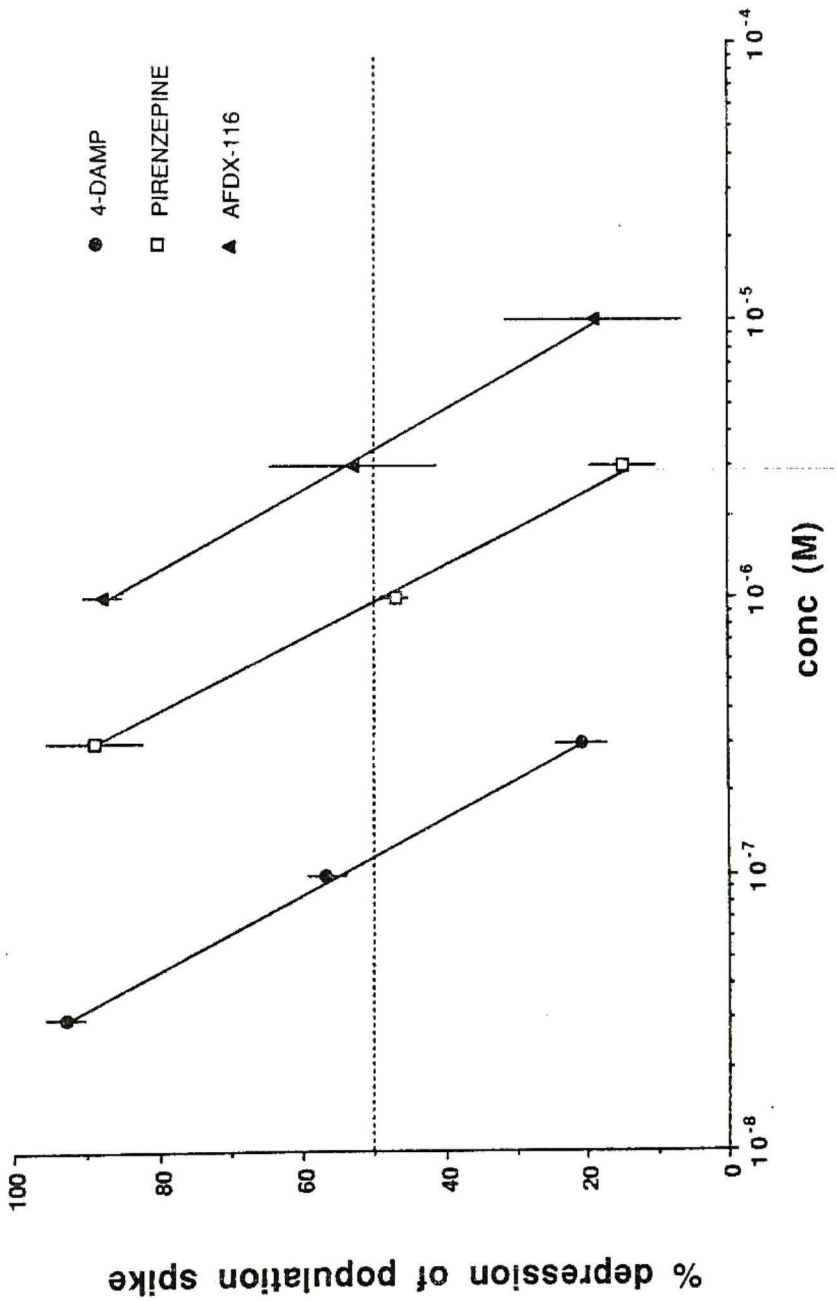
4-DAMP
PIRENZEPINE
AFDX-116
% depression of population spike
100
80
60
40
20
0
10^{-8}
10^{-7}
10^{-6}
10^{-5}
10^{-4}
conc (M)

Fig 14. Representative traces demonstrating the efficacy of muscarinic receptor antagonists. A. Population spikes recorded before (base) and in the presence of 10μM muscarine (10 min MUSC). In all successive traces, the solid trace is a baseline response, and the broken trace was recorded in the presence of 10μM muscarine plus antagonist. Antagonists were applied 10 min prior to and during muscarine application. B. The M1 receptor antagonist pirenzepine completely blocked 10μM muscarine-induced depression at a concentration of 10μM. C. The M2 receptor antagonist AFDX-116 had no effect on muscarinic depression, and required a high concentration (50μM) for complete antagonism. D. The nonselective muscarinic receptor antagonist atropine produced a complete antagonism of muscarinic depression at a concentration of 1μM. E. The mixed M1 / M3 receptor antagonist 4-DAMP similarly produced complete antagonism of muscarinic depression at a low concentration of 1μM.

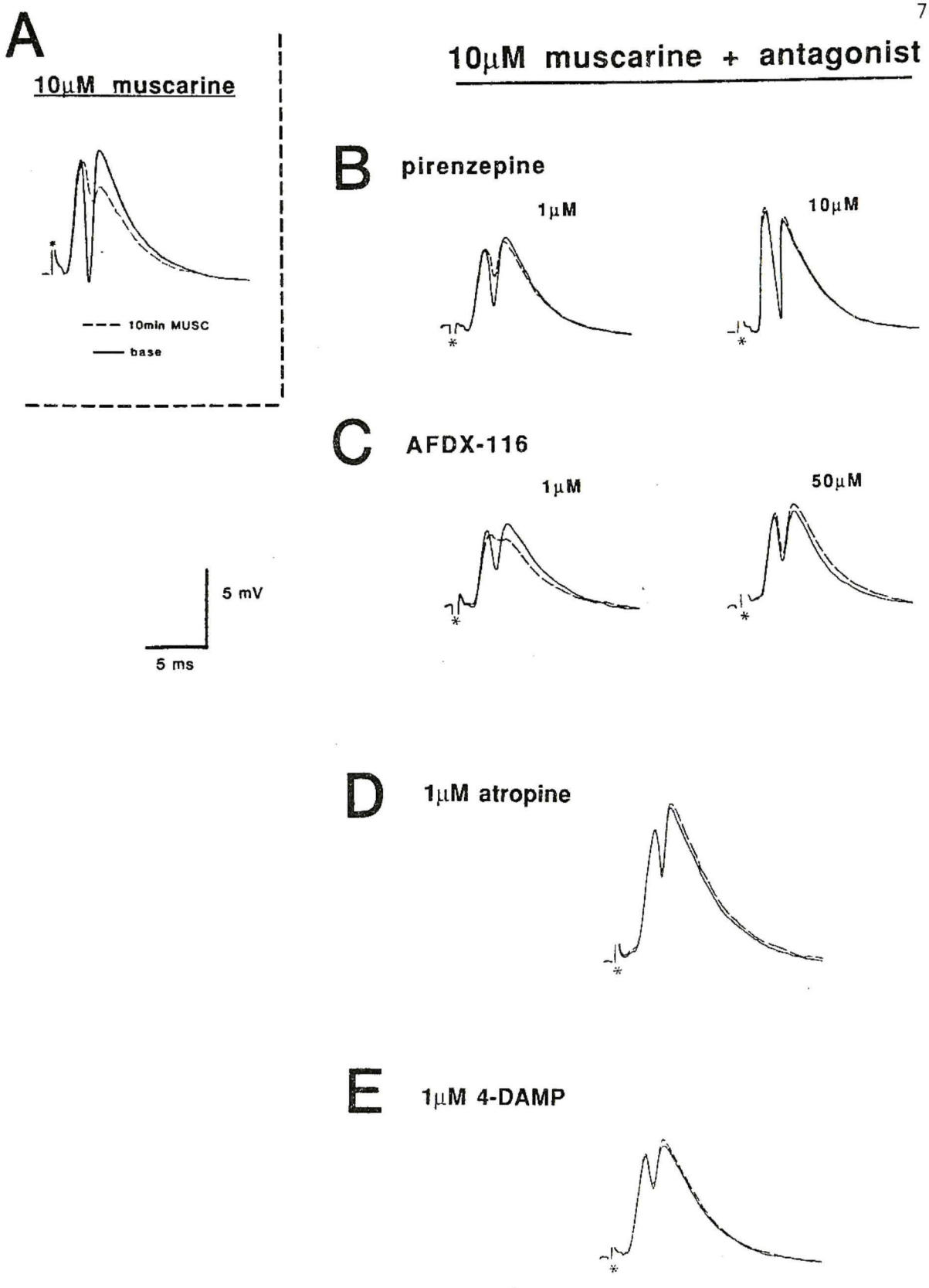
A
10μM muscarine
10min MUSC
base
5 mV
5 ms
10μM muscarine + antagonist
B
pirenzepine
1μM
10μM
C
AFDX-116
1μM
50μM
D
1μM atropine
E
1μM 4-DAMP

To determine the subtype(s) of muscarinic receptor which mediates the muscarine-induced depression of evoked responses, the PTx sensitivity of this response was examined. PTx injections were performed *in vivo*, and slices prepared from PTx-treated hippocampi (see Materials and Methods, and Burgard and Sarvey, in press). Bath application of 10μM muscarine for 10 min produced a significant depression of both the population spike (31 $\pm$ 8.8% of baseline) and the EPSP (74 $\pm$ 7.5%, n=4, Fig 15) which was reversible upon washout of the drug. The depression of the population spike or EPSP in slices from PTx-treated rats was not significantly different than that of slices from untreated rats (n.s., Student's t-test).

The efficacy of the PTx injection was determined by its ability to block $GABA_B$-mediated responses, which are PTx-sensitive. The effects of the $GABA_B$ receptor agonist baclofen on evoked responses were analyzed both in slices previously exposed to 10μM muscarine (n=4), and nonexposed slices (n=2). The disinhibitory effects of baclofen usually seen in naive slices were significantly reduced or abolished with PTx treatment (see Fig 3 of Burgard and Sarvey, in press). In slices exposed to muscarine, a 20 min washout of muscarine always preceeded the baclofen exposure, to allow for washout of muscarine. There were no differences in the responses to baclofen in slices exposed to muscarine or those not exposed. This demonstrates that the PTx treatments were effective in blocking PTx-sensitive G-protein-mediated responses, as determined by the responses to baclofen.

Fig 15. Pertussis toxin insensitivity of muscarinic depression. A. In slices from PTx-treated rats, a 10 min bath application of 10μM muscarine transiently depressed both the mean amplitude of the population spike (left ordinate) and the mean slope of the EPSP (right ordinate). Muscarine was bath applied at the bar, and responses recorded in the presence of muscarine were significantly depressed as compared to baseline values (asterisk, $P<0.05$, ANOVA plus SNK). The depression produced in slices from PTx-treated rats was not significantly different than that recorded in untreated rats (see Fig 11). Each data point represents the mean % $\pm$ SEM of 4 responses. B. Representative population spikes and EPSPs recorded before (baseline) and at the end of a 10 min bath application of 10μM muscarine in a slice from a PTx-treated rat. The stimulus intensity used to evoke the population spike was greater than that used for the EPSP. Asterisk denotes stimulus artifact, and calibration bar is 5mV, 5msec.

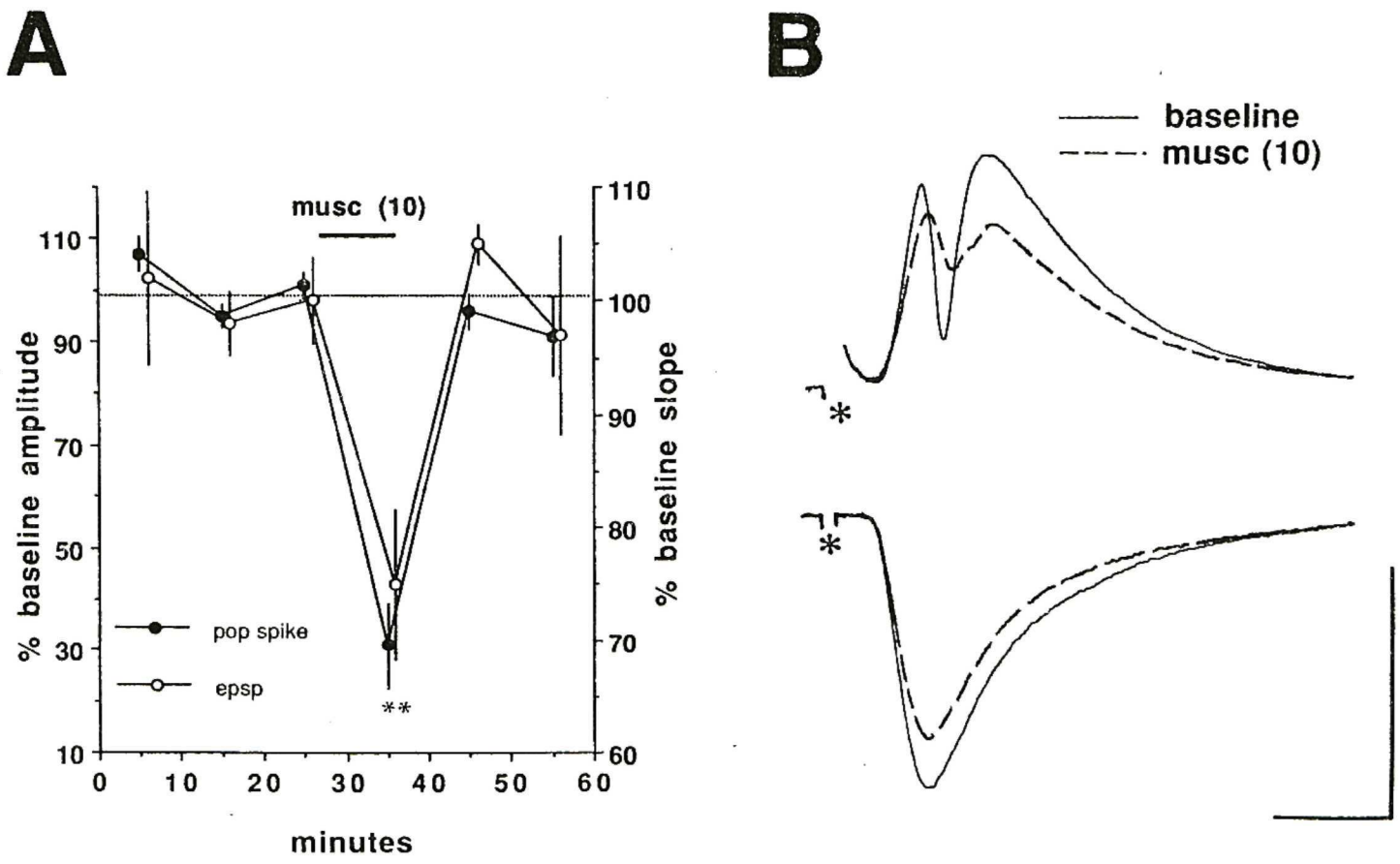
A
musc (10)
110
90
70
50
30
10
% baseline amplitude
110
100
90
80
70
60
% baseline slope
pop spike
epsp
**
0
10
20
30
40
50
60
minutes
B
baseline
musc (10)
*
*

Muscarinic facilitation of LTP

The effects of various concentrations of muscarine on LTP induction using both sub- and suprathreshold high frequency stimulation were examined. Muscarine (1 and 10μM) was bath applied for 10 minutes prior to and during the delivery of a subthreshold high frequency stimulus train. 1μM muscarine itself had no significant effect on the population spike or EPSP (Fig 11C). Likewise, a subthreshold HFT did not have any significant effect on either the population spike or the EPSP. However, delivery of a subthreshold HFT during bath application of 1μM muscarine resulted in potentiation (Fig 16) of both the population spike (responses in 6 of 6 slices potentiated to 265 $\pm$ 33% of baseline) and the EPSP (responses in 6 of 6 slices potentiated to 155 $\pm$ 8.9%) measured 30 min after delivery of the HFT. As can be seen in Fig 16, the responses were potentiated within 5 minutes after the HFT and remained potentiated throughout the recording period.

In other experiments, the M1 receptor antagonist pirenzepine (1μM) was bath applied before and during application of muscarine plus delivery of a subthreshold HFT. Fig 16 also demonstrates the effect of pirenzepine on muscarine-facilitated LTP of both the population spike (responses in 2 of 5 slices potentiated, 138 $\pm$ 8.4%) and the EPSP (responses in 3 of 5 slices potentiated, 117 $\pm$ 7.6%). In these experiments, 1μM pirenzepine alone did not affect evoked responses (population spike: 103 $\pm$ 2.9%, EPSP: 105 $\pm$ 3.1%), but reduced both the probability and the degree of muscarine-facilitated potentiation. Thirty minutes after the subthreshold HFT, neither the amplitude nor the

Fig 16. Pirenzepine-sensitive facilitation of LTP by a low concentration of muscarine. A. Time course of population spike amplitudes under 3 different experimental conditions. A subthreshold HFT was applied at the arrow (squares, solid line; n=5); 1μM muscarine was bath applied for 10 min before and during a subthreshold HFT delivered at the arrow (circles, dotted line; n=6); or 1μM pirenzepine was applied 10 min prior to and during 1μM muscarine + subthreshold HFT (triangles, broken line; n=5). Asterisk denotes a significant difference compared to both the subthreshold HFT group and the pirenzepine-treated group ($P<0.05$, ANOVA plus SNK at each time point). B. Time course of EPSP slopes under the same experimental conditions as 16A. The symbols and number of experiments are the same as in 16A. The arrow denotes the delivery of a subthreshold HFT. Asterisk denotes significant difference compared to both the subthreshold HFT group and the pirenzepine-treated group ($P<0.05$, ANOVA plus SNK at each time point). (From Burgard and Sarvey, 1990)

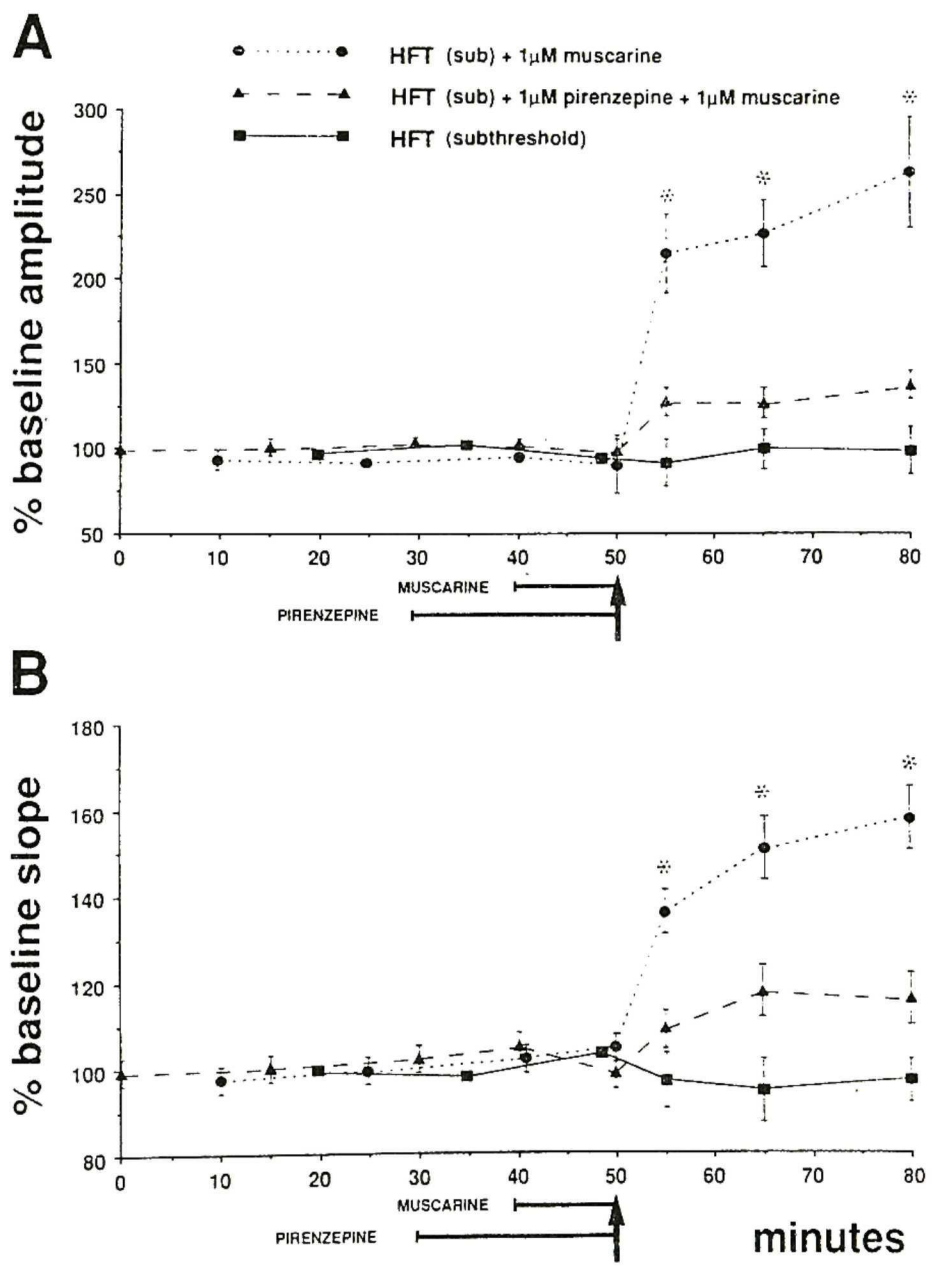
A
HFT (sub) + 1μM muscarine
HFT (sub) + 1μM pirenzepine + 1μM muscarine
HFT (subthreshold)
% baseline amplitude
300
250
200
150
100
50
0
10
20
30
40
50
60
70
80
MUSCARINE
PIRENZEPINE
B
% baseline slope
180
160
140
120
100
80
0
10
20
30
40
50
60
70
80
MUSCARINE
PIRENZEPINE
minutes

slope of the pirenzepine plus muscarine-treated group was significantly different from the group that received no drugs; but both the amplitude and slope were significantly less than those of the group treated with muscarine alone ($P<0.05$, ANOVA plus SNK). A concentration of 20μM pirenzepine did not block induction of LTP (n=1).

When the muscarine concentration was increased to 10μM, a subthreshold HFT did not facilitate LTP induction. Neither the population spike (responses in 1 of 6 slices potentiated, 107 $\pm$ 12% of baseline) nor the EPSP (responses in 1 of 6 slices potentiated, 111 $\pm$ 6.2%) was potentiated compared to either subthreshold HFT alone or 1μM muscarine + subthreshold HFT (n.s., ANOVA plus SNK). The lack of effect of a high concentration (10μM) of muscarine on LTP induction might be explained by activation of a second muscarinic receptor subtype which counteracts the effects of M1 receptor activation. A 10μM concentration of muscarine also had no effect on LTP elicited by a suprathreshold HFT (4 of 4 population spikes potentiated to 202 $\pm$ 22% and 4 of 4 EPSPs potentiated to 134 $\pm$ 10%; $P>0.05$, t-test compared to suprathreshold HFT alone).

For all experiments, the stimulus intensity of the subthreshold HFT was carefully adjusted to compensate for any effects of muscarine on evoked responses. At the stimulus intensities chosen for subthreshold HFTs, the mean slopes of the EPSPs did not differ significantly between groups (subthreshold HFT alone: 47 $\pm$ 3.8% of maximum baseline slope; 1μM muscarine + subthreshold HFT: 56 $\pm$ 6.1%; and 10μM muscarine + subthreshold HFT: 47 $\pm$ 3.7%, n.s., ANOVA). Within the narrow range of EPSP slopes used for subthreshold HFTs, there was also no correlation

between the slope of the EPSP and its ability to produce LTP, regardless of treatment group. This suggests that muscarinic facilitation of LTP is not simply due to an increase in the initial slope of the EPSP at the stimulus intensity used for the HFT.

Muscarinic inhibition of LLP

Bath application of muscarine for 10 min prior to, during, and for 10 min after a 20 minute application of 1μM isoproterenol had concentration-dependent effects on the induction of LLP. Fig 17A demonstrates the time course of the effects of 10μM muscarine on isoproterenol-induced LLP of the population spike. A 20 min application of 1μM isoproterenol produced LLP (squares). Pre- and concurrent treatment with 10μM muscarine depressed the population spike and also blocked LLP (circles). A high concentration of pirenzepine (20μM) was necessary to block the effects of muscarine on LLP (triangles). LLP of the EPSP parallelled the population spike in its blockade by 10μM muscarine (see Fig 17B). Fig 17B is a summary of the 10μM muscarine data for both population spike and EPSP recorded following the 30 min final wash. As shown in this figure, LLP of both EPSP and population spike was significantly reduced in the presence of muscarine as compared to isoproterenol alone. This reduction could be prevented by pre- and coapplication of a high concentration of pirenzepine (20μM).

Application of a lower concentration of muscarine (1μM) for 10 min prior to and during a 20 min exposure to 1μM isoproterenol reduced,

Fig 17. Blockade of LLP by a high concentration of muscarine. A. Time course of population spike amplitudes under 3 different experimental conditions. A 20 min application of 1μM isoproterenol (ISO) was applied at the bar (between minutes 50 - 70, squares, solid line; n=5); 10μM muscarine was bath applied for 10 min before, during, and for 5 min after application of 1μM ISO (circles, dotted line; n=6); or 20μM pirenzepine was applied 10 min prior to and during 10μM muscarine + 1μM ISO (triangles, broken line; n=4). Asterisk denotes a significant difference compared to both the 1μM ISO group and the pirenzepine-treated group ($P<0.05$, ANOVA plus SNK at each time point). B. Summary of both population spike amplitudes (PS, left ordinate, open bars) and EPSP slopes (right ordinate, hatched bars) recorded at the end of a 30 min wash period. The treatment groups are the same as those described in 17A, and the number of responses appears within each bar. Asterisk denotes significant difference compared to both the 1μM ISO group and the pirenzepine-treated group ($P<0.05$, ANOVA plus SNK).

A

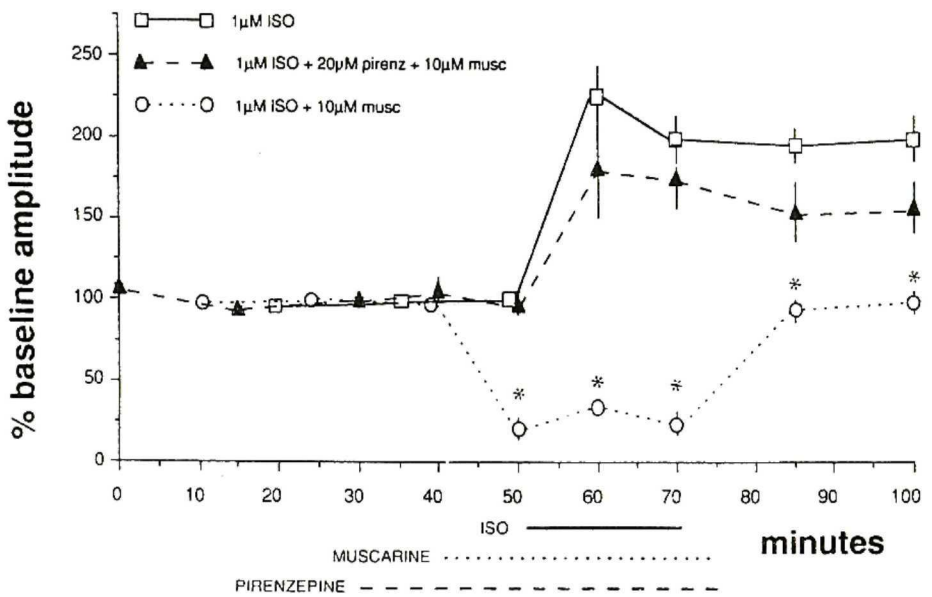
1μM ISO
1μM ISO + 20μM pirenz + 10μM musc
1μM ISO + 10μM musc
% baseline amplitude
250
200
150
100
50
0
0
10
20
30
40
50
60
70
80
90
100
minutes
ISO
MUSCARINE
PIRENZEPINE

B

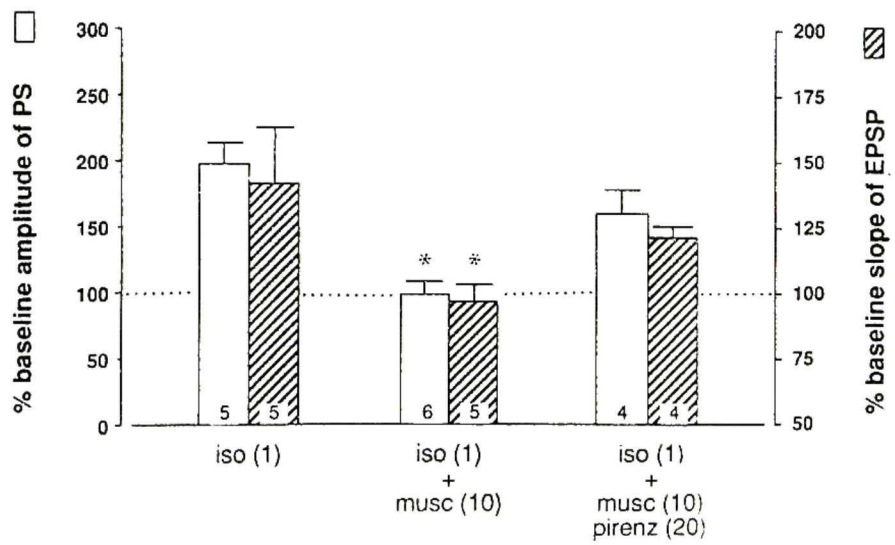
% baseline amplitude of PS
% baseline slope of EPSP
300
250
200
150
100
50
0
200
175
150
125
100
75
50
5
5
6
5
4
4
iso (1)
iso (1)
+
musc (10)
iso (1)
+
musc (10)
pirenz (20)

but did not block, LLP of either the population spike or the EPSP. In the presence of 1μM muscarine, isoproterenol produced both an acute potentiation (population spike: 138 $\pm$ 10% of baseline, EPSP: 114 $\pm$ 2.7%), and an LLP measured at the end of a 30 min wash (population spike: 157 $\pm$ 19% of baseline, EPSP: 115 $\pm$ 3.7%, $P<0.05$ for both compared to baseline, Student's t-test, n=10).

From the above experiments, it appeared that muscarine produced a concentration-dependent reduction of LLP. However, since muscarine could facilitate LTP induction, the facilitation of LLP induction with muscarine was examined. Since a low concentration of muscarine (1μM) was able to facilitate the induction of LTP, this concentration of muscarine was applied 10 min prior to and during a 20 min exposure to 0.1μM isoproterenol, which is 'subthreshold' for induction of LLP. This concentration of isoproterenol can be used to demonstrate facilitation of LLP induction by other agents (see Fig 4 of Burgard and Sarvey, in press). In three slices from three rats, 1μM muscarine did not facilitate LLP induction. However, in these three slices, 1μM muscarine also depressed the population spike to 69 $\pm$ 12% of baseline, and the EPSP to 95 $\pm$ 3.9%. In the presence of 1μM muscarine, 0.1μM isoproterenol produced neither acute potentiation (population spike: 72 $\pm$ 14%, EPSP: 90 $\pm$ 7.1%) measured in the presence of both, nor LLP (population spike: 103 $\pm$ 13%, EPSP: 95 $\pm$ 7.9%) measured at the end of a 30 min wash. These results suggest that 1μM muscarine does not facilitate the induction of LLP as it facilitates LTP induction.

V. Stimulation of [cAMP] in the dentate gyrus

These experiments were aimed at correlating electrophysiological responses with regulation of cAMP accumulation using the same concentrations of ligands. The approach used was to find a concentration of isoproterenol which would produce a measurable increase in [cAMP], and then attempt to block this increase with exposure to muscarine. The biochemical methods used for determination of cAMP production by slices of dentate gyrus are outlined in the Materials and Methods.

ß-Adrenergic-induced changes in [cAMP]

A 10 min incubation of dentate gyrus slices with 1μM isoproterenol produced a significant increase in the accumulation of cAMP. As can be seen in Fig 18, 1μM isoproterenol significantly increased cAMP accumulation from a basal concentration of 6.9 $\pm$ 0.5 pmol to a stimulated level of 11.5 $\pm$ 0.8 pmol ($P<0.05$, Student's t-test). Increasing the concentration of isoproterenol to 10μM produced no further increase in the accumulation of cAMP (93 $\pm$ 8.3% of 1μM isoproterenol-stimulated level, n=3).

All of the experiments included in Fig 18 were performed in the presence of 1mM IBMX to inhibit phosphodiesterase activity. 1mM IBMX

Fig 18. Inability of muscarine to block isoproterenol-stimulated increase in cAMP. Bar graph demonstrating the effects of 3 different treatments on [cAMP] produced by slices of dentate gyrus. The three treatment groups were: 1) 10μM muscarine alone, 2) 1μM isoproterenol alone, and 3) 10μM muscarine plus 1μM isoproterenol. Each bar represents the mean + SEM pmol cAMP accumulated from each slice. The number of slices appears within each bar. Asterisk denotes significant difference compared to control values ($P<0.05$, Student's t-test).

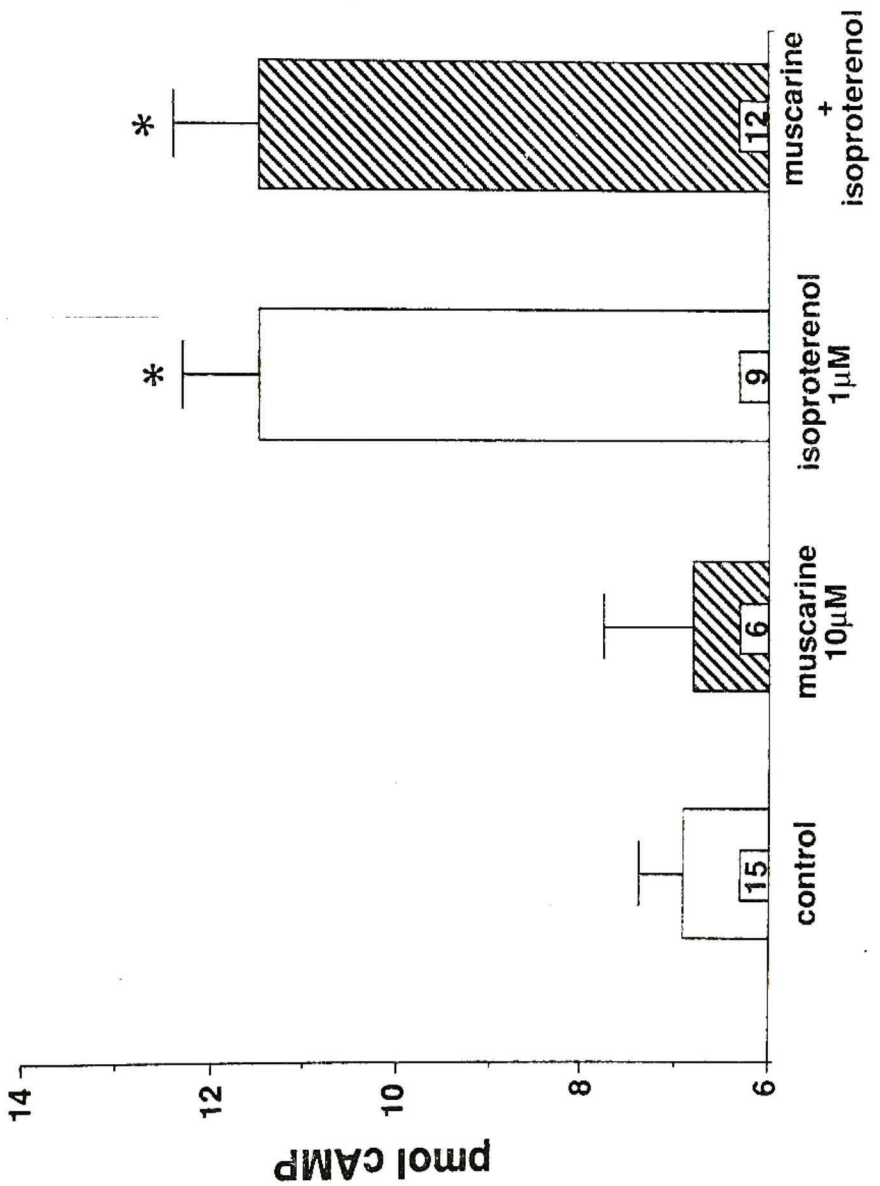
pmol cAMP
14
12
10
8
6
*
*
15
6
9
12
control
muscarine 10μM
isoproterenol 1μM
muscarine + isoproterenol

alone had no significant effect on the basal accumulation of cAMP in dentate gyrus slices (97 ± 25% of control, n=3).

The amount of protein per slice in the cAMP experiments was not determined. However, in other experiments, the average amount of protein in slices of dentate gyrus was determined in 18 slices. The protein determinations were performed according to the method of Lowry (1951). The mean protein content was 97 ± 6.1 μg protein per slice. This value was used as a guide for determination of pmol cAMP produced per mg protein in dentate gyrus slices. In general, the mean pmol cAMP displayed in Fig 18, if presented as pmol cAMP/mg protein, would be approximately 10-fold greater than that shown.

Muscarinic-induced changes in [cAMP]

A concentration of 10μM muscarine did not affect basal accumulation of cAMP, as depicted in Fig 18 (6.8 ± 1.0 pmol vs 6.9 ± 0.5 basal pmol cAMP). Increasing the concentration of muscarine to 100μM did not produce a further significant change in cAMP accumulation (86 ± 12% of basal level, n=3). When slices were incubated in the presence of both 1μM isoproterenol and 10μM muscarine, the accumulation of cAMP was almost identical to that stimulated by 1μM isoproterenol alone (11 ± 0.9 vs 11 ± 0.8 for 1μM isoproterenol). These data indicate that accumulation of isoproterenol-stimulated cAMP was not blocked by muscarine, at concentrations of muscarine effective in blocking LLP.

Discussion

NMDA receptors and synaptic plasticity

I have demonstrated that long-lasting changes in synaptic activity can be induced in medial perforant path/granule cell synapses of the rat dentate gyrus. High-frequency stimulation of the medial perforant path at a stimulus intensity suprathreshold for evoking a population spike reliably induced LTP. LTP was measured as a significant increase in both the amplitude of the population spike and the initial negative slope of the dendritic EPSP. Similarly, LLP of both population spike and EPSP were produced by bath application of either 1μM isoproterenol or 50μM norepinephrine. Both LTP and LLP were shown to be dependent on NMDA receptor activation, in that D(-)APV and CPP could block the induction of both (Burgard et al., 1989). In addition, D(-)APV was unable to reverse LLP. Both D(-)APV and CPP have been shown to have high affinity for NMDA binding sites (Davies et al., 1986; Watkins and Olverman, 1987) and to be effective in blocking LTP (Collingridge et al., 1983; Errington et al., 1987; Harris et al., 1986; Wigstrom et al., 1986). The results of these and other studies (Stanton, et al., 1989) demonstrate that LLP, like LTP, is a form of NMDA receptor-dependent neuronal plasticity.

I have also characterized the NMDA receptor-dependence of evoked responses recorded in the dentate gyrus (Burgard et al., 1989; Dahl et al., 1990). Both D(-)APV and CPP, at concentrations known to block LTP

at medial perforant path/granule cell synapses, depressed selective aspects of synaptic transmission. This indicates that NMDA receptors are activated during, and significantly contribute to, low frequency-evoked synaptic transmission in the medial perforant path. The effects of D(-)APV were stereospecific and restricted to orthodromic activation of granule cells, since antidromic activation was not affected by D(-)APV. This implies that D(-)APV did not produce a nonspecific depression of the granule cell action potential-generating mechanism. Specificity is also demonstrated by the ability of D(-)APV and CPP to produce a selective depression of medial, but not lateral, perforant path-evoked EPSP amplitudes (Dahl et al., 1990). NMDA receptor antagonists did not depress the initial negative slope of the medial perforant path-evoked EPSP, but depressed both the peak amplitude and area of the EPSP. The lack of effect on the initial negative slope indicates that NMDA receptors do not play a significant role in the initial synaptic depolarization of granule cell dendrites. This activity is mediated mainly by non-NMDA receptors (Kauer et al., 1988). However, as the membrane becomes more depolarized, NMDA receptors become activated due to their voltage sensitivity (Mayer and Westbrook, 1985). The activation of NMDA receptors at more depolarized potentials is reflected in the ability of NMDA receptor antagonists to reduce only the peak amplitude and area of the EPSP, as well as the amplitude of the population spike. The activation kinetics of the NMDA receptor-mediated component of the EPSP also predict the presence of a D(-)APV-sensitive component at longer latencies (Hestrin et al., 1990). Due to the slow onset of NMDA receptor activation, D(-)APV-induced depression should not

be recorded during the period of initial negative slope, but in the peak amplitude and area. In agreement with these findings, NMDA receptor-mediated EPSPs have been recorded in field CA1 neurons (Collingridge et al., 1988) and NMDA receptor antagonists have been shown to depress synaptic transmission in both field CA1 (Hablitz and Langmoen, 1986; Sah et al., 1989) and the dentate gyrus (Abraham and Mason, 1988). The ability of D(-)APV to cause an 'apparent' increase in paired-pulse inhibition in dentate gyrus (see Fig 6 of Burgard and Sarvey, in press) adds support to the idea that NMDA receptor-mediated long-latency EPSPs may be activated in granule cells. Reduction of these EPSPs by D(-)APV would cause a decrease in paired-pulse facilitation, which would be manifested as an increase in paired-pulse inhibition.

These results indicate that NMDA receptors contribute significantly to synaptic activity evoked in the medial perforant path. They also demonstrate that both LTP and LLP of synaptic activity in the medial perforant path are dependent upon NMDA receptor activation. Consistent with these findings, there is neurochemical evidence to indicate that the major excitatory neurotransmitter of the perforant path is glutamate (White et al., 1977). In addition, the molecular layer of the dentate gyrus contains one of the highest levels of NMDA-sensitive ^{3}H-glutamate binding sites in the rat brain (Monaghan and Cotman, 1985). LTP of the perforant path has been shown to be sensitive to NMDA receptor antagonists (Errington et al., 1987, Wigstrom et al., 1986), although separation of medial vs lateral perforant path was not specified in these studies.

The mechanisms behind NMDA receptor regulation of LLP remain

unclear. It is clear, however, that both ß-adrenergic and NMDA receptor activation are required for either LTP or LLP induction in the dentate gyrus. Previous studies have demonstrated that LTP in the dentate gyrus can be blocked or significantly reduced by either ß-adrenergic receptor antagonists or chronic norepinephrine depletion *in vivo* (Stanton and Sarvey, 1985b; 1987). LLP can also be blocked by ß-adrenergic receptor antagonists (Stanton and Sarvey, 1985a; Dahl and Sarvey 1989). I have considered three possible mechanisms which could explain the NMDA receptor-dependence of LLP:

1) ß-adrenergic receptor activation facilitates the activation of NMDA receptors by a postsynaptic mechanism independent of NMDA receptors. Studies have shown that norepinephrine causes an initial ß-receptor-mediated reduction in a Ca^{++}-dependent K^{+} conductance (Haas and Rose, 1987) in dentate granule cells. This is believed to be the mechanism responsible for the decrease in accommodation, increase in input resistance, and membrane depolarization produced by ß-adrenergic receptor activation in these cells (Stanton et al., 1989). Norepinephrine also stimulates a cAMP-regulated voltage-dependent calcium current (Gray and Johnston, 1987) in dentate granule cells. All of these effects could facilitate postsynaptic NMDA receptor activation by increasing postsynaptic excitability, leading to LLP. This hypothesis could be directly tested by experimentally holding the postsynaptic membrane (under voltage clamp) at resting membrane potential during application of ß-adrenergic agonists. In this way, the depolarization induced by ß-adrenergic receptor activation could be prevented, and the induction of LLP could be monitored.

2) Activation of postsynaptic ß-adrenergic receptors directly modulates NMDA receptors through a second messenger system. I have demonstrated that activation of ß-adrenergic receptors produces an increase in cAMP accumulation in slices of dentate gyrus. cAMP acts as an intracellular second messenger which activates cAMP-dependent protein kinase (PKA). PKA could then activate or phosphorylate the NMDA receptor to cause a transient activation of the receptor. Although this is purely speculative, it is a testable hypothesis. Using intracellular and/or patch clamp recording techniques to record from individual neurons, the NMDA receptor-mediated component of the intracellular EPSP could be monitored. Application of norepinephrine, or intracellular injections of cAMP analogs or PKA should all produce a transient enhancement of the NMDA receptor-mediated component of the EPSP, and this effect should be blocked by inhibitors of PKA. These experiments would have to be performed under voltage clamp conditions to exclude depolarization-induced effects such as described in 1), above. The fact that D(-)APV can block phorbol ester-induced potentiation (see Results) sets a precedent for this hypothesis. Possibly, stimulation of PKC by phorbol esters also produces a transient enhancement of the NMDA receptor-mediated component of the EPSP. This could lead to D(-)APV-sensitive long-lasting potentiation of evoked responses, as proposed above for the cAMP system.

3) ß-adrenergic receptor activation induces LLP by a presynaptic mechanism. There is evidence to suggest a ß-adrenergic modulation of glutamate release in the dentate (Lynch and Bliss, 1986). On the other hand, NMDA receptor activation may occur presynaptically to

modulate glutamate release (Errington et al., 1987). An increase in glutamate release could also increase the probability of postsynaptic NMDA receptor activation leading to potentiation of evoked responses. Interestingly, Dahl and Sarvey (1990) have shown that LLP, although blocked by NMDA receptor antagonists, does not require low-frequency electrical stimulation of the presynaptic terminals. Possibly a ß-adrenergic-induced increase in resting glutamate release, coupled with significant NMDA receptor activation in the resting state is sufficient to induce LLP. The ability of D(-)APV to block phorbol ester-induced potentiation also supports a presynaptic locus for induction of long-lasting potentiation. Possibly, activation of PKC by phorbol esters increases glutamate release from presynaptic terminals, leading to a postsynaptic NMDA receptor-mediated potentiation of synaptic transmission.

Muscarinic receptors and synaptic plasticity

I have demonstrated that muscarine, a nonselective muscarinic receptor agonist, produced a concentration-dependent depression of evoked responses in the dentate gyrus. At concentrations $\leq 1\mu M$, muscarine produced no significant depression, but at concentrations $\geq 10\mu M$, muscarine produced almost complete depression of the population spike amplitude, along with a reduction in the slope of the EPSP. The depression of the population spike produced by $10\mu M$ muscarine was not PTx-sensitive, and was blocked by three competitive muscarinic receptor

antagonists with relative potencies: 4-DAMP > pirenzepine > AFDX-116.

Pharmacological data from a number of laboratories (Hammer et al., 1980; Doods et al., 1987; Micheletti et al., 1987; Eltze, 1988) indicate that three muscarinic receptor subtypes can be relatively selectively identified. As indicated in Table 1, atropine, a nonselective antagonist, displays a high affinity (high pA_2) for all three subtypes. Pirenzepine has a high affinity for M1 receptors, while AFDX-116 displays a relatively high affinity for M2 receptors. 4-DAMP has a high affinity for both M1 and M3 receptors. The three subtypes can also be distinguished on the basis of their coupling mechanisms to intracellular second messenger systems. It has generally been accepted that both M1 and M3 receptor activation initiates the hydrolysis of phosphotidylinositol 4,5 bisphosphate (PI) through a PTx-insensitive G protein. M2 receptor activation inhibits adenylyl cyclase through a PTx-sensitive G protein (G_i), leading to a decrease in intracellular cAMP (see Hulme et al., 1990). In the dentate gyrus, autoradiographic studies have revealed high concentrations of pirenzepine-sensitive M1 receptors (Cortes and Palacios, 1986; Mash and Potter, 1986). *In situ* hybridization has also revealed high levels of M1 and M3 mRNA in the dentate gyrus, with lower levels of M4, and virtually no M2 mRNA (Bonner et al., 1987; Mei et al., 1989).

My results indicate that depression of evoked responses by muscarine involves activation of M1 or M3 receptors. Increasing concentrations of pirenzepine shifted the concentration-response curve for muscarine to the right in a competitive manner. The EC50s for muscarine in the presence of various concentrations of pirenzepine were

increased, while there appeared to be no change in the maximal depression produced by muscarine. Construction of a Schild plot from the EC50s of muscarinic depression in the presence of pirenzepine revealed an estimated pA_2 value for pirenzepine of 6.2. The slope of the line fit to the data points in this plot revealed a slope of -1.04, indicating competitive antagonism of muscarinic depression by pirenzepine (Tallarida et al., 1979).

The pA_2 value for pirenzepine obtained in this study is much less than those listed for antagonism of the M1 receptor in Table 1. This may be due to the experimental design used in these experiments. In these experiments, pirenzepine was applied for 10 min before, and during a 10 min application of muscarine. Realistically, a Schild plot relies on the ability of the antagonist to reach equilibrium binding to the receptor (Tallarida et al., 1979). Studies examining the ability of compounds to wash into hippocampal slices in a recording chamber have shown that it may take hours to actually reach equilibrium (Muller et al., 1988). The pirenzepine plus muscarine experiments outlined above were initially designed to examine muscarinic effects on either LTP or LLP, where complete washout of compounds following the induction of LTP or LLP is critical. This made it impractical to bath apply muscarinic receptor antagonists for extended periods of time. In retrospect, the method used by Sheridan and Sutor (1990) to study antagonism of muscarinic depression by pirenzepine in field CA1 of the hippocampus could have been used. They exposed slices to pirenzepine for 45 min before adding muscarine, but then performed cumulative concentration-response curves, and arrived at a higher pA_2 value (7.4). However, the

addition of cumulative concentrations of agonists to a single slice assumes the absence of desensitization of the response. Although I never observed any desensitization of muscarinic depression, I chose to limit exposure of a slice to one agonist concentration, or if a subsequent agonist application was used, it was separated from the first by at least 20 min of drug-free wash.

A concentration of 10μM muscarine produced almost complete depression of the population spike and a significant depression of the EPSP. This concentration was chosen for use in many subsequent experiments, because it was greater than the estimated EC50, but less than maximum. The relative potency of muscarinic receptor antagonists was estimated by their ability to antagonize 10μM muscarine-induced depression of the population spike. The relative EC50s were: 4-DAMP, 0.12μM; pirenzepine, 1.0μM; and AFDX-116, 3.3μM. The EC50 for 4-DAMP was approximately a log concentration less than that for pirenzepine. Since the EC50 for pirenzepine was approximately the same as its pA_2 value in these experiments, (1.0μM vs 0.63μM), then the same might apply to 4-DAMP. Following this assumption, the pA_2 for 4-DAMP would also be approximately a log concentration greater than that for pirenzepine. This is consistent with the data presented in Table 1. This table shows that 4-DAMP has a pA_2 for M1 receptors approximately a log concentration greater than pirenzepine. This suggests that both pirenzepine and 4-DAMP block muscarinic depression by antagonism at M1 receptors. However, the pA_2 of 4-DAMP for M3 receptors is also comparably high. Blockade of muscarinic depression by 4-DAMP via antagonism of M3 receptors cannot be ruled out. AFDX-116 was the least potent antagonist

in these experiments. According to Table 1, if muscarinic depression was mediated by M2 receptors, then AFDX-116 should be a more potent antagonist of this effect than pirenzepine, based on the published pA_2 values. From the pharmacological data, it appears that muscarinic depression is produced by activation of either M1 or M3 receptors.

Evidence supporting the hypothesis that M1 or M3 receptor activation mediates muscarinic depression comes from two additional sets of experiments. In the first, PTx was used to discriminate between receptor subtypes. PTx catalyzes the ADP-ribosylation of selective G proteins (Gilman, 1987). PTx-treatment blocks the activity of these G proteins, and functionally uncouples the receptor from its intracellular effector mechanism. In these experiments, hippocampal slices from PTx-treated rats were exposed to a 10 min bath application of 10μM muscarine, as above. The efficacy of the injection was analyzed by its ability to block $GABA_B$-mediated responses. In these slices, muscarine produced a depression of evoked responses that was not significantly different than that produced in untreated control slices. Since M2 (Ashkenazi et al., 1987; Hulme et al., 1990), but not M1 or M3 (Jones et al., 1990) receptors appear to be linked to PTx-sensitive G proteins, it does not appear that M2 receptor activation mediates muscarinic depression.

In the second set of experiments examining possible involvement of M2 receptors, cAMP accumulation was measured from slices of dentate gyrus. M2 receptors have been shown to be linked to inhibition of adenylyl cyclase through activation of a PTx-sensitive G protein, G_i (Ashkenazi, et al., 1987). A substantial basal accumulation of cAMP

from dentate gyrus slices was measured (6.9 ± 0.5 pmol). The slices were capable of producing cAMP, as recorded in response to activation of ß-adrenergic receptors (11.5 ± 0.8 pmol). A concentration of 10μM (or up to 100μM) muscarine did not affect basal accumulation of cAMP in these slices. In addition, 10μM muscarine had no effect on the isoproterenol-induced increase in [cAMP]. The concentration of isoproterenol (1μM) that produced a significant increase in [cAMP] was the same as that which induced LLP. The inability of muscarine, at concentrations of 10 - 100μM, to modulate either basal or stimulated cAMP levels suggests that M2 receptors may not be involved in muscarinic depression. To further test this hypothesis, intracellular injections of cAMP analogs could be analyzed in terms of their abilities to prevent and/or reverse muscarinic depression.

I have also demonstrated that muscarine can differentially regulate the induction of either LTP or LLP. Both LTP and LLP displayed 'thresholds' for induction, below which neither was reliably induced. High-frequency stimulation of the medial perforant path, at an intensity that was subthreshold for evoking a population spike, did not induce LTP. Likewise, bath application of 0.1μM isoproterenol did not induce LLP (see Burgard and Sarvey, in press), and was therefore considered a subthreshold concentration. The ability to define a stimulus and/or concentration parameter, above (but not below) which long-lasting changes in synaptic activity could be produced, allowed an examination of either facilitation or inhibition of these changes.

Application of a low concentration (1μM) of muscarine, while producing no significant depression of evoked responses, facilitated the

induction of LTP (Burgard and Sarvey, 1990). The facilitation of LTP induction could be blocked with a low concentration (1μM) of pirenzepine. However, when the concentration of muscarine was increased to 10μM, induction of LTP was not facilitated. On the other hand, 10μM muscarine did not block the induction of LTP induced by a suprathreshold stimulus intensity. These results suggest a 'biphasic' effect of muscarine on LTP induction at different concentrations. At a concentration below that which produces a measurable depression, LTP induction can be facilitated. This facilitation is blocked by pirenzepine, and is therefore probably M1 receptor-mediated. When the concentration is increased, the facilitation is lost, although no inhibitory effect on LTP induction is observed.

M1 receptor activation produces a slow depolarization in dentate granule cells (Muller and Misgeld, 1986) and also blocks a K^+-mediated afterhyperpolarization in CA1 pyramidal neurons (Cole and Nicoll, 1983; Dutar and Nicoll, 1988). These effects could lead to an increased excitability of granule cells, which could facilitate LTP induction by facilitating granule cell depolarization during an HFT. In addition, M1 receptor activation has been linked to activation of phospholipase C and phosphatidylinositol turnover (Gil and Wolfe, 1985; Peralta et al., 1988; Audigier et al., 1988). These intracellular second messengers may play a role in the induction and maintenance of LTP via phosphorylation of certain cellular proteins such as B-50 (Linden and Routtenberg, 1989), which have also been found to be substrates for muscarinic receptor-induced phosphorylation (Van Hooff et al., 1989).

In contrast to the facilitatory effects of muscarine on the

induction of LTP, muscarinic modulation of LLP was inhibitory. At a concentration of 1μM, muscarine reduced, and at 10μM, completely blocked the induction of LLP. The blockade of LLP by 10μM muscarine could be prevented by pre- and coapplication of 20μM pirenzepine. In addition, 1μM muscarine could not facilitate the induction of LLP, as it facilitated the induction of LTP. There was a positive correlation between the concentration-dependent depression of evoked responses and the inhibition of LLP by muscarine. It appeared as if blockade of inhibition of LLP was dependent on the amount of depression produced by muscarine. As demonstrated earlier, muscarinic inhibition could be competitively antagonized by pirenzepine. A concentration of 20μM pirenzepine was needed to block the depression of evoked responses produced by 10μM muscarine. This concentration of pirenzepine also prevented blockade of LLP by 10μM muscarine. In agreement with these observations, the depression of medial perforant path-evoked responses by a high concentration (10μM) of the muscarinic agonist carbachol has been described by Kahle and Cotman (1989), who also showed that high concentrations (10μM) of pirenzepine were required to block the depression. It appears that M1 or M3 receptor-mediated depression of evoked responses is responsible for blockade of LLP.

Why are pirenzepine-sensitive receptors responsible for both facilitation of LTP induction and depression of evoked responses leading to inhibition of LLP? There may be different explanations for this. Sheridan and Sutor (1990), recording both extracellular dendritic EPSPs and intracellular responses in field CA1 demonstrated that 1 - 3μM carbachol (another nonselective muscarinic agonist) would increase

excitability of pyramidal cells in response to depolarizing current pulses. Increased excitability was measured as a membrane depolarization, increased input resistance, reduced accommodation of spike firing, and a decreased afterhyperpolarization (AHP) associated with the spike train. At the same concentrations, however, extracellular EPSPs were depressed. This depression was competetively antagonized by pirenzepine, with a pA_2 of 7.4. These data suggest that increased excitability is a postsynaptic effect, and the pirenzepine-sensitive depression of evoked responses is presynaptic. Other studies have shown that increased neuronal (postsynaptic) excitability is also pirenzepine sensitive. Depolarization of dentate granule cells (Muller and Misgeld, 1986) and substantia nigra neurons (Lacey et al., 1990) are both sensitive to antagonism by pirenzepine ($\leq 1\mu M$), as are the blockade of a K^+-mediated AHP and depolarization in CA1 pyramidal cells (Cole and Nicoll, 1983; Dutar and Nicoll, 1988). These studies support the hypothesis that both facilitation of LTP (via increased postsynaptic excitability) and depression of evoked responses (via presynaptic inhibition) leading to a blockade of LLP are mediated by pirenzepine-sensitive M1 receptors. In addition, Markram and Segal (1990) have shown that muscarinic receptor activation can potentiate postsynaptic pyramidal cell responses to NMDA. Potentiation of NMDA receptor activity could also facilitate LTP induction. On the other hand, voltage-dependent postsynaptic effects of muscarinic receptor activation have also been reported. Akins et al., (1990) reported that muscarinic receptor modulation of the A current, a fast transient outward K^+ current, was voltage dependent. At relatively hyperpolarized membrane

potentials, carbachol decreased excitability by activation of the A current, whereas at depolarized potentials, carbachol increased excitability by inactivation of this current. Inactivation of the A current during a depolarizing stimulus train could also explain facilitation of LTP by muscarine. However, the pirenzepine sensitivity of this effect was not reported.

A testable hypothesis for the mechanisms of action of muscarine on the induction of synaptic plasticity can be constructed. The facilitation of LTP induction in the dentate gyrus is hypothesized to be due to preferential activation of postsynaptic M1 receptors at low concentrations of muscarine. Activation of these receptors increases the excitability of the granule cell, and facilitates depolarization during application of a subthreshold high frequency stimulus train. This is sufficient to activate otherwise nonactivated NMDA receptors, leading to LTP. As the concentration of muscarine is increased, presynaptic M1 (or M3) receptors are activated, which function to depress synaptic activity by decreasing sustained release of glutamate from the nerve terminal. This inhibitory effect is sufficient to counteract the postsynaptic depolarization, and block facilitation of LTP. However, with application of a suprathreshold stimulus train, presynaptic inhibition is overcome, and induction of LTP is not affected. By monitoring the intracellular NMDA receptor-mediated component of the EPSP, a transient concentration-dependent increase in this component would be recorded at low concentrations of muscarine. At higher concentrations, an overall reduction in the EPSP would counteract the increased NMDA component, blocking facilitation.

The same mechanisms could be responsible for blockade of LLP by muscarine. LLP is dependent on NMDA receptor activation, and is hypothesized to increase the NMDA receptor-mediated component of the intracellularly-recorded EPSP. This action, coupled with tonic release of glutamate from perforant path terminals, and a substantial NMDA receptor-mediated component of the extracellularly-recorded EPSP, is sufficient to induce LLP. A concentration-dependent increase in presynaptic inhibition by muscarine would decrease the amount of glutamate available for NDMA receptor activation, thus blocking LLP. Alternatively, the site of LLP induction may be presynaptic, acting to increase glutamate release. If the site of induction was presynaptic, ß-adrenergic and muscarinic receptor activation would have opposite effects on neurotransmitter release. By monitoring stimulus-induced glutamate release from the perforant path, the concentration-dependent effects of muscarinic and ß-adrenergic agonists on neurotransmitter release could be assessed. The inability of low concentrations of muscarine to facilitate LLP induction may be due to the inability of muscarine to sufficiently excite (or depolarize) the postsynaptic membrane as may be the case with a subthreshold HFT or baclofen application. This could be tested by performing intracellular and/or patch clamp recordings, comparing membrane depolarizations produced by muscarine, baclofen, and subthreshold HFTs, and their abilities to facilitate induction of long-lasting synaptic plasticity.

The immediate goal of this dissertation was to investigate the muscarinic cholinergic modulation of two similar, yet different, forms of synaptic plasticity: LTP and ß-adrenergic agonist-induced LLP.

However, the ultimate goal was to determine the degree of similarity between these two phenomena. Their response to modulation by different neurotransmitter systems may indicate which cellular processes underlie each form of plasticity, and may also reveal which processes are universally required for induction of long-lasting plasticity. For example, both LTP and ß-adrenergic LLP are 1) induced in both the population spike and EPSP in the dentate gyrus (Stanton and Sarvey, 1987), 2) blocked by ß-adrenergic antagonists (Stanton and Sarvey, 1985b), 3) blocked by inhibitors of protein synthesis (Stanton and Sarvey, 1985a), 4) blocked by NMDA receptor antagonists (Burgard et al., 1989), and 5) facilitated by the $GABA_B$ receptor agonist baclofen in the dentate gyrus (see Burgard and Sarvey, in press; Mott et al., 1990). From the above data it appears that the two forms of synaptic plasticity are very similar. However, LTP and ß-adrenergic LLP are very different in their response to muscarinic receptor activation. It is in this context, that the differences and similarities between LTP and ß-adrenergic LLP may be discerned through their modulation by various neurotransmitter systems, that this dissertation should be viewed.

References

Abraham, W.C., and Mason, S.E., Effects of the NMDA receptor/channel antagonists CPP and MK801 on hippocampal field potentials and long-term potentiation in anaesthetized rats, Brain Res., 462 (1988) 40-46.

Akins, P.T., Surmeier, D.J., and Kitai, S.T., Muscarinic modulation of a transient K^+ conductance in rat neostriatal neurons, Nature, 344 (1990) 240-242.

Alger, B.E., and Teyler, T.J., Long-term and short-term plasticity in the CA1, CA3, and dentate regions of the rat hippocampal slice, Brain Res., 110, (1976) 463-480.

Artola, A., and Singer, W., Long-term potentiation and NMDA receptors in rat visual cortex, Nature, 330 (1987) 649-652.

Arunlakshana, O., and Schild, H.O., Some Quantitative uses of drug antagonists, Brit. J. Pharmacol., 14 (1959) 48-58.

Ashkenazi, A., Winslow, J.W., Peralta, E.G., Peterson, G.L., Schimerlik, M.I., Capon, D.J., and Ramachandran, J., An M2 muscarinic receptor subtype coupled to both adenylyl cyclase and phosphoinositide turnover, Science, 238 (1987) 672-675.

Audigier, S.M.P., Wang, J.K.T., and Greengard, P., Membrane depolarization and carbamoylcholine stimulate phosphatidylinositol turnover in intact nerve terminals, Proc. Natl. Acad. Sci., 85 (1988) 2859-2863.

Bekkers, J.M., and Stevens, C., Presynaptic mechanism for long-term

potentiation in the hippocampus, Nature, 346 (1990) 724-728.

Berger, T.W., Long-term potentiation of hippocampal synaptic transmission affects rate of behavioral learning, Science, 224 (1984) 627-630.

Bliss, T.V.P., and Gardner-Medwin, A.R., Long-lasting potentiation of synaptic transmission in the dentate area of the unanaesthetized rabbit following stimulation of the perforant path, J. Physiol., 232 (1973) 357-374.

Bliss, T.V.P., and Lømo, T., Long-lasting potentiation of synaptic transmission in the dentate area of the anaesthetized rabbit following stimulation of the perforant path, J. Physiol., 232 (1973) 331-356.

Bonner, T.I., Buckley, N.J., Young, A., and Brann, M.R., Identification of a family of muscarinic receptor genes, Science, 237 (1987) 527-532.

Brown, B.L., Albano, J.D.M., Ekins, R.P., Sgherzi, A.M., and Tampion, W., A simple and sensitive saturation assay method for the measurement of adenosine 3′:5′-cyclic monopohosphate, Biochem. J., 121 (1971) 561-562.

Buckley, N.J., Bonner, T.I., and Brann, M.R., Localization of a family muscarinic receptor mRNAs in rat brain, J. Neurosci., 8 (1988) 4646-4652.

Burgard, E.C., Decker, G., and Sarvey, J.M. NMDA receptor antagonists block norepinephrine-induced long-lasting potentiation and long-term potentiation in rat dentate gyrus, Brain Res., 482 (1989) 351-355.

Burgard, E.C., and Sarvey, J.M., Baclofen-induced epileptiform activity is reduced by the NMDA receptor antagonist D-2-amino-5-phosphonovaleric acid (APV) in rat dentate gyrus, Society for Neuroscience Abstracts, 15 (1989) 1214.

Burgard, E.C., and Sarvey, J.M., Muscarinic receptor activation facilitates the induction of long-term potentiation (LTP) in the rat dentate gyrus, Neurosci. Lett., 116 (1990) 34-39.

Burgard, E.C., and Sarvey, J.M., Long-lasting potentiation and epileptiform activity produced by $GABA_B$ receptor activation in the dentate gyrus of rat hippocampal slice, J. Neurosci., (in press).

Chandler, J.P., and Crutcher, K.A., The septohippocampal projection in the rat: an electron microscopic horseradish peroxidase study, Neuroscience, 10 (1983) 685-696.

Clarke, D.J., Cholinergic innervation of the rat dentate gyrus: an immunocytochemical and electron microscopical study, Brain Res., 360 (1985) 349-354.

Cline, H.T., and Constantine-Paton, M., NMDA receptor agonist and antagonists alter retinal ganglion cell arbor structure in the developing frog retinotectal projection, J. Neurosci., 10 (1990) 1197-1216.

Coan, E.J., and Collingridge, G.L., Characterization of an N-methyl-D-aspartate receptor component of synaptic transmission in rat hippocampal slices, Neuroscience, 22 (1987) 1-8.

Cole, A.E., and Nicoll, R.A., Acetylcholine mediates a slow synaptic potential in hippocampal pyramidal cells, Science, 221 (1983) 1299-1301.

Collingridge, G.L., Kehl, S.J., and McLennan, H., Excitatory amino acids in synaptic transmission in the Schaffer collateral-commissural pathway of the rat hippocampus, J. Physiol., 334 (1983) 33-46.

Collingridge, G.L., Herron, C.E., and Lester, R.A.J., Synaptic activation of N-methyl-D-aspartate receptors in the Schaffer collateral-commissural pathway of rat hippocampus, J. Physiol., 399 (1988) 283-300.

Cortes, R., and Palacios, J.M., Muscarinic cholinergic receptor subtypes in the rat brain. I. Quantitative autoradiographic studies, Brain Res., 362 (1986) 227-238.

Cotman, C.W., and Monaghan, D.T., Organization of excitatory amino acid receptors: functional implications, in Excitatory Amino Acid Transmission, (1987) Alan R. Liss, Inc., 325-332.

Crutcher, K.A., and Davis, J.N., Hippocampal a- and ß-adrenergic receptors: comparison of [^{3}H]dihydroalprenolol and [^{3}H]WB4101 binding with noradrenergic innervation in the rat, Brain Res., 182 (1980) 107-117.

Dahl, D., and Sarvey, J.M., Norepinephrine induces pathway-specific long-lasting potentiation and depression in the hippocampal dentate gyrus, Proc. Natl. Acad. Sci., 86 (1989) 4776-4780.

Dahl, D., and Sarvey, J.M., ß-Adrenergic agonist-induced long-lasting synaptic modifications in hippocampal dentate gyrus require activation of NMDA receptors, but not electrical activation of afferents, Brain Res., 526 (1990) 347-350.

Dahl, D., Burgard, E.C., and Sarvey, J.M., NMDA receptor antagonists reduce medial, but not lateral, perforant pathway-evoked EPSPs in

dentate gyrus of rat hippocampal slices, Exp. Brain Res., (1990) in press.

Davies, J., Evans, R.H., Herrling, P.L., Jones, A.W., Olverman, H.J., Pook, P., and Watkins, J.C., CPP, a new potent and selective NMDA antagonist. Depression of central neuron responses, affinity for [^{3}H]D-AP5 binding sites on brain membranes and anticonvulsant activity, Brain Res., 382 (1986) 169-173.

Davies, S.N., Alford, S.T., Coan, E.J., Lester, R.A.J., and Collingridge, G.L., Ketamine blocks an NMDA receptor-mediated component of synaptic transmission in rat hippocampus in a voltage-dependent manner, Neurosci. Lett., 92 (1988) 213-217.

Davies, S.N., Lester, R.A.J., Reymann, K.G., and Collingridge, G.L., Temporally distinct pre- and post-synaptic mechanisms maintain long-term potentiation, Nature, 338 (1989) 500-503.

Deutsch, J.A., The cholinergic synapse and the site of memory, Science, 174 (1971) 788-794.

Doods, H.N., Mathy, M., Davidesko, K., van Charldorp, K.J., de Jonge, A., and van Zwieten, P.A., Selectivity of muscarinic antagonists in radioligand and in vivo experiments for the putative M1, M2, and M3 receptors, J. Pharm. Exp. Ther., 242 (1987) 257-262.

Douglass, R.M., and Goddard, G.V., Long-term potentiation of the perforant path-granule cell synapse in the rat hippocampus, Brain Research, 86 (1975) 205-215.

Durkin, T., Central cholinergic pathways and learning and memory processes: presynaptic aspects, Comp. Biochem. Physiol., 93A (1989) 273-280.

Dutar, P., and Nicoll, R.A., Classification of muscarinic responses in hippocampus in terms of receptor subtypes and second-messenger systems: electrophysiological studies in vitro, J. Neurosci., 8 (1988) 4214-4224.

Egan, T.M., and North, R.A., Acetylcholine hyperpolarizes central neurones by acting on an M_2 muscarinic receptor, Nature, 319 (1986) 405-407.

Eltze, M., Muscarinic M_1 and M_2 receptors mediating opposite effects on neuromuscular transmission in rabbit vas deferens, Eur. J. Pharmacol., 151 (1988) 205-221.

Errington, M.L., Lynch, M.A., and Bliss, T.V.P., Long-term potentiation in the dentate gyrus: induction and increased glutamate release are blocked by D(-)aminophosphonovalerate, Neuroscience, 20 (1987) 279-284.

Fagg, G.E., Foster, A.C., and Ganong, A.H., Excitatory amino acid synaptic mechanisms and neurological function, Trends Pharmacol. Sci., 7 (1986) 357-363.

Foster, A.C., and Fagg, G.E., Acidic amino acid binding sites in mammalian neuronal membranes: their characteristics and relationship to synaptic receptors, Brain Res. Reviews, 7 (1984) 103-164.

Frey, E.A., and Gosse, M., Determination of adenylate cyclase activity by the Brown method, Laboratory Manual, (1989).

Frotscher M., and Leranth C., Cholinergic innervation of the rat hippocampus as revealed by choline acetyltransferase immunocytochemistry: a combined light and electron microscopic

study, J. Comp. Neurol., 239 (1985) 237-246.

Gil, D.W., and Wolfe, B.B., Pirenzepine distinguishes between muscarinic receptor-mediated phosphoinositide breakdown and inhibition of adenylate cyclase, J. Pharm. Exp. Ther., 232 (1985) 608-616.

Gilman, A.G., G proteins: transducers of receptor-generated signals, Annu. Rev. Biochem., 56 (1987) 615-649.

Giraldo, E., Hammer, R., and Ladinsky, H., Distribution of muscarinic receptor subtypes in rat brain as determined in binding studies with AFDX-116 and pirenzepine, Life Sciences, 40 (1987) 833-840.

Gray, R., and Johnston, D., Noradrenaline and ß-adrenoceptor agonists increase activity of voltage-dependent calcium channels in hippocampal neurons, Nature, 327 (1987) 620-622.

Haas, H.L., and Rose, G.M., Noradrenaline blocks potassium conductance in rat dentate granule cells in vitro, Neurosci. Lett., 78 (1987) 171-174.

Hablitz, J.J., and Langmoen, I.A., N-methyl-D-aspartate receptor antagonists reduce synaptic excitation in the hippocampus, J. Neurosci., 6 (1986) 102-106.

Hammer R., Berrie, C.P., Birdsall, N.J.M., Burgen, A.S.V., and Hulme, E.C., Pirenzepine distinguishes between different subclasses of muscarinic receptors, Nature, 283 (1980) 90-92.

Harris, E.W., and Cotman, C.W., Long-term potentiation of guinea pig mossy fiber responses in not blocked by N-methyl D-aspartate antagonists, Neurosci. Lett., 70 (1986) 132-137.

Harris, E.W., Ganong, A.H., and Cotman, C.W., Long-term potentiation in the hippocampus involves activation of N-methyl-D-aspartate

receptors, Brain Res., 323 (1984) 132-137.

Harris, E.W., Ganong, A.H., Monaghan, D.T., Watkins, J.C., and Cotman, C.W., Action of 3-((+)-2-carboxypiperazin-4-yl)-propyl-1-phosphonic acid (CPP): a new and highly potent antagonist of N-methyl-D-aspartate receptors in the hippocampus, Brain Res., 382 (1986) 174-177.

Hebb, D.O., The Organization of Behavior, (1949) Wiley, New York, 62-66, 126-134.

Hestrin, S., Nicoll, R.A., Perkel, D.J., and Sah, P., Analysis of excitatory synaptic action in pyramidal cells using whole-cell recording from rat hippocampal slices, J. Physiol., 422 (1990) 203-225.

Hirotsu, I., Hori, N., Katsuda, N., and Ishihara, T., Effect of anticholinergic drug on long-term potentiation in rat hippocampal slices, Brain Res., 482 (1989) 194-197.

Hjorth-Simonsen, A., Projection of the lateral part of the entorhinal area to the hippocampus and fascia dentata, J. Comp. Neurol., 146 (1972) 219-232.

Hjorth-Simonsen, A., and Jeune, B., Origin and termination of the hippocampal perforant path in the rat studied by silver impregnation, J. Comp. Neurol., 144 (1972) 215-232.

Hopkins, W.F., and Johnston, D., Frequency-dependent noradrenergic modulation of long-term potentiation in hippocampus, Science, 226 (1984) 350-352.

Hopkins, W.F., and Johnston, D., Noradrenergic enhancement of long-term potentiation at mossy fiber synapses in the hippocampus, J.

Neurophysiol., 59 (1988) 667-687.

Hulme, E.C., Birdsall, N.J.M., and Buckley, N.J., Muscarinic receptor subtypes, Anna. Rev. Pharmacol. Toxicol., 30 (1990) 633-673.

Jones, S.M., Snell, L.D., and Johnson, K.M., Phencyclidine selectively inhibits N-methyl-D-aspartate-induced hippocampal [^{3}H]norepinephrine release, J. Pharm. Expt. Therap., 240 (1987) 492-497.

Jones, S.V.P., Barker, J.L., Goodman, M.B., and Brann, M.R., Inositol trisphosphate mediates cloned muscarinic receptor-activated conductances in transfected mouse fibroblast A9 L Cells, J. Physiol., 421 (1990) 499-519.

Kahle, J.S., and Cotman, C.W., Carbachol depresses synaptic responses in the medial but not the lateral perforant path, Brain Res., 482 (1989) 159-163.

Kandel, E.R., and Schwartz, J.H., Molecular biology of learning: modulation of transmitter release, Science, 218 (1982) 433-443.

Kauer, J., Malenka, R.C., and Nicoll, R.A., persistent postsynaptic modification mediates long-term potentiation in the hippocampus, Neuron, 1 (1988) 911-917.

Kelso, S.R., Ganong, A.H., and Brown, T.H., Hebbian synapses in hippocampus, Proc. Natl, Acad. Sci. USA, 83 (1986) 5326-5330.

Kleinschmidt, A., Bear, M.F., and Singer, W., Blockade of "NMDA" receptors disrupts experience-dependent plasticity of kitten striate cortex, Science, 238 (1987) 355-358.

Lacaille, J.-C., and Harley C.W., The action of norepinephrine in the dentate gyrus: Beta-mediated facilitation of evoked responses in

vitro, Brain Res., 358 (1985) 210-220.

Lacaille, J.-C., and Schwartzkroin, P.A., Intracellular responses of rat hippocampal granule cells in vitro to discrete applications of norepinephrine, Neurosci. Lett., 89 (1988) 176-181.

Lacey, M.G., Calabresi, P., and North, R.A., Muscarine depolarizes rat substantia nigra zona compacta and ventral tegmental neurons in vitro through M1-like receptors, J. Pharm. Expt. Therap., 253 (1990) 395-400.

Linden, D.J., and Routtenberg, A., The role of protein kinase C in long-term potentiation: a testable model, Brain Res. Rev., 14 (1989) 279-296.

Lowry, O.H., Rosebrough, N.J., Farr, A.L., and Randall, R.J., Protein measuremens with Folin phenol reagent, J. Biol. Chem., 193 (1951) 265-275.

Loy, R., Koziell, D.A., Lindsey, J.D., and Moore, R.Y., Noradrenergic innervation of the adult rat hippocampal formation, J. Comp. Neurol., 189 (1980) 699-710.

Lynch, G., Larson, J., Kelso, S., Barrionuevo, G., and Schottler, F., Intracellular injections of EGTA block induction of hippocampal long-term potentiation, Nature, 305 (1983) 719-721.

Lynch, M.A., and Bliss, T.V.P., Noradrenaline modulates the release of [14C]glutamate from dentate but not from CA1/CA3 slices of rat hippocampus, Neuropharmacology, 25 (1986) 493-498.

MacDermott, A.B., Mayer, M.L., Westbrook, G.L., Smith, S.J., and Barker, J.L., NMDA-receptor activation increases cytoplasmic calcium concentration in cultured spinal cord neurones, Nature,

321 (1986) 519-522.

Madison, D.V., and Nicoll, R. A., Cyclic adenosine 3',5'-monophosphate mediates ß-receptor actions of noradrenaline in rat hippocampal pyramidal cells, J. Physiol., 372 (1986) 245-259.

Malenka, R.C., Kauer, J.A., Zucker, R.S., and Nicoll, R.A., Postsynaptic calcium is sufficient for potentiation of hippocampal synaptic transmission, Science, 242 (1988) 81-84.

Malenka, R.C., Kauer, J.A., Perkel, D.J., and Nicoll, R.A., The impact of postsynaptic calcium on synaptic transmission - its role in long-term potentiation, Trends Neurosci., 12 (1989) 444-450.

Malinow, R., and Tsien, R.W., Presynaptic enhancement shown by whole-cell recordings of long-term potentiation in hippocampal slices, Nature, 346 (1990) 177-180.

Markram, H., and Segal, M., Acetylcholine potentiates responses to N-methyl-D-aspartate in the rat hippocampus, Neurosci. Lett., 113 (1990) 62-65.

Mash, D.C., and Potter, L.T., Autoradiographic localization of M1 and M2 muscarine receptors in the rat brain, Neuroscience, 19 (1986) 551-564.

Matthies, H., Ruethrich, H., Ott, T., Matthies, H.K., and Matthies, R., Low frequency perforant path stimulation as a conditioned stimulus demonstrates correlations between long-term synaptic potentiation and learning, Physiol. and Behav., 36 (1986) 811-821.

Mayer, M.L., and Westbrook, G.L., Mixed-agonist action of excitatory amino acids on mouse spinal cord neurons under voltage clamp, J. Physiol., 354 (1984) 29-53.

Mayer, M.L., and Westbrook, G.L., The action of N-methyl-D-aspartic acid on mouse spinal neurones in culture, J. Physiol., 361 (1985) 65-90.

Mayer, M.L., and Westbrook, G.L., The physiology of excitatory amino acids in the vertebrate central nervous system, Prog. Neurobiol., 28 (1987) 197-276.

Mayer, M.L., Westbrook, G.L., and Guthrie, P.B., Voltage-dependent block by Mg2+ of NMDA responses in spinal cord neurons, Nature, 309 (1984) 261-263.

McKinney, M., Anderson, D., and Vella-Rountree, L., Different agonist-receptor active conformations for rat brain M1 and M2 muscarinic receptors that are separately coupled to two biochemical effector systems, Mol. Pharmacol., 35 (1989) 39-47.

McNaughton, B.L., Evidence for two physiologically distinct perforant pathways to the fascia dentata, Brain Res., 199 (1980) 1-19.

Mei, L., Roeske, W.R., and Yamamura, H.I., Molecular pharmacology of muscarinic receptor heterogeneity, Life Sci., 45 (1989) 1831-1851.

Michel, A.D., Stefanich, E., and Whiting R.L., Direct labeling of rat M3-muscarinic receptors by [^{3}H]4DAMP, Eur. J. Pharmacol., 166 (1989) 459-466.

Micheletti, R., Montagna, E., and Giachetti, A., AF-DX 116, a cardioselective muscarinic antagonist, J. Pharmacol. Exp. Ther., 241 (1987) 628-634.

Monaghan, D.T., and Cotman, C.W., Distribution of N-methyl-D-aspartate-sensitive L-[^{3}H]glutamate-binding sites in rat brain, J. Neurosci., 5 (1985) 2909-2919.

Morris, R.G.M., Anderson, E., Lynch, G., and Baudry, M., Selective impairment of learning and blockade of long-term potentiation by an N-methyl-D-aspartate receptor antagonist, AP5, Nature, 319 (1986) 774-776.

Mosko, S., Lynch, G., and Cotman, C.W., The distribution of septal projections to the hippocampus in the rat, J. Comp. Neurol., 52 (1973) 163-174.

Mott, D.D., Lewis, D.V., Ferrari, C.M., Wilson, W.A., and Swartzwelder, H.S., Baclofen facilitates the development of long-term potentiation in the rat dentate gyrus, Neurosci. Lett., 113 (1990) 222-226.

Mueller, A.L., Hoffer, B.J., and Dunwiddie, T.V., Noradrenergic responses in rat hippocampus: evidence for mediation by alpha and ß receptors in the in vitro slice, Brain Res., 214 (1981) 113-126.

Muller, D., and Lynch, G., N-Methyl-D-Aspartate receptor-mediated component of synaptic responses to single-pulse stimulation in rat hippocampal slices, Synapse, 2 (1988) 666-668.

Muller, W., and Misgeld, U., Slow cholinergic excitation of guinea pig hippocampal neurons is mediated by two muscarinic receptor subtypes, Neurosci. Lett., 67 (1986) 107-112.

Muller, W., Misgeld, U., and Heinemann, U., Carbachol effects on hippocampal neurons in vitro: dependence on the rate of rise of carbachol tissue concentration, Exp. Brain. Res., 72 (1988) 287-298.

Newman, R.S., and Harley, C.W., Long-lasting potentiation of the dentate gyrus population spike by norepinephrine, Brain Res., 273

(1983) 162-165.

Nowak, L., Bregestovski, P., Ascher, P., Herbet, A., and Prochiants, A., Magnesium gates glutamate-activated channels in mouse central neurons, Nature, 307, (1984) 462-465.

Oleskevich, S., and Descarries, L., Regional and laminar density of the noradrenaline innervation in adult rat hippocampus, Soc. Neurosci. Abstr. 14 (1988) 778.

Olverman, H.J., Jones, A.W., and Watkins, J.C., L-Glutamate has higher affinity than other amino acids for [^{3}H]-D-AP5 binding sites in rat brain membranes, Nature, 307 (1984) 460-462.

Peralta, E.G., Ashkenazi, A., Winslow, J.W., Ramachandran, J., and Capon, D.J., Differential regulation of PI hydrolysis and adenylyl cyclase by muscarinic receptor subtypes, Nature, 334 (1988) 434-437.

Piercey, M.F., Vogelsang, G.D., Franklin, S.R., and Tang, A.H., Reversal of scopolamine-induced amnesia and alterations in energy metabolism by the nootropic piracetam: implications regarding identification of brain structures involved in consolidation of memory traces, Brain Res., 424 (1987) 1-9.

Pitler, T.A., and Alger, B.E., Evidence of the M3 muscarinic receptor subtype in hippocampal neurons, Soc. Neurosci. Abstracts, 15 (1989).

Quirion R., Araujo, D.M., and Lapchak, P.A., Binding characteristics of ^{3}H-4DAMP, a putative muscarinic-M3 antagonist, in rat brain, Soc. Neurosci. Abstracts, 15 (1989).

Regenold, W., Araugo, D.M., and Quirion, R., Quantitative

autoradiographic distribution of [^{3}H]AF-DX 116 muscarinic-M2 receptor binding sites in rat brain, Synapse, 4 (1989) 115-125.

Rothman, S.M., and Olney, J.W., Excitotoxicity and the NMDA receptor, Trend. Neur. Sci., 10 (1987) 299-302.

Rothman, S.M., Thurston, J.H., Hauhart, R.E., Clark, G.D., and Soloman, J.S., Ketamine protects hippocampal neurons from anoxia in vitro, Neuroscience, 21 (1987) 673-678.

Sah, P., Hestrin, S., and Nicoll, R.A., Tonic activation of NMDA receptors by ambient glutamate enhances excitability of neurons, Science, 246 (1989) 815-818.

Sarvey, J.M., ß-adrenergic mechanisms in long-term potentiation and norepinephrine-induced long-lasting potentiation, in Cellular Mechanisms of Conditioning and Behavioral Plasticity, ed. Woody, Alkon and McGaugh, (1988) 65-76.

Schacher, S., Castellucci, V.F., and Kandel, E.R., cAMP evokes long-term facilitation in Aplysia sensory neurons that requires new protein synthesis, Science, 240 (1988) 1667-1669.

Scharfman, H.E., and Sarvey, J.M., Responses to g-aminobutyric acid applied to cell bodies and dendrites of rat visual cortical neurons, Brain Res., 358 (1985) 385-389.

Scharfman, H.E., and Schwartzkroin, P.A., Protection of dentate hilar cells from prolonged stimulation by intracellular calcium chelation, Science, 246 (1989) 257-260.

Scholz, K.P., and Byrne, J.H., Intracellular injection of cAMP induces a long-term reduction of neuronal K+ currents, Science, 240 (1988) 1664-1666.

Schwartzkroin, P.A., and Wester, K., Long-lasting facilitation of a synaptic potential following tetanization in the in vitro hippocampal slice, Brain Res., 89 (1975) 107-119.

Sheridan, R.D., and Sutor, B., Presynaptic M_1 muscarinic cholinoceptors mediate inhibition of excitatory synaptic transmission in the hippocampus in vitro, Neurosci. Lett., 108 (1990) 273-278.

Skrede, K.K., and Malthe-Sørenssen, D., Increased resting and evoked release of transmitter following repetitive electrical tetanization in hippocampus: a biochemical correlate to long-lasting synaptic potentiation, Brain Res., 208 (1981) 436-441.

Stanton, P.K., Mody, I., and Heinemann, U. A role for N-methyl-D-aspartate receptors in norepinephrine-induced long-lasting potentiation in the dentate gyrus, Exp. Brain Res., 77 (1989) 517-530.

Stanton, P.K., and Sarvey, J.M., Blockade of norepinephrine-induced long-lasting potentiation in the hippocampal dentate gyrus by an inhibitor of protein synthesis, Brain Res., 361 (1985a) 276-283.

Stanton, P.K., and Sarvey, J.M., Depletion of norepinephrine, but not serotonin, reduces long-term potentiation in the dentate gyrus of rat hippocampal slices, J. Neurosci., 5 (1985b) 2169-2176.

Stanton, P.K., and Sarvey, J.M., The effect of high frequency electrical stimulation and norepinephrine on cyclic AMP levels in normal versus norepinephrine-depleted rat hippocampal slices, Brain Res., 358 (1985c) 343-348.

Stanton, P.K., and Sarvey, J.M., Norepinephrine regulates long-term

potentiation of both the population spike and dendritic EPSP in hippocampal dentate gyrus, Brain Res. Bull., 18 (1987) 115-119.

Steward, O., Topographic organization of the projections from the entorhinal area to the hippocampal formation of the rat, J. Comp. Neurol., 167 (1976) 285-314.

Stringer, J.L., and Guyenet, P.G., Elimination of long-term potentiation in the hippocampus by phencyclidine and ketamine, Brain Res., 258 (1983) 159-164.

Tallarida, R.J., Cowan, A., and Adler, M.W., pA_2 and receptor differentiation: a statistical analysis of competitive antagonism, Life Sci., 25 (1979) 637-654.

Tanaka, Y., Sakurai, M., and Hayashi, S., Effect of scopolamine and HP 029, a cholinesterase inhibitor, on long-term potentiation in hippocampal slices of the guinea pig, Neurosci. Lett., 98 (1989) 179-183.

Thompson, A.M., West, D.C., and Lodge, D., An N-methylaspartate-mediated synapse in rat cerebral cortex: a site of action of ketamine?, Nature, 313 (1985) 479-481.

Van Hooff, C.O.M., De Graan, P.N.E., Oestreicher, A.B., and Gispen, W.H., Muscarinic receptor activation stimulates B-50/GAP43 phosphorylation in isolated nerve growth cones, J. Neurosci., 9 (1989) 3753-3759.

Watkins, J.C., and Olverman, H.J., Agonists and antagonists for excitatory amino acid receptors, Trends Neurosci., 10 (1987) 265-272.

Watkins, J.C., Krogsgaard-Larsen, P., and Honore, T., Structure-activity

relationships in the development of excitatory amino acid receptor agonists and competitive antagonists, Trends Pharmacol. Sci., 11 (1990) 25-33.

Werling, L.L., McMahon, P.N., and Cox, B.M., Opioid inhibition of amino acid elicited catecholamine release from hippocampal and striatal slices of rat brain, Soc. Neurosci. Abstr., 13 (1988) 1212.

White, W.F., Nadler, J.V., Hamberger, A., Cotman, C.W., and Cummins, J.T., Glutamate as transmitter of hippocampal perforant path, Nature, 270 (1977) 356-357.

Wigstrom, H., Gustafsson, B., and Huang, Y.-Y., Mode of action of excitatory amino acid receptor antagonists on hippocampal long-lasting potentiation, Neuroscience, 17 (1986) 1105-1115.

Williams, S., and Johnston, D., Muscarinic depression of long-term potentiation in CA3 hippocampal neurons, Science, 242 (1988) 84-87.

Worley, P.F., Baraban, J.M., and Snyder, S.H., Heterogeneous localization of protein kinase C in rat brain: autoradiographic analysis of phorbol ester receptor binding, J. Neurosci., 6 (1986) 199-207.